Supporting Information For

Osmium-Promoted Transformation of Alkyl Nitriles to Secondary Aliphatic Amines: Scope and Mechanism

Juan C. Babón, Miguel A. Esteruelas,*Ana M. López, and Enrique Oñate

Departamento de Química Inorgánica, Instituto de Síntesis Química y Catálisis Homogénea (ISQCH), Centro de Innovación en Química Avanzada (ORFEO-CINQA), Universidad de Zaragoza-CSIC, 50009 Zaragoza, Spain.

* Corresponding author's e-mail address: maester@unizar.es

The supplemental file om0c00236_si_002.xyz contains the computed Cartesian coordinates of all of the molecules reported in this study. The file may be opened as a text file to read the coordinates, or opened directly by a molecular modeling program such as Mercury (version 3.3 or later, http://www.ccdc.cam.ac.uk/pages/Home.aspx) for visualization and analysis.

Contents:

Experimental Section: General information. All reactions were performed with rigorous exclusion of air at an argon/vacuum manifold using standard Schlenk-tube or glovebox techniques. Solvents were dried by the usual procedures and distilled under argon prior to use or obtained oxygen- and water-free from an MBraun solvent purification apparatus. Complex $OsH_6(P^iPr_3)_2$ (**1**) was prepared according to the published method.[1] Nitriles and amines were purchased from commercial sources and distilled in a Kugelrohr distillation oven. NMR spectra were recorded on a Bruker ARX 300, Bruker Avance 300 MHz, or a Bruker Avance 400 MHz instruments. Chemical shifts (expressed in parts per million) are referenced to residual solvent peaks (^{1}H, ^{13}C{^{1}H}) and external H_3PO_4 (^{31}P{^{1}H}). Coupling constants *J* are given in Hertz. High-resolution (HRMS) and low-resolution (LRMS) electrospray mass spectra were acquired using a MicroTOF-Q hybrid quadrupole time-of-flight spectrometer and an Esquire 3000+ spectrometer, respectively (Bruker Daltonics, Bremen, Germany). C, H, and N analyses were carried out in a Perkin-Elmer 2400-B Series II CHNS-Analyzer. Attenuated total reflection infrared spectra (ATR-IR) of solid samples were run on a Perkin-Elmer Spectrum 100 FT-IR spectrometer.

Structural Analysis of Complexes 3, 5, and 6. X-ray data were collected for the complexes on a Bruker Smart APEX diffractometer equipped with a normal focus, and 2.4 kW sealed tube source (Mo radiation, λ = 0.71073 Å). Data were collected over the complete sphere covering 0.3^o in ω. Data were corrected for absorption by using a multiscan method applied with the SADABS program.[2] The structures were solved by Patterson or direct methods and refined by full-matrix least squares on F^2 with SHELXL2016,[3] including isotropic and subsequently anisotropic displacement parameters. The hydrogen atoms were observed in the last Fourier Maps or calculated, and refined freely or using a restricted riding model. The hydrides were located but refined with fixed Os-H distances (1.59 Å).

The azavinylidene ligand of complex **3** was observed disordered and was refined with two moieties, complementary occupancy factors, and isotropic displacement parameters. The hydrides (also disordered) were refined with a fixed distance Os-H using the expected geometry as template.

The crystal of **6** is the result of the co-crystallization 0.75/0.25 of amine/imine (**5**) complexes. The disordered ligands were refined with complementary occupancy factors. The mayor component (**6**) was refined freely with anisotropic thermal

parameters. The minor component was refined with restricted geometry, and isotropic displacement parameters.

Crystal data for **3** (1993553): $C_{23}H_{55}NOsP_2$, M_W 597.82, orange, irregular block (0.159 x 0.152 x 0.147 mm^3), triclinic, space group P-1, *a*: 9.6213(6) Å, *b*: 11.1004(7) Å, *c*: 14.9218(9) Å, ◘: 76.6170(10)°, ◘: 76.0920(10)°, ◘: 66.6920(10)°, V = 1403.97(15)$Å^3$, Z = 2, Z' = 1, D_{calc}: 1.414 g cm^{-3}, F(000): 612, T = 100(2) K, μ 4.664 mm^{-1}. 24571 measured reflections (2θ: 3-57°, ω scans 0.3°), 6696 unique (R_{int} = 0.0268); min./max. transm. Factors 0.654/0.862. Final agreement factors were R^1 = 0.0239 (6117 observed reflections, I > 2σ(I)) and wR^2 = 0.0598; data/restraints/parameters 6696/28/263; GoF = 1.001. Largest peak and hole 1.715 (close to osmium atoms) and -0.719 e/ $Å^3$.

Crystal data for **5** (1993555): $C_{40}H_{98}N_2OOs_2P_4$, M_W 1127.48, colorless, irregular block (0.243 x 0.166 x 0.026 mm^3), monoclinic, space group $P2_1/n$, *a*: 12.1110(10) Å, *b*: 23.0715(19) Å, *c*: 18.6300(15) Å, ◘: 102.2410(10)°, V = 5087.2(7) $Å^3$, Z = 4, Z' = 1, D_{calc}: 1.472 g cm^{-3}, F(000): 2288, T = 100(2) K, μ 5.145 mm^{-1}. 115178 measured reflections (2θ: 3-57°, ω scans 0.3°), 12470 unique (R_{int} = 0.0893); min./max. transm. Factors 0.520/0.862. Final agreement factors were R^1 = 0.0646 (10083 observed reflections, I > 2σ(I)) and wR^2 = 0.1392; data/restraints/parameters 12470/7/494; GoF = 1.191. Largest peak and hole 4.333 (close to osmium atoms) and -2.341 e/ $Å^3$.

Crystal data for **6** (1993554): 0.75($C_{40}H_{100}N_2OOs_2P_4$), 0.25($C_{40}H_{98}N_2OOs_2P_4$), M_W 1128.99, colourless, irregular block (0.219 x 0.041 x 0.041 mm^3), triclinic, space group P-1, *a*: 11.5140(13) Å, *b*: 12.9055(14) Å, *c*: 18.259(2) Å, ◘: 108.1990(10)°, ◘: 99.3720(10)°, ◘: 101.0170(10)°, V = 2456.9(5)$Å^3$, Z = 2, Z' = 1, D_{calc}: 1.526 g cm^{-3}, F(000): 1147, T = 100(2) K, μ 5.327 mm^{-1}. 35603 measured reflections (2θ: 3-57°, ω scans 0.3°), 11556 unique (R_{int} = 0.0869); min./max. transm. Factors 0.646/0.862. Final agreement factors were R^1 = 0.0476 (7137 observed reflections, I > 2σ(I)) and wR^2 = 0.0705; data/restraints/parameters 11556/12/ 483; GoF = 1.088. Largest peak and hole 1.566 (close to osmium atoms) and -1.806 e/ $Å^3$.

Computational Details. All calculations in the mechanistic studies were performed at the DFT level using the B3LYP functional[4] supplemented with the Grimme's dispersion correction D3[5] including an ultrafine integration grid, as implemented in Gaussian09.[6] Os atom was described by means of an effective core potential SDD for the inner electron[7] and its associated double-◘ basis set for the outer ones, complemented with a set of f-polarization functions.[8] The 6-31G** basis set was used for the H, C, N and P

atoms.[9] All geometries were fully optimized in toluene (◘ = 2.37) solvent using the continuum SMD model.[10] Transition states were identified by having one imaginary frequency in the Hessian matrix. It was confirmed that transition states connect with the corresponding intermediates by means of application of an eigenvector corresponding to the imaginary frequency and subsequent optimization of the resulting structures. Gibbs energies were computed at 298.15 K and 1 atmosphere. All values collected in schemes and figures correspond to Gibbs energies in toluene in kcal mol^{-1}. **t_2 + H_2** and **t_7 + H_2** are the **t_2** and **t_7** model complexes with an explicit hydrogen molecule necessary to study the reactivity with the gas.

Analytical data of the isolated amine hydrochloride salts

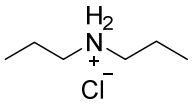

a·HCl:[11a] ^{1}H NMR (300.13 MHz, $CDCl_3$, 298 K): δ 9.33 (br, 2H, NH_2), 2.89 (t, $^3J_{H\text{-}H}$ = 8.1, 4H, NCH_2), 1.94 (m, 4H, CH_2CH_3), 1.01 (t, $^3J_{H\text{-}H}$ = 7.3, 6H, CH_3). $^{13}C\{^1H\}$ APT NMR (75.48 MHz, $CDCl_3$, 298 K): ◘ 49.5 (NCH_2), 19.6 (CH_2CH_3), 11.4 (CH_3). HR-MS (electrospray): m/z calcd for $C_6H_{16}N^+$ $[M]^+$ 102.1277; found 102.1267.

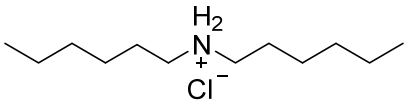

b·HCl:[12] ^{1}H NMR (400.16 MHz, $CDCl_3$, 298 K): δ 9.37 (br, 2H, NH_2), 2.83 (br, 4H, NCH_2), 1.83 (m, 4H, CH_2CH_2N), 1.31-1.23 (br, 12H, $CH_3CH_2CH_2CH_2$) 0.81 (t, $^3J_{H\text{-}H}$ = 6.8, 6H, CH_3). $^{13}C\{^1H\}$ APT NMR (100.63 MHz, $CDCl_3$, 298 K): ◘ 47.9 (NCH_2), 31.2 (CH_2), 26.5 (CH_2), 25.9 (CH_2), 22.5 (CH_2), 13.9 (CH_3). HR-MS (electrospray): m/z calcd for $C_{12}H_{28}N^+$ $[M]^+$ 186.2216; found 186.2213.

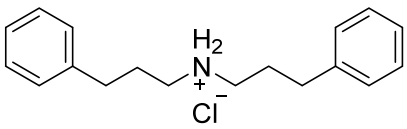

c·HCl: ^{1}H NMR (400.16 MHz, $CDCl_3$, 298 K): δ 9.35 (br, 2H, NH_2), 7.17 (m, 4H, CH_{Ph}), 7.09 (m, 6H, CH_{Ph}), 2.76 (m, 4H, NCH_2), 2.54 (t, $^3J_{H\text{-}H}$ = 7.3, 4H, CH_2), 2.09 (m, 4H, CH_2). $^{13}C\{^1H\}$ APT NMR (100.63 MHz, $CDCl_3$, 298 K): ◘ 139.8 (C_q), 128.6 (s, CH_{Ph}), 128.4 (CH_{Ph}), 126.4 (CH_{Ph}), 47.2 (NCH_2), 32.7 (CH_2), 27.2 (CH_2). HR-MS (electrospray): m/z calcd for $C_{18}H_{24}N^+$ $[M]^+$ 254.1903; found. 254.1936.

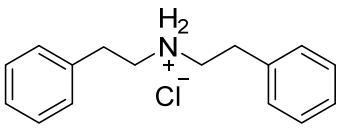

d·HCl: ^{1}H NMR (400.16 MHz, $CDCl_3$, 298 K): δ 9.87 (br, 2H, NH_2), 7.24-7.10 (m, 10 H, CH_{Ar}), 3.26-3.07 (m, 8H, NCH_2). $^{13}C\{^1H\}$ APT NMR (100.63 MHz, $CDCl_3$, 298 K):

◘ 136.3 (C_q), 128.9 (CH_{Ar}), 128.7 (CH_{Ar}), 127.2 (CH_{Ar}), 49.2 (NCH_2), 32.4 (CH_2). HR-MS (electrospray): m/z calcd for $C_{16}H_{20}N^+$ $[M]^+$ 226.1590; found. 226.1602.

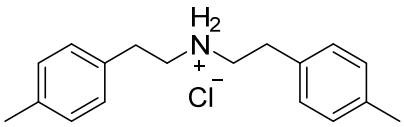

e·HCl: ^{1}H NMR (400.16 MHz, $(CD_3)_2SO$, 298 K): δ 8.21 (br, 2H, NH_2), 7.12 (m, 8H, CH_{Ar}), 3.02 (m, 4H, NCH_2), 2.85 (m, 4H, CH_2), 2.27 (s, 6H, CH_3). $^{13}C\{^1H\}$ APT NMR (75.48 MHz, $(CD_3)_2SO$, 298 K): ◘ 136.0 (C_q), 129.6 (CH_{Ar}), 128.9 (CH_{Ar}), 49.0 (NCH_2), 32.6 (CH_2), 21.1 (CH_3). HR-MS (electrospray): m/z calcd for $C_{18}H_{24}N^+$ $[M]^+$ 254.1903; found 254.1922.

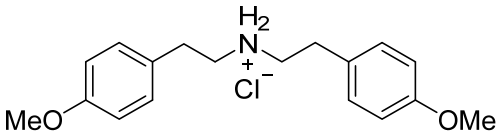

f·HCl: ^{1}H NMR (400.16 MHz, $(CD_3)_2SO$, 298 K): δ 9.06 (br, 2H, NH_2), 7.17 (d, $^3J_{H\text{-}H}$ = 8.6, 4H, CH_{Ar}), 6.89 (d, $^3J_{H\text{-}H}$ = 8.6, 4H, CH_{Ar}), 3.73 (s, 6H, CH_3), 3.07 (t, $^3J_{H\text{-}H}$ = 7.9, 4H, NCH_2), 2.90 (t, $^3J_{H\text{-}H}$ = 8.0, 4H, CH_2). $^{13}C\{^1H\}$ APT NMR (75.48 MHz, $(CD_3)_2SO$, 298 K): ◘ 158.9 (C_q), 130.1 (C_q), 129.7 (CH_{Ar}), 114.5 (CH_{arom}), 55.5 (OCH_3), 48.9 (NCH_2), 31.3 (CH_2). HR-MS (electrospray): m/z calcd for $C_{18}H_{24}NO_2^+$ $[M]^+$ 286.1802; found 286.1800.

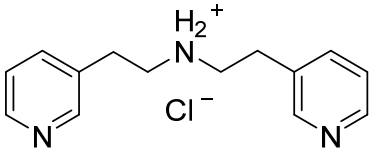

g·HCl: ^{1}H NMR (300.13 MHz, $(CD_3)_2SO$, 298 K): δ 8.84 (br, 2H, CH_{Ar}), 8.77 (br, 2H, CH_{Ar}), 8.39 (br, 2H, CH_{Ar}), 8.14 (br, 2H, NH), 7.93 (br, 2H, CH_{Ar}), 3.16 (m, 4H, NCH_2), 3.10 (m, 4H, CH_2). $^{13}C\{^1H\}$ APT NMR (100.63 MHz, $(CD_3)_2SO$, 298 K): ◘ 149.3 (CH_{Ar}), 147.4 (CH_{Ar}), 136.9 (CH_{Ar}), 133.5 (C_q), 124.0 (CH_{Ar}), 64.9 (NCH_2), 30.0 (CH_2). LR-MS (electrospray): m/z calcd for $C_{14}H_{18}N_3^+$ $[M]^+$ 228.15; found 228.04.

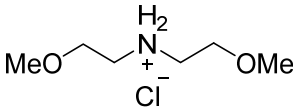

h·HCl: ^{1}H NMR (400.16 MHz, $CDCl_3$, 298 K): δ 5.39 (br, 2H, NH_2), 3.73 (m, 4H, CH_2O), 3.35 (s, 6H, OCH_3), 3.17 (m, 4H, NCH_2). $^{13}C\{^1H\}$ APT NMR (100.63 MHz, $CDCl_3$, 298 K): ◘ 67.9 (CH_2O), 59.0 (OCH_3), 47.7 (NCH_2). HR-MS (electrospray): m/z calcd for $C_6H_{16}NO_2^+$ $[M]^+$ 134.1176; found. 134.1180.

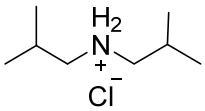

i·HCl:[11b] ^{1}H NMR (300.13 MHz, $CDCl_3$, 298 K): δ 9.05 (br, 2H, NH_2), 2.88 (br, 4H, NCH_2), 2.33 (m, 2H, CH), 1.13 (d, $^3J_{H\text{-}H}$ = 6.3, 12H, CH_3). $^{13}C\{^1H\}$ APT NMR (75.48 MHz, $CDCl_3$, 298 K): ◘ 55.4 (NCH_2), 25.5 (CH), 20.8 (CH_3). HR-MS (electrospray): m/z calcd for $C_8H_{20}N^+$ $[M]^+$ 130.1590; found 130.1592.

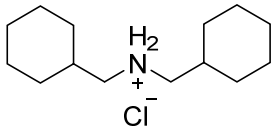

j·HCl ^{1}H NMR (400.16 MHz, $CDCl_3$, 298 K): δ 7.98 (br, 2H, NH_2), 2.75 (br, 4H, NCH_2), 1.82-1.63 (m, 11H, Cy), 1,23-0.9 (m, 11H, Cy). ^{13}C{^{1}H} APT NMR (100.63 MHz, $CDCl_3$, 298 K): δ 35.9 (CH), 30.4, 25.9, 25.5 (all CH_2), NCH_2 not observed. Secondary amine: HR-MS (electrospray): m/z calcd for $C_{14}H_{28}N^+$ $[M]^+$ 210.2216; found. 210.2223. Primary amine is also detected: HR-MS (electrospray): m/z calcd for $C_7H_{16}N^+$ $[M]^+$ 114.1277; found. 114.1293.

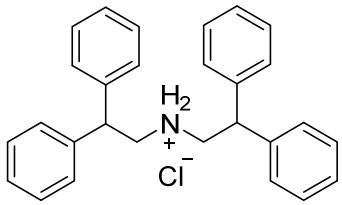

k·HCl: ^{1}H NMR (400.16 MHz, $(CD_3)_2SO$, 298 K): δ 8.07 (br, 2H, NH_2), 7.39-7.34 (m, 16H, CH_{Ar}), 7.24 (m, 4H, CH_{arom}), 4.35 (t, $^{3}J_{H\text{-}H}$ = 7.9, 2H, C*H*Ph_2), 3.54 (m, 4H, NCH_2). ^{13}C{^{1}H} APT NMR (100.63 MHz, $(CD_3)_2SO$, 298 K): ◘ 141.0 (C_{Ar}), 128.7 (CH_{Ar}), 127.8 (CH_{Ar}), 127.0 (CH_{Ar}), 48.6 (*C*HPh_2), 42.3 (NCH_2). HR-MS (electrospray): m/z calcd for $C_{28}H_{28}N^+$ $[M]^+$ 378.2216; found. 378.2274.

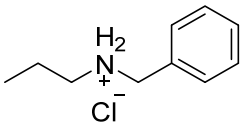

l·HCl:[13] ^{1}H NMR (400.16 MHz, $CDCl_3$, 298 K): δ 9.68 (br, 2H, NH_2), 7.54 (m, 2H, CH_{Ph}), 7.32 (m, 3H, CH_{Ph}), 3.98 (br, 2H, NC*H*$_2$Ph), 2.66 (m, 2H, NCH_2), 1.79 (m, 2H, CH_2), 0.87 (t, $^{3}J_{H\text{-}H}$ = 6.7 Hz, 3H, CH_3). ^{13}C{^{1}H} APT NMR (100.63 MHz, $CDCl_3$, 298 K): ◘ 134.1 (C_q), 128.9 (CH_{Ar}), 128.5 (s, CH_{Ar}), 128.4 (s, CH_{Ar}), 61.3 (N*C*H_2Ph), 49.7 (NCH_2), 42.1 (CH_2), 32.8 (CH_3). LR-MS (electrospray): m/z calcd for $C_{10}H_{16}N^+$ $[M]^+$ 150.13; found 150.13.

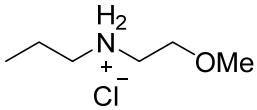

m·HCl: ^{1}H NMR (400.16 MHz, $CDCl_3$, 298 K): δ 8.99 (br, 2H, NH_2), 3.78 (br, 2H, OCH_2), 3.36 (s, 3H, OCH_3), 3.12 (br, 2H, N*CH*$_2$$CH_2$O), 2.97 (br, 2H, N*CH*$_2$$CH_2CH_3$), 1.88 (m, 2H, NCH_2*CH*$_2$$CH_3$), 0.97 (t, $^{3}J_{H\text{-}H}$ = 7.3 Hz, 3H, NCH_2CH_2*CH*$_3$). ^{13}C{^{1}H} APT NMR (100.63 MHz, $CDCl_3$, 298 K): ◘ 67.9 (OCH_2), 59.1 (OCH_3), 50.1 (N*CH*$_2$$CH_2$O), 47.0 (N*CH*$_2$$CH_2CH_3$), 19.8 ($NCH_2$*CH*$_2$$CH_3$), 11,3 ($NCH_2CH_2$*CH*$_3$). HR-MS (electrospray): m/z calcd for $C_6H_{16}NO^+$ $[M]^+$ 118.1226 found 118.1230.

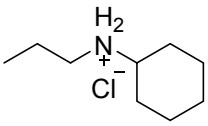

n·HCl:[13] ^{1}H NMR (400.16 MHz, $CDCl_3$, 298 K): δ 9.16 (br, 2H, NH_2), 2.98 (br, 1H, NCH), 2.82 (br, 2H, NCH_2), 2.17 (br, 2H, CH_2), 1.88 (br, 2H, CH_2), 1.78 (br, 2H, CH_2), 1.19 (br, 6H, CH_2), 0.93 (t, $^{3}J_{H\text{-}H}$ = 6 Hz, 3H, CH_3). ^{13}C{^{1}H} APT NMR (100.63 MHz, $CDCl_3$, 298 K): ◘ 57.2

(NCH), 46.2 (NCH_2), 29.2, 24.8, 24.6, 19.6 (all CH_2), 11,5 (CH_3). LR-MS (electrospray): m/z calcd for $C_9H_{20}N^+$ $[M]^+$ 142.16; found 142.14.

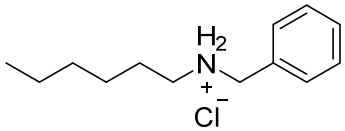

o·HCl: ^{1}H NMR (400.16 MHz, $CDCl_3$, 298 K): δ 9.75 (br, 2H, NH_2), 7.61 (m, 2H, CH_{Ar}), 7.40 (m, 3H, CH_{Ar}), 4.01 (s, 2H, NCH_2), 2.74 (br, 2H, NCH_2), 1.84 (br, 2H, CH_2), 1.28 (m, 6H, CH_2), 0.84 (t, $^3J_{H\text{-}H}$ = 6.8 Hz, 3H, CH_3). $^{13}C\{^1H\}$ APT NMR (100.63 MHz, $CDCl_3$, 298 K): ◘ 127.6 (s, CH_{Ar}), 127.2 (s, C_q), 126.5 (CH_{Ar}), 126.2 (CH_{Ar}), 47.6 (NCH_2), 43.1 (NCH_2), 28.2, 23.6, 23.0, 19.5 (all CH_2), 11,3 (CH_3). HR-MS (electrospray): m/z calcd for $C_{13}H_{22}N^+$ $[M]^+$ 192.1747 found 192.1739.

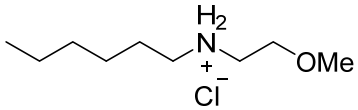

p·HCl: ^{1}H NMR (300.13 MHz, $CDCl_3$, 298 K): δ 9.26 (br, 2H, NH_2), 3,85 (br, 2H, OCH_2), 3.43 (s, 3H, OCH_3), 3.20 (br, 2H, NCH_2), 3.07 (br, 2H, NCH_2), 1.34 (m, 8H, CH_2), 0.90 (br, 3H, CH_3). $^{13}C\{^1H\}$ APT NMR (75.48 MHz, $CDCl_3$, 298 K): ◘ 67.7 (OCH_2), 59.0 (OCH_3), 48.5 (NCH_2), 46.9 (s, NCH_2), 31.2, 26.4, 26.2, 22.4 (all CH_2), 13,9 (CH_3). HR-MS (electrospray): m/z calcd for $C_9H_{22}NO^+$ $[M]^+$ 160.1696 found 160.1686.

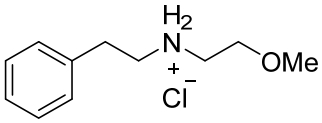

q·HCl: ^{1}H NMR (400.16 MHz, $CDCl_3$, 298 K): δ 9.01 (br, 2H, NH_2), 7.19 (m, 5H, Ph), 3.74 (br, 2H, OCH_2), 3.29 (m, 3H, OCH_3), 3.21-3.15 (br, 6H, $3CH_2$). $^{13}C\{^1H\}$ APT NMR (100.63 MHz, $CDCl_3$, 298 K): ◘ 136.5 (s, C_q), 128.9 (CH_{Ph}), 128.8 (CH_{Ph}), 127.1 (CH_{Ph}), 67.6 (OCH_2), 59.0 (OCH_3), 49.5, 46.9 (both NCH_2), 32.4 (s, CH_2Ph). LR-MS (electrospray): m/z calcd for $C_{11}H_{18}NO^+$ $[M]^+$ 180.14; found 180.07.

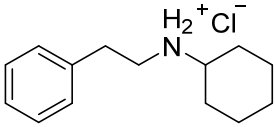

r·HCl:[14] ^{1}H NMR (400.16 MHz, $CDCl_3$, 298 K): δ 9.67 (br, 2H, NH_2), 7.17 (m, 5H, Ph), 3.22 (br, 2H, NCH_2), 3.11 (br, 2H, CH_2), 2.93 (br, 1H, NCH), 2.20 (br, 2H, CH_2), 1.77 (br, 2H, CH_2), 1.58 (br, 3H, CH_2), 1.18 (br, 3H, CH_2). 13C{^{1}H} APT NMR (100.63 MHz, $CDCl_3$, 298 K): ◘ 136.6 (C_q Ph), 128.8 (CH_{Ph}), 128.8 (CH_{Ph}), 127.1 (CH_{Ph}) 57.5 (NCH), 49.4 (s, NCH_2), 46.1 (PhCH_2*C*H_2), 32.5, 29.3, 24.6 (CH_2 Cy). HR-MS (electrospray): m/z calcd for $C_{14}H_{22}N^+$ $[M]^+$ 204.1731; found 204.1747.

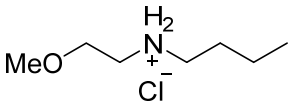

s·HCl: ^{1}H NMR (400.16 MHz, $CDCl_3$, 298 K): δ 9.21 (br, 2H, NH_2), 3.76 (t, $^3J_{H\text{-}H}$ = 5.2 Hz, 2H, OCH_2), 3.33 (s, 3H, OCH_3),

3.11 (t, $^{3}J_{H\text{-}H}$ = 5.2 Hz, 2H, N*CH*$_2$CH$_2$O), 2.98 (m, 2H, NCH$_2$), 1.81 (m, 2H, CH$_2$), 1.35 (m, 2H, CH$_2$), 0.88 (t, $^{3}J_{H\text{-}H}$ = 7.4 Hz, 3H, CH$_3$). ^{13}C{^{1}H} APT NMR (100.63 MHz, CDCl$_3$, 298 K): δ 67.6 (OCH$_2$), 58.9 (OCH$_3$), 48.1 (N*CH*$_2$CH$_2$O), 46.6, 27.9, 20.0 (all CH$_2$), 13.5 (CH$_3$). HR-MS (electrospray): m/z calcd for $C_7H_{18}NO^+$ $[M]^+$ 132.1383; found 132.1390.

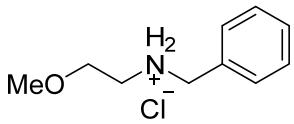

t·HCl: ^{1}H NMR (400.16 MHz, CDCl$_3$, 298 K): δ 9.74 (br, 2H, NH$_2$), 7.54 (m, 2H, Ph), 7.32 (m, 3H, Ph), 4.11 (br, 2H, NC*H*$_2$Ph), 3.71 (m, 2H, OCH$_2$), 3.31 (s, 3H, OCH$_3$), 2.95 (br, 2H, N*CH*$_2$CH$_2$). ^{13}C{^{1}H} APT NMR (100.63 MHz, CDCl$_3$, 298 K): ◘ 136.1 (C$_q$), 130.5 (s, CH$_{Ph}$), 129.5 (s, CH$_{Ph}$), 129.2 (s, CH$_{Ph}$), 68.3, 67.6 (NCH$_2$Ph and OCH$_2$), 59.0 (OCH$_3$), 45.0 (s, N*CH*$_2$CH$_2$). HR-MS (electrospray): m/z calcd for $C_{10}H_{16}NO^+$ $[M]^+$ 166.1226; found 166.1224.

Figures of the ^{1}H NMR spectra of the reaction crude of the catalytic nitrile hydrogenations and ^{1}H NMR and ^{13}C{^{1}H} APT NMR spectra of the hydrochloride salts.

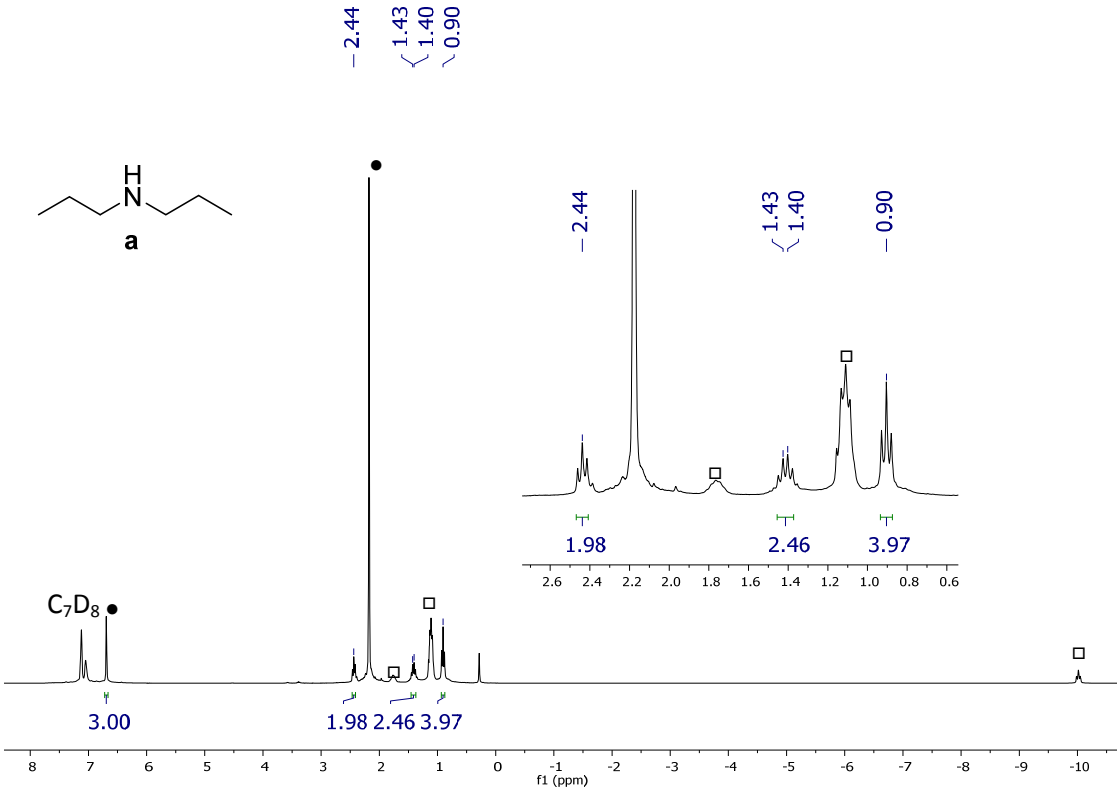

Figure S1. ^{1}H NMR (300.13 MHz, C_7D_8, 298 K) spectrum of the reaction mixture of the hydrogenation of propionitrile: formation of di-*n*-propylamine (**a**). • Mesitylene. □ $OsH_6(P^iPr_3)_2$ (**1**).

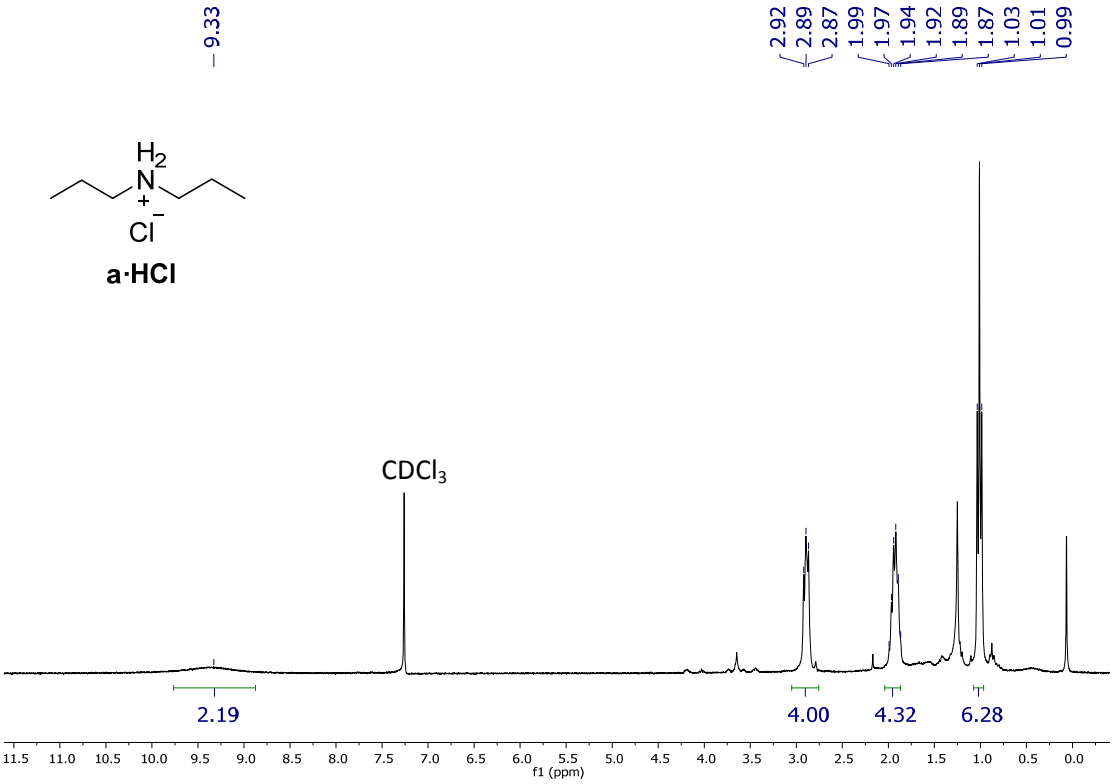

Figure S2. ^{1}H NMR (300.13 MHz, $CDCl_3$, 298 K) spectrum of **a·HCl**.

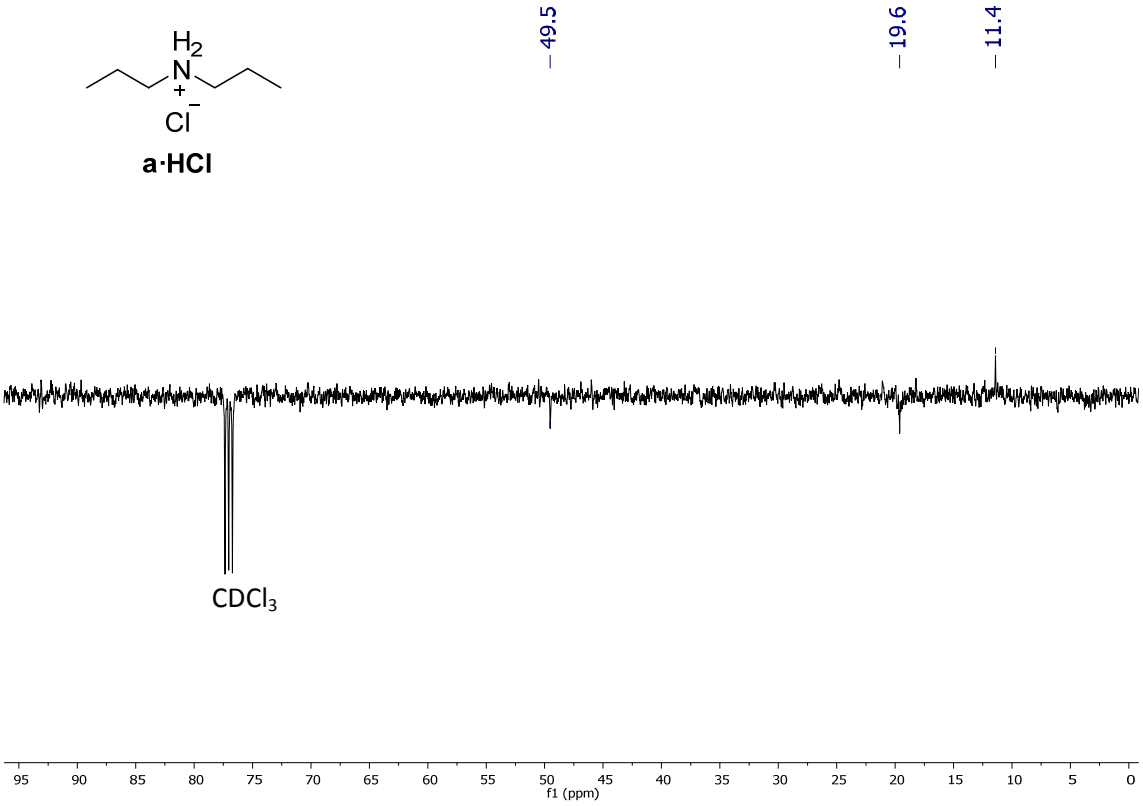

Figure S3. $^{13}C\{^{1}H\}$ APT NMR (75.48 MHz, $CDCl_3$, 298 K) spectrum of **a·HCl**.

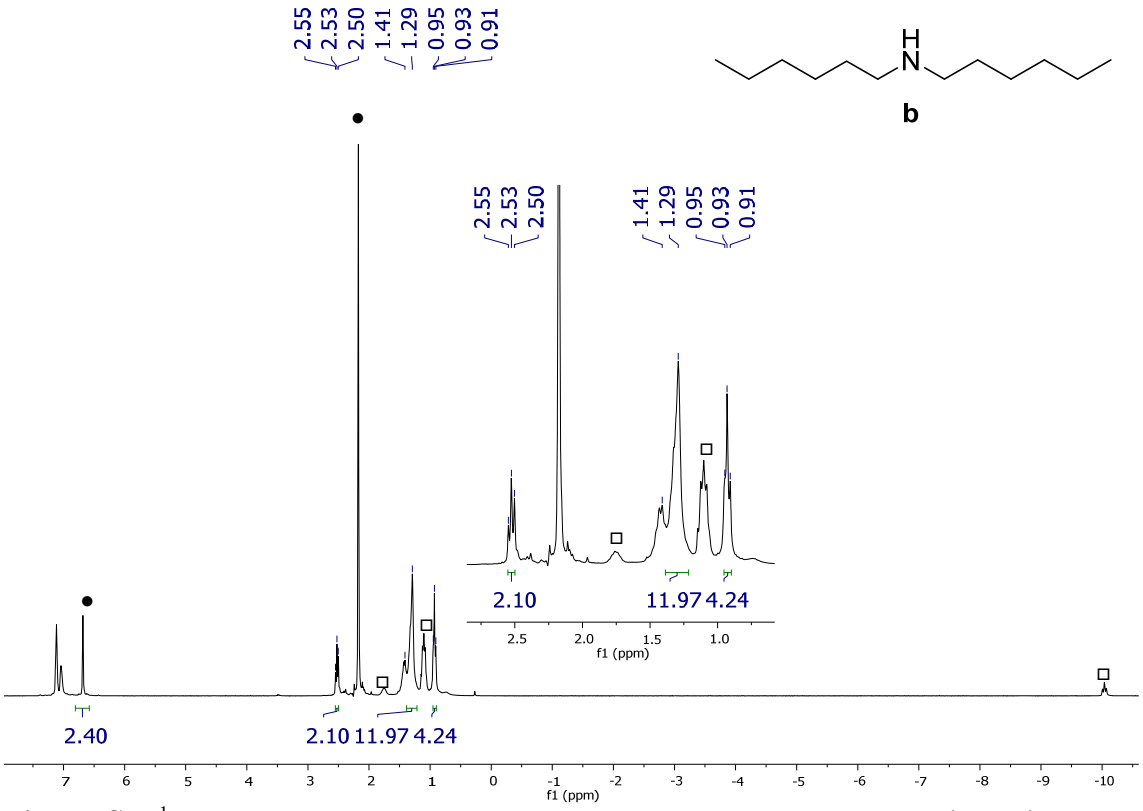

Figure S4. ^{1}H NMR (300.13 MHz, C_7D_8, 298 K) spectrum of the reaction mixture of the hydrogenation of hexanenitrile: formation of di-*n*-hexylamine (**b**). • Mesitylene. □ $OsH_6(P^iPr_3)_2$ (**1**).

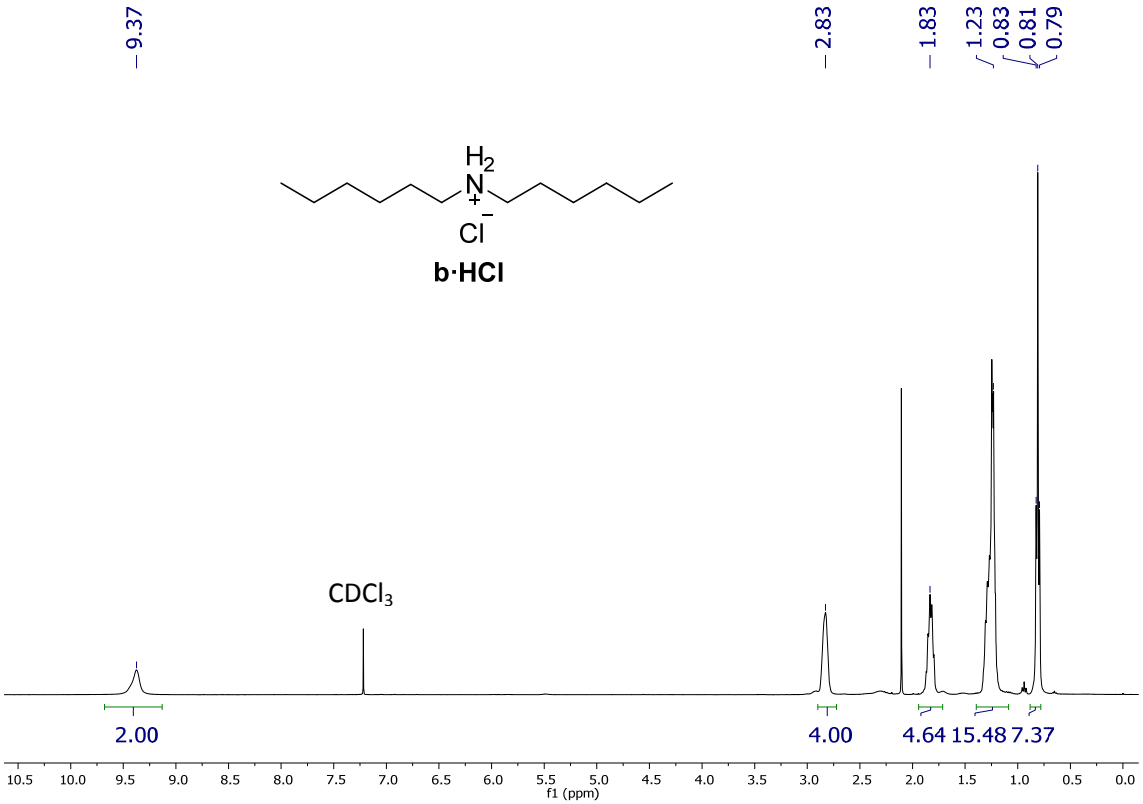

Figure S5. ^{1}H NMR (400.16 MHz, $CDCl_3$, 298 K) spectrum of **b·HCl**.

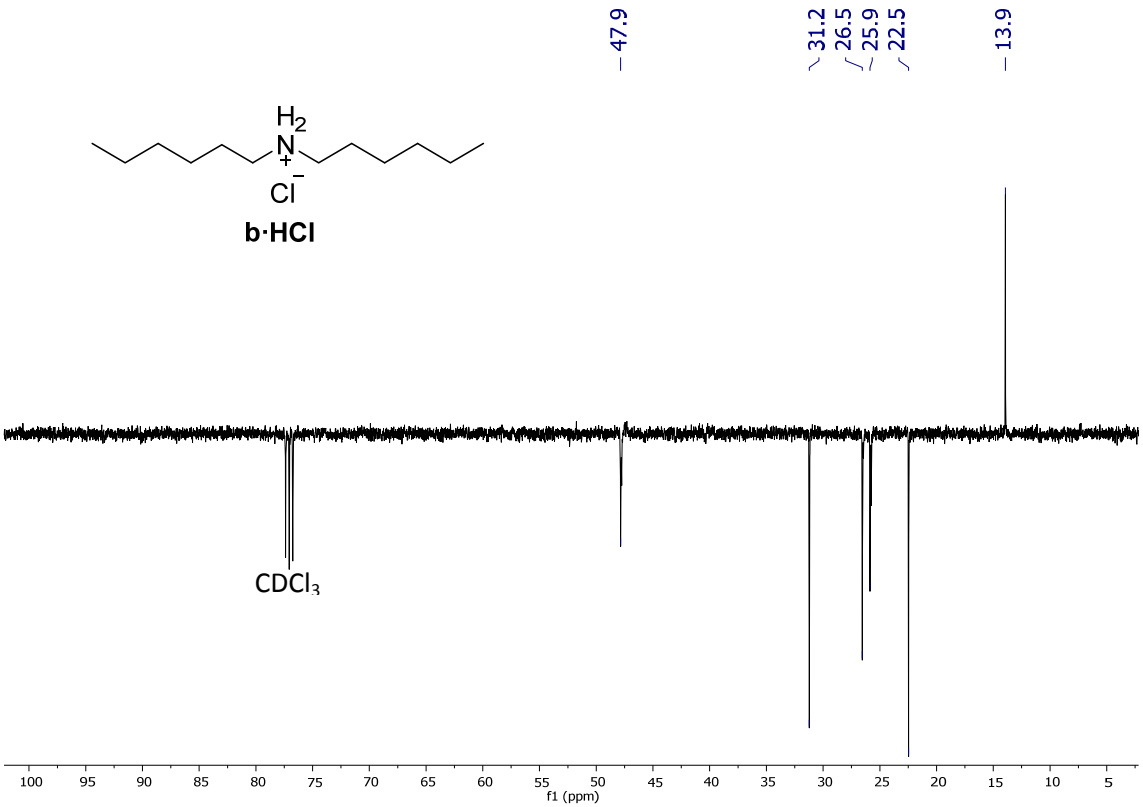

Figure S6. ^{13}C{^{1}H} APT NMR (100.63 MHz, $CDCl_3$, 298 K) spectrum of **b·HCl**.

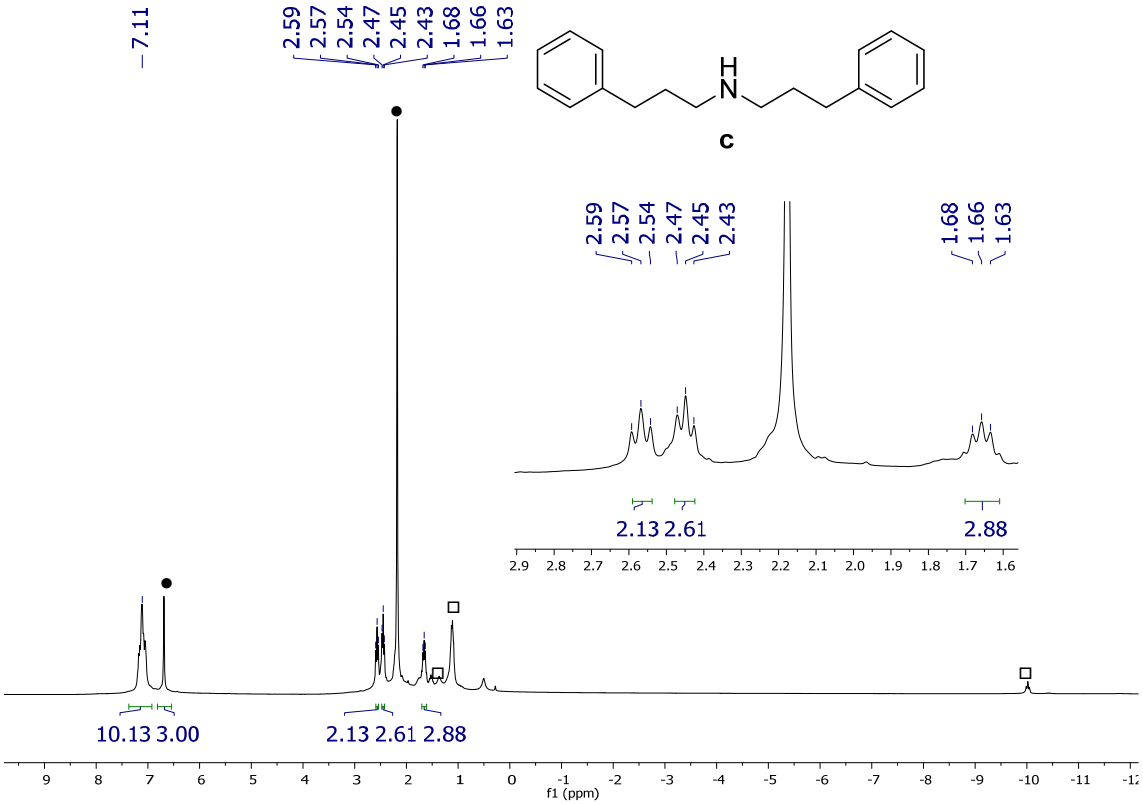

Figure S7. ^{1}H NMR (300.13 MHz, C_7D_8, 298 K) spectrum of reaction mixture of the hydrogenation of 3-phenylpropanenitrile: formation of bis(3-phenylpropyl)amine (**c**).[15] • Mesitylene. □ $OsH_6(P^iPr_3)_2$ (**1**)

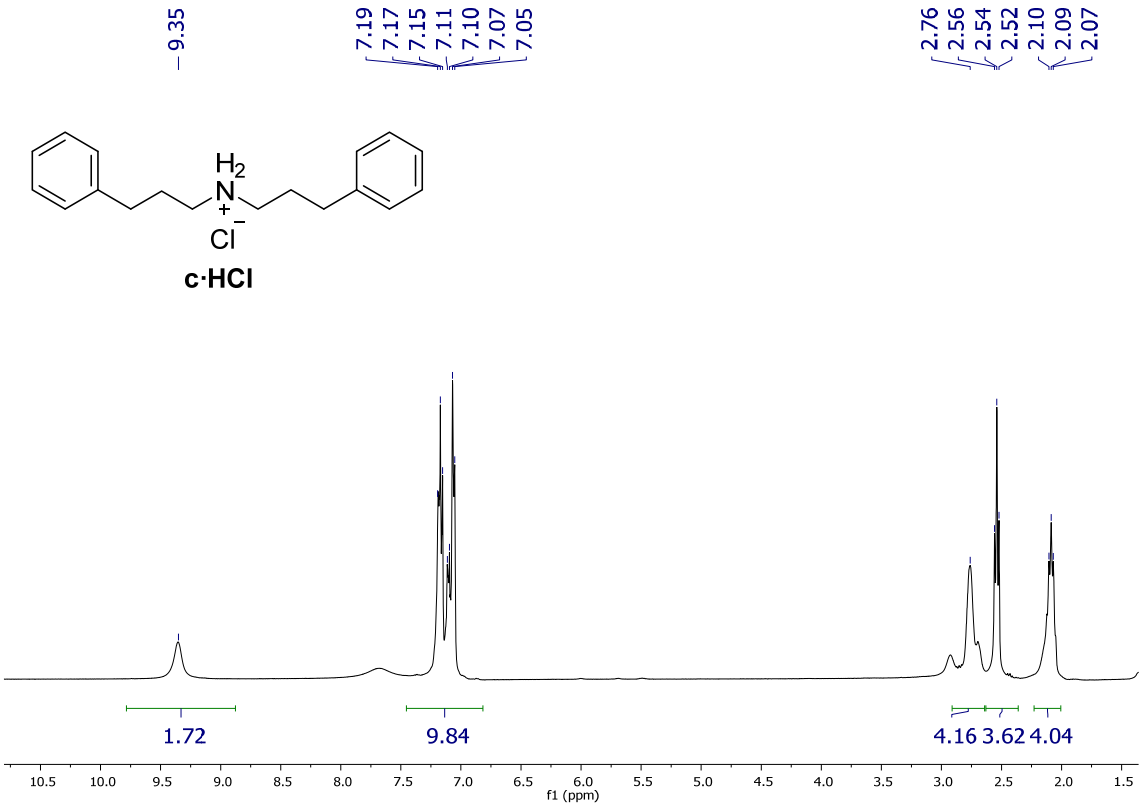

Figure S8. ^{1}H NMR (400.16 MHz, $CDCl_3$, 298 K) spectrum of **c·HCl**.

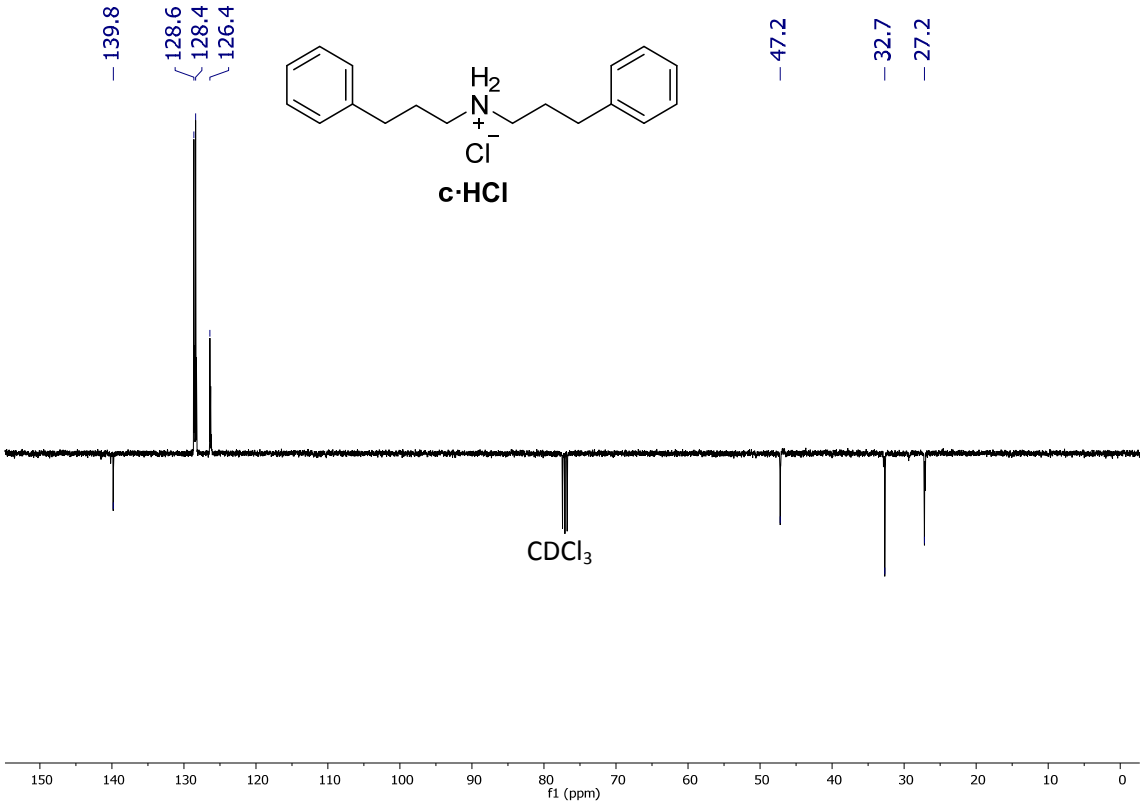

Figure S9. $^{13}C\{^{1}H\}$ APT NMR (100.63 MHz, $CDCl_3$, 298 K) spectrum of **c·HCl**.

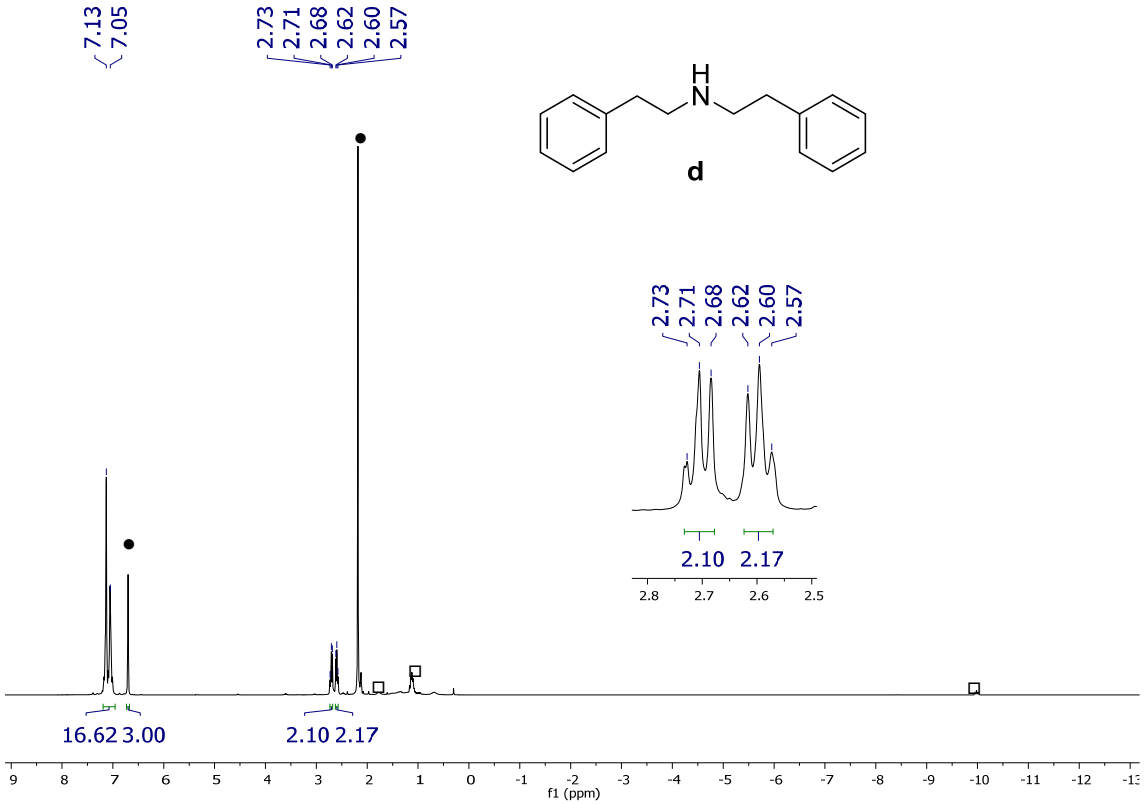

Figure S10. ^{1}H NMR (300.13 MHz, C_7D_8, 298 K) spectrum of the reaction mixture of the hydrogenation of 2-phenylacetonitrile: formation of diphenethylamine (**d**).[16] • Mesitylene. □ $OsH_6(P^iPr_3)_2$ (**1**).

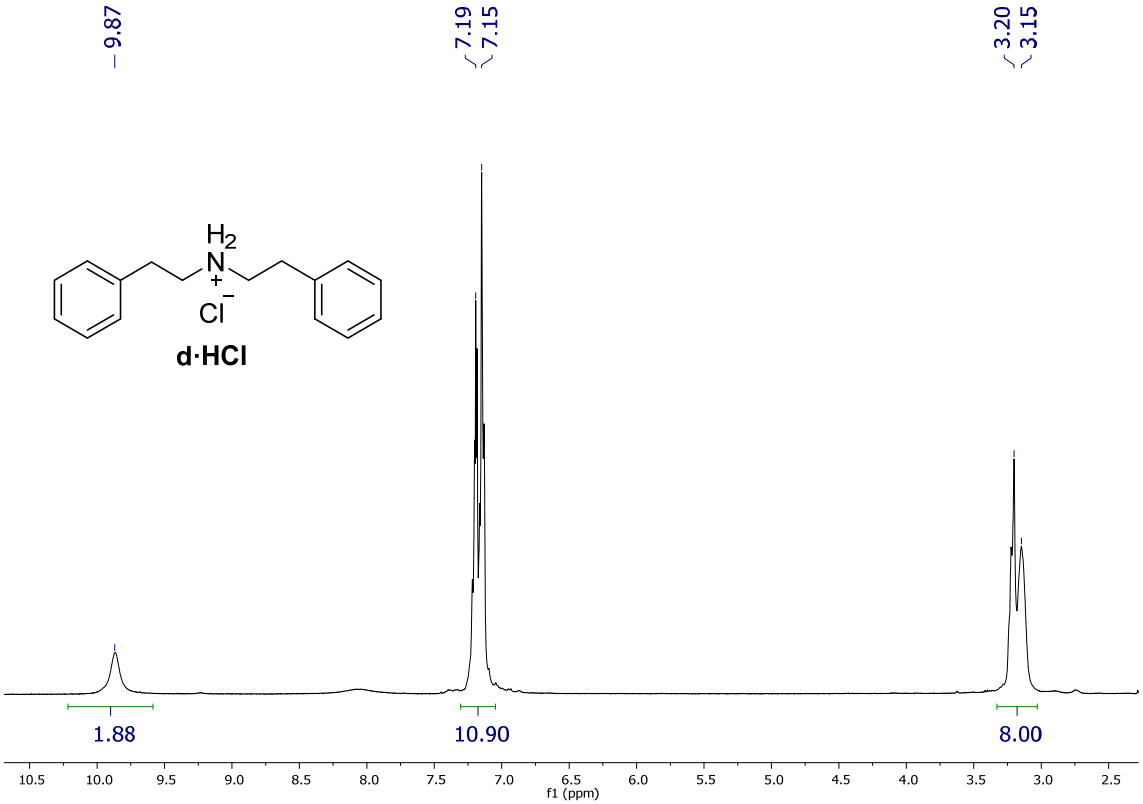

Figure S11. ^{1}H NMR (400.16 MHz, $CDCl_3$, 298 K) spectrum of **d·HCl**.

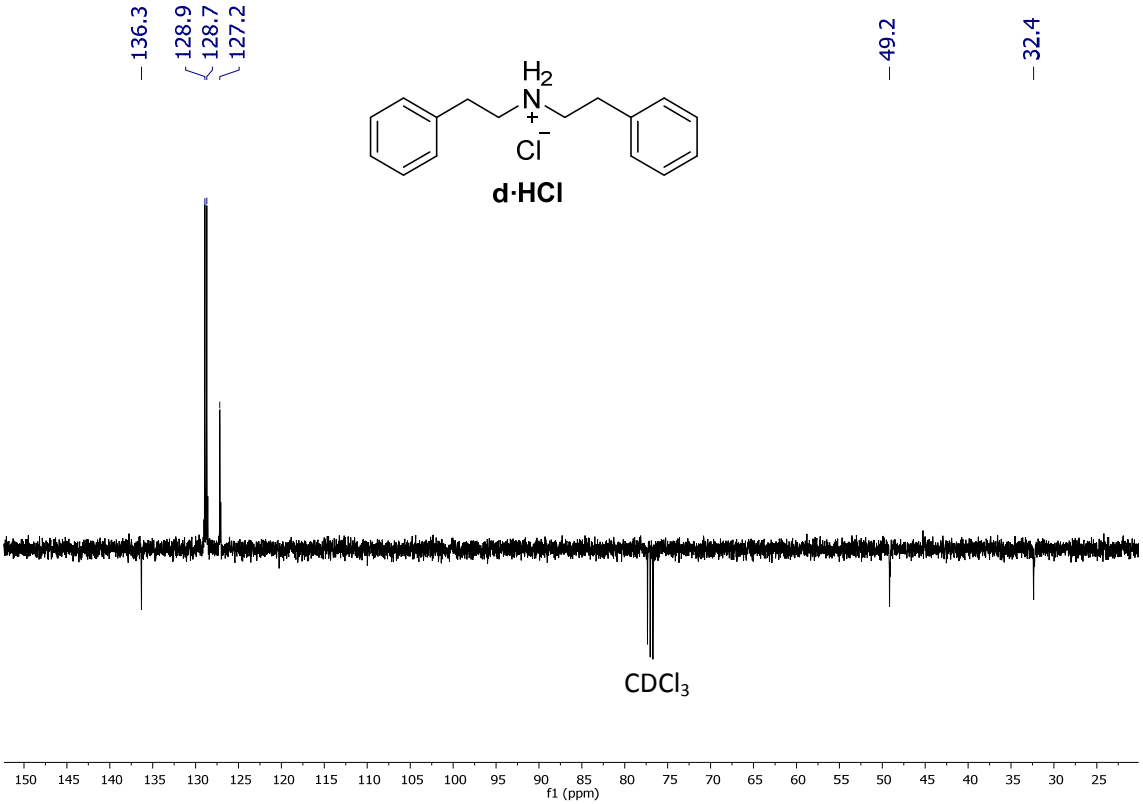

Figure S12. ^{13}C{^{1}H} APT NMR (100.63 MHz, $CDCl_3$, 298 K) spectrum of **d·HCl**.

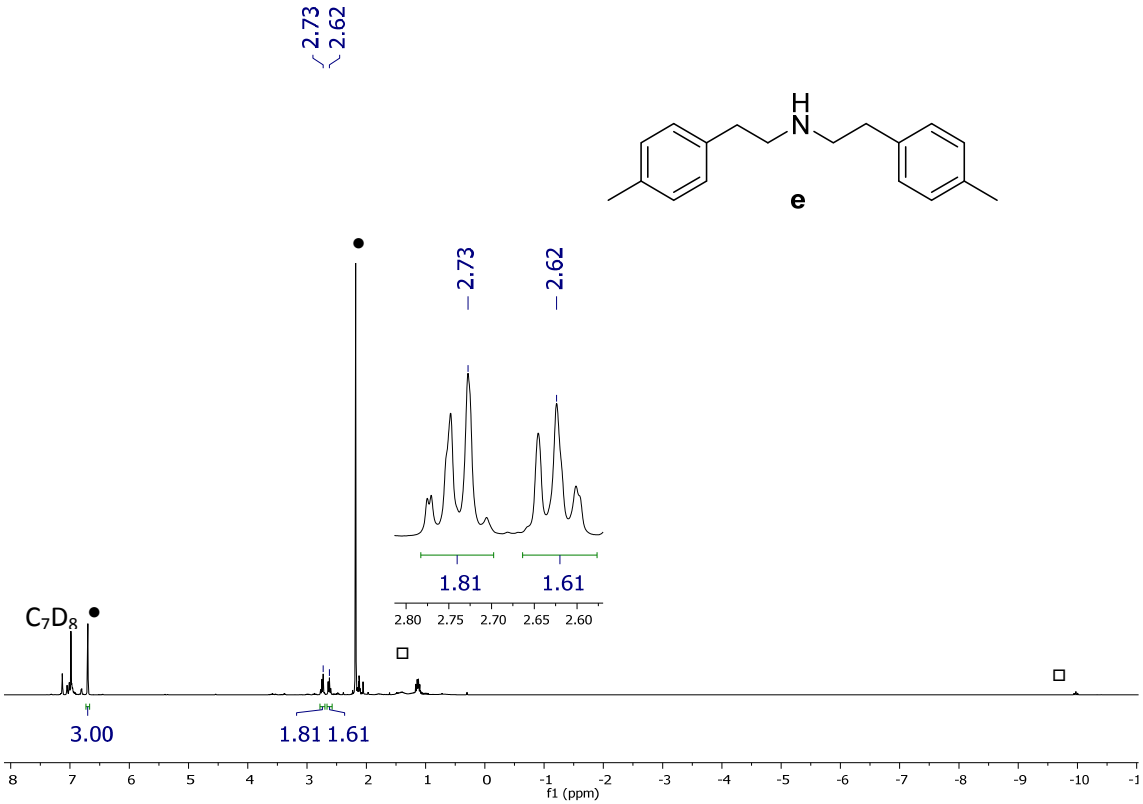

Figure S13. ^{1}H NMR (300.13 MHz, C_7D_8, 298 K) spectrum of the reaction mixture of the hydrogenation of 2-(*p*-tolyl)acetonitrile: formation of bis(4-methylphenethyl)amine (**e**). • Mesitylene. □ $OsH_6(P^iPr_3)_2$ (**1**).

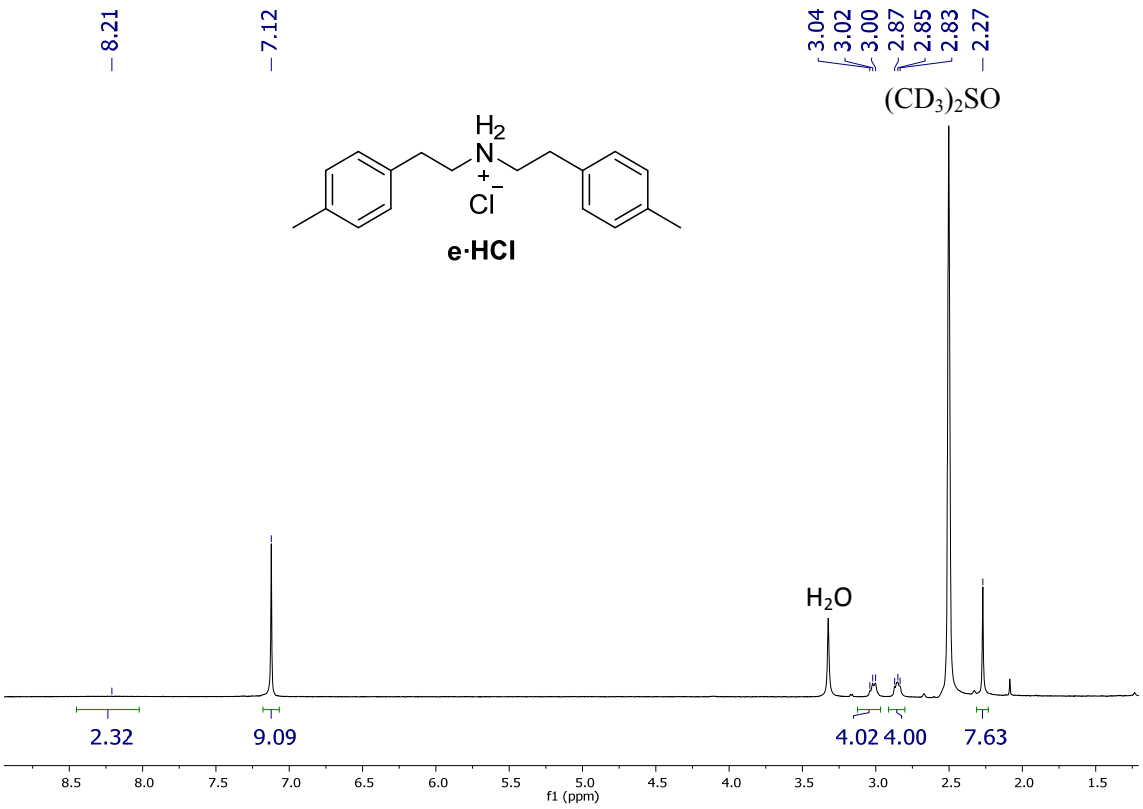

Figure S14. ^{1}H NMR (400.13 MHz, $(CD_3)_2SO$, 298 K) spectrum of **e·HCl**.

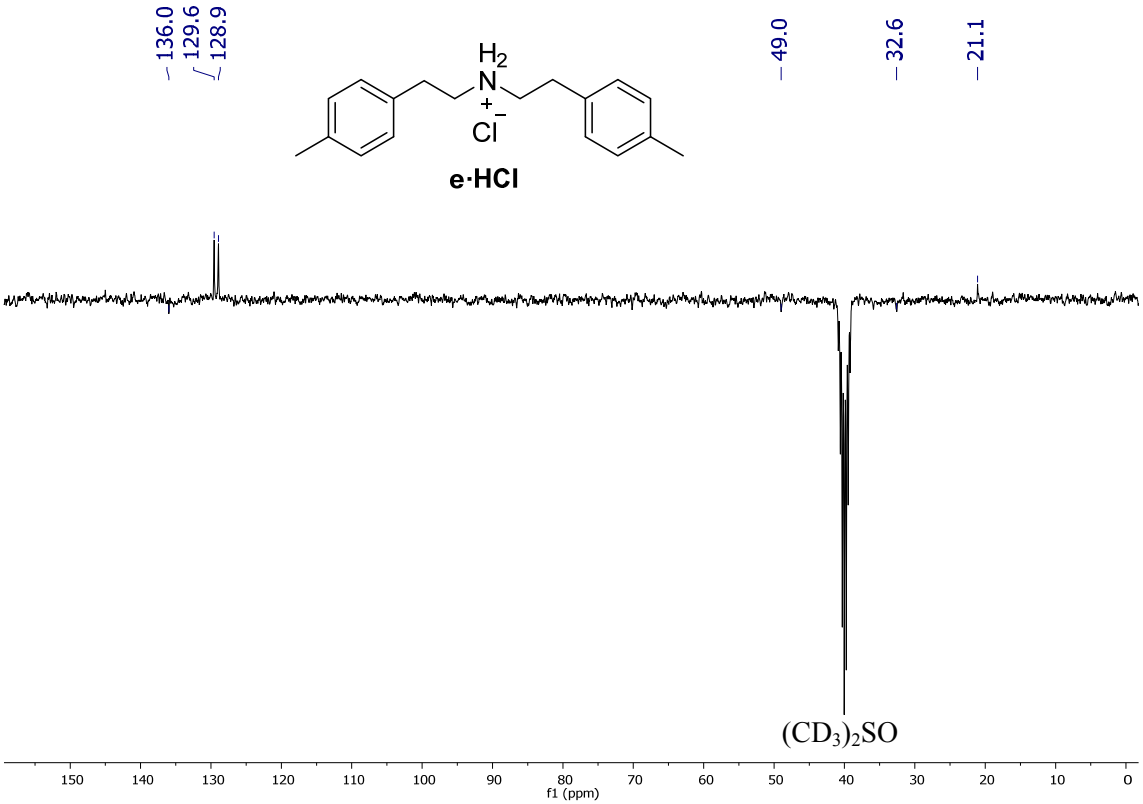

Figure S15. $^{13}C\{^{1}H\}$ APT NMR (75.48 MHz, $(CD_3)_2SO$, 298 K) spectrum of **e·HCl**.

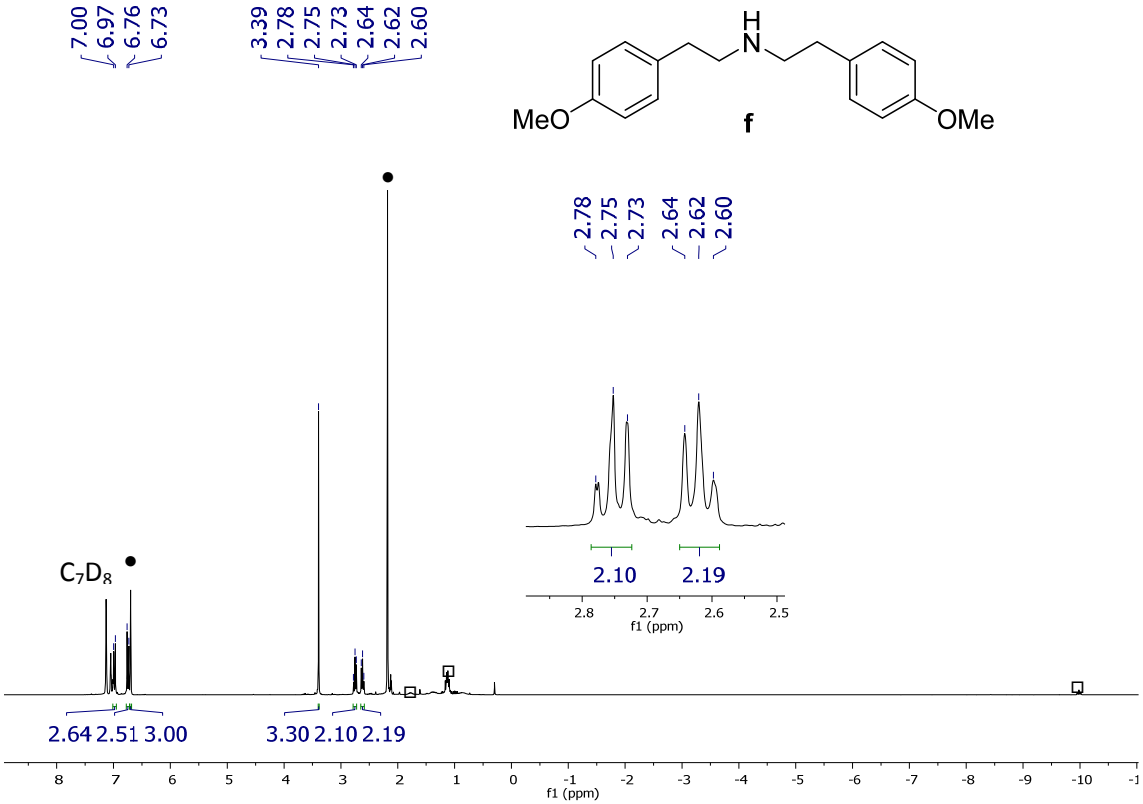

Figure S16. ^{1}H NMR (300.13 MHz, C_7D_8, 298 K) spectrum of the reaction mixture of the hydrogenation of 2-(4-methoxyphenyl)acetonitrile: formation of bis(4-methoxyphenethyl)amine (**f**). • Mesitylene. □ $OsH_6(P^iPr_3)_2$ (**1**).

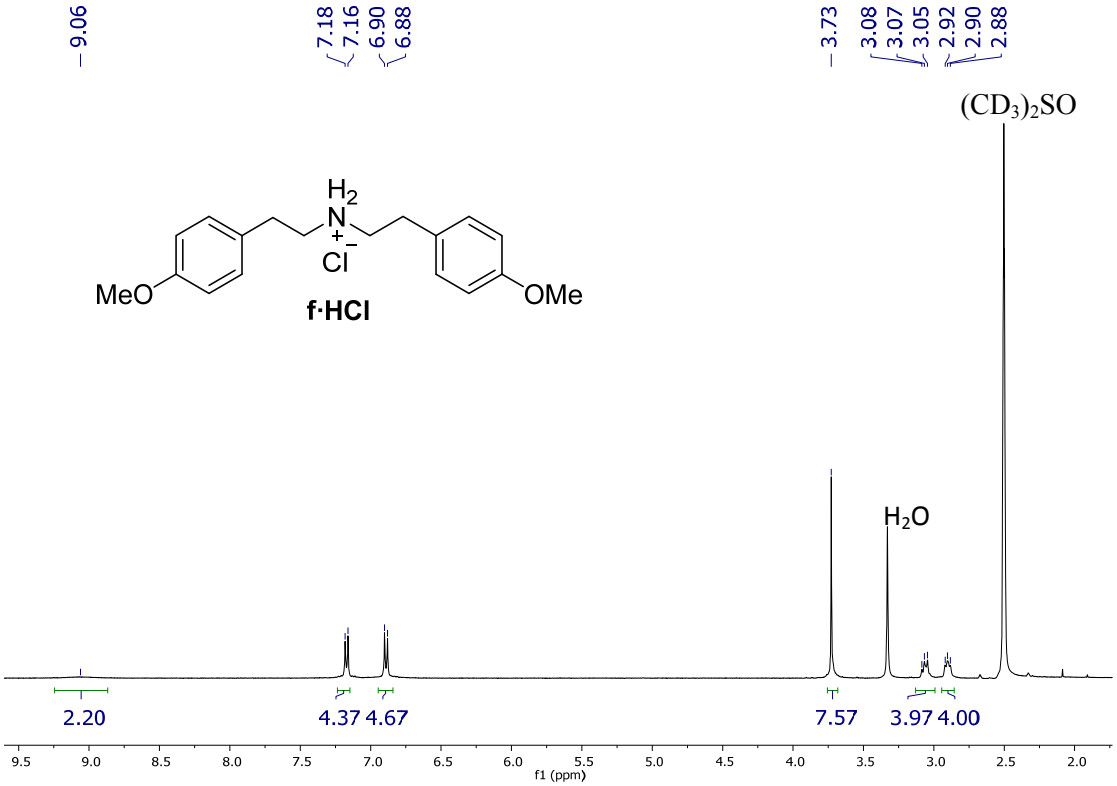

Figure S17. ^{1}H NMR (400.13 MHz, $(CD_3)_2SO$, 298 K) spectrum of **f·HCl**.

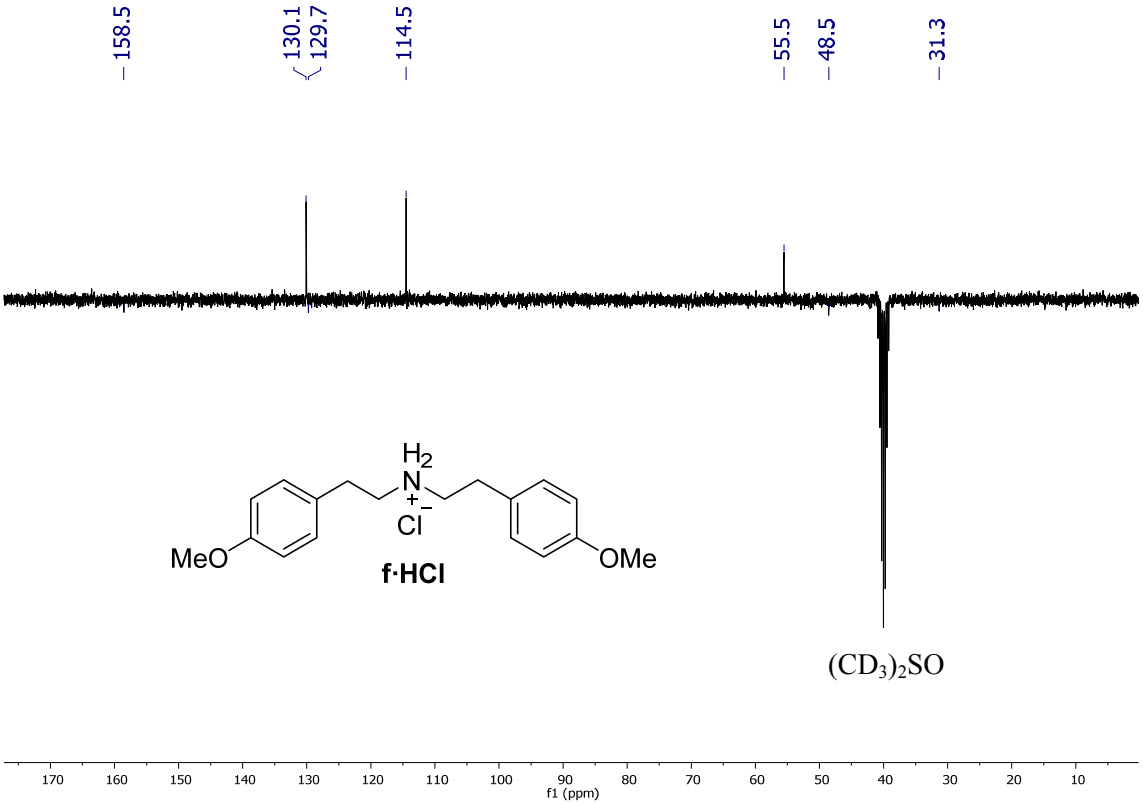

Figure S18. ^{13}C{^{1}H} APT NMR (75.48 MHz, $(CD_3)_2SO$, 298 K) spectrum of **f·HCl.**

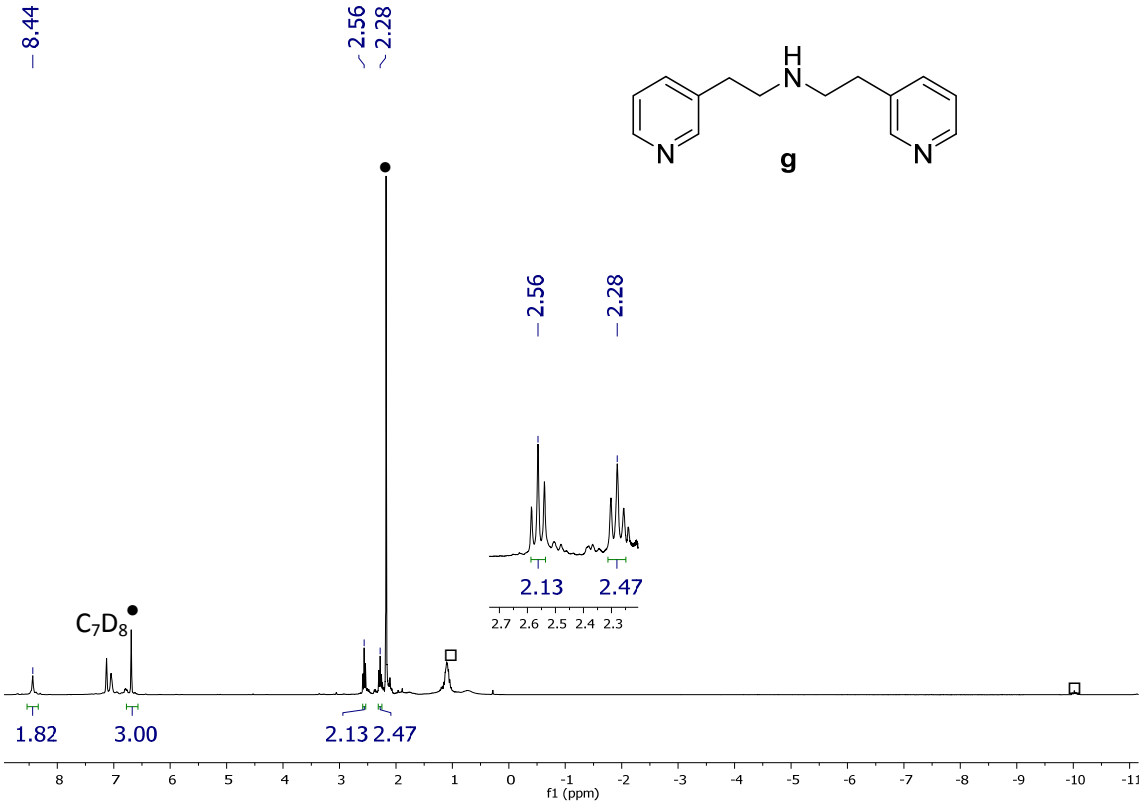

Figure S19. ^{1}H NMR (300.13 MHz, C_7D_8, 298 K) spectrum of the reaction mixture of the hydrogenation of 2-(pyridin-3-yl)acetonitrile: formation of bis(2-(pyridin-3-yl)ethyl)amine (**g**). • Mesitylene. □ $OsH_6(P^iPr_3)_2$ (**1**).

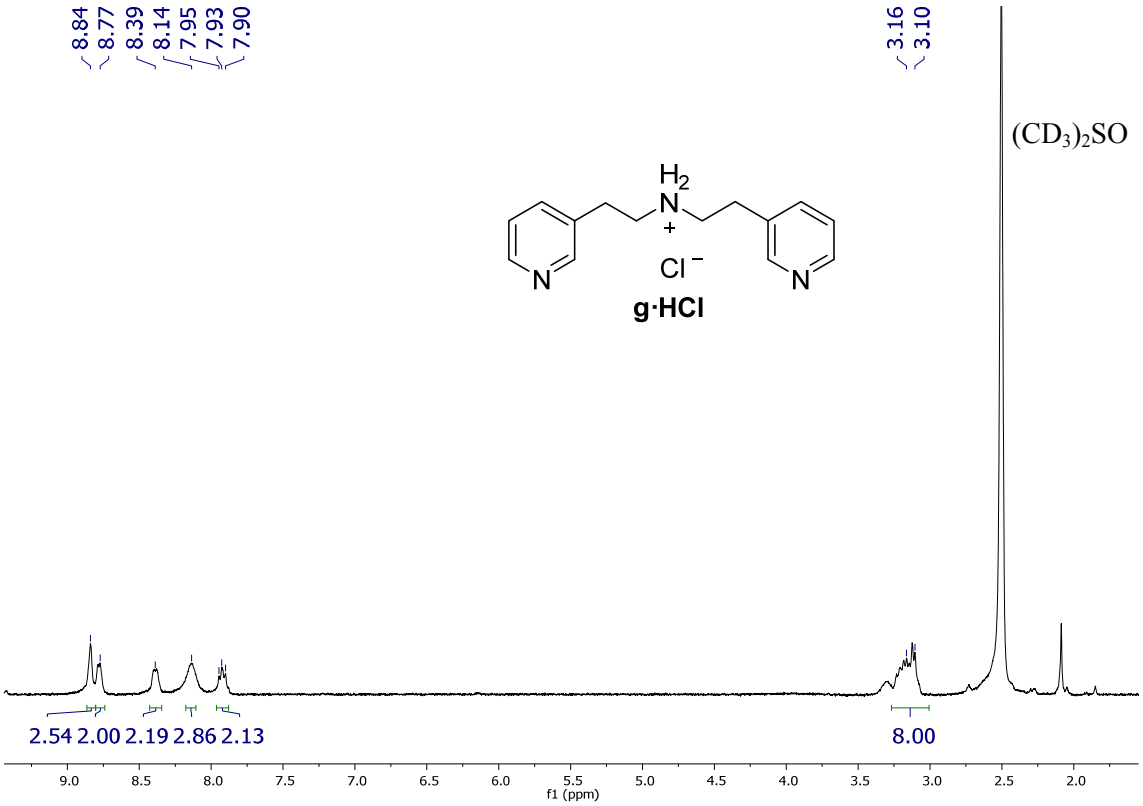

Figure S20. ^{1}H NMR (300.13 MHz, $(CD_3)_2SO$, 298 K) spectrum of **g·HCl**.

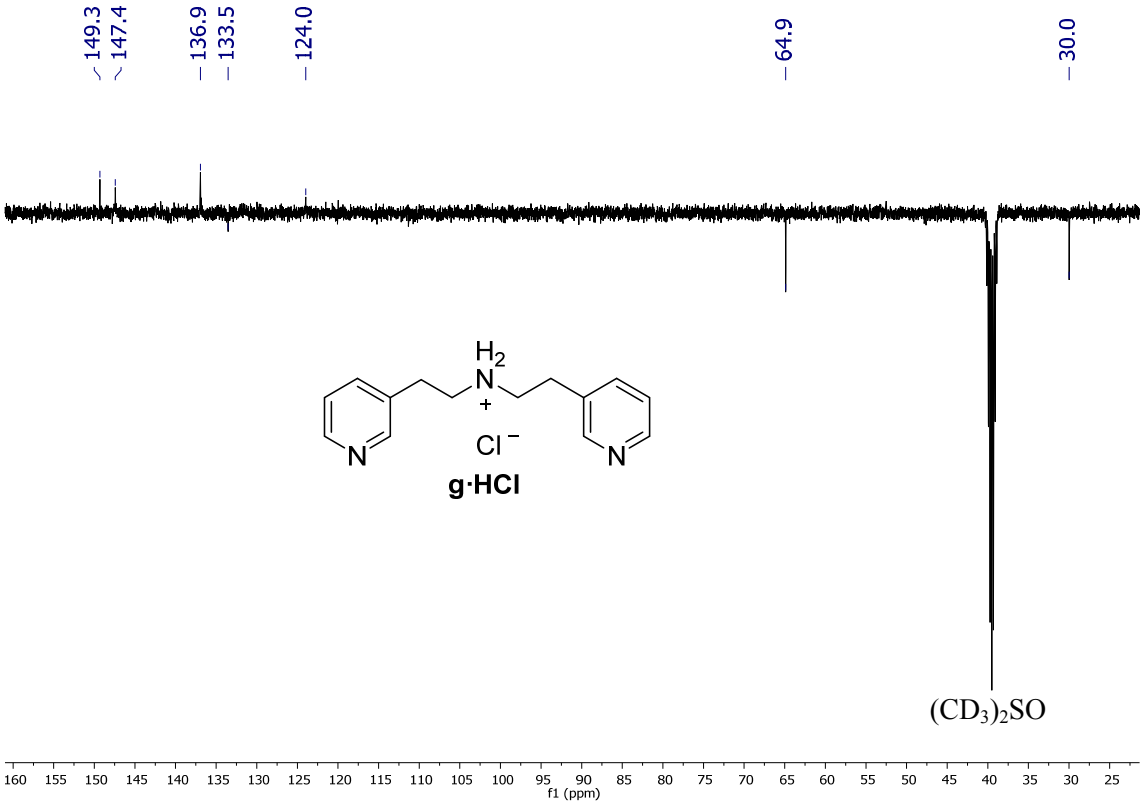

Figure S21. $^{13}C\{^{1}H\}$ APT NMR (100.63 MHz, $(CD_3)_2SO$, 298 K) spectrum of **g·HCl.**

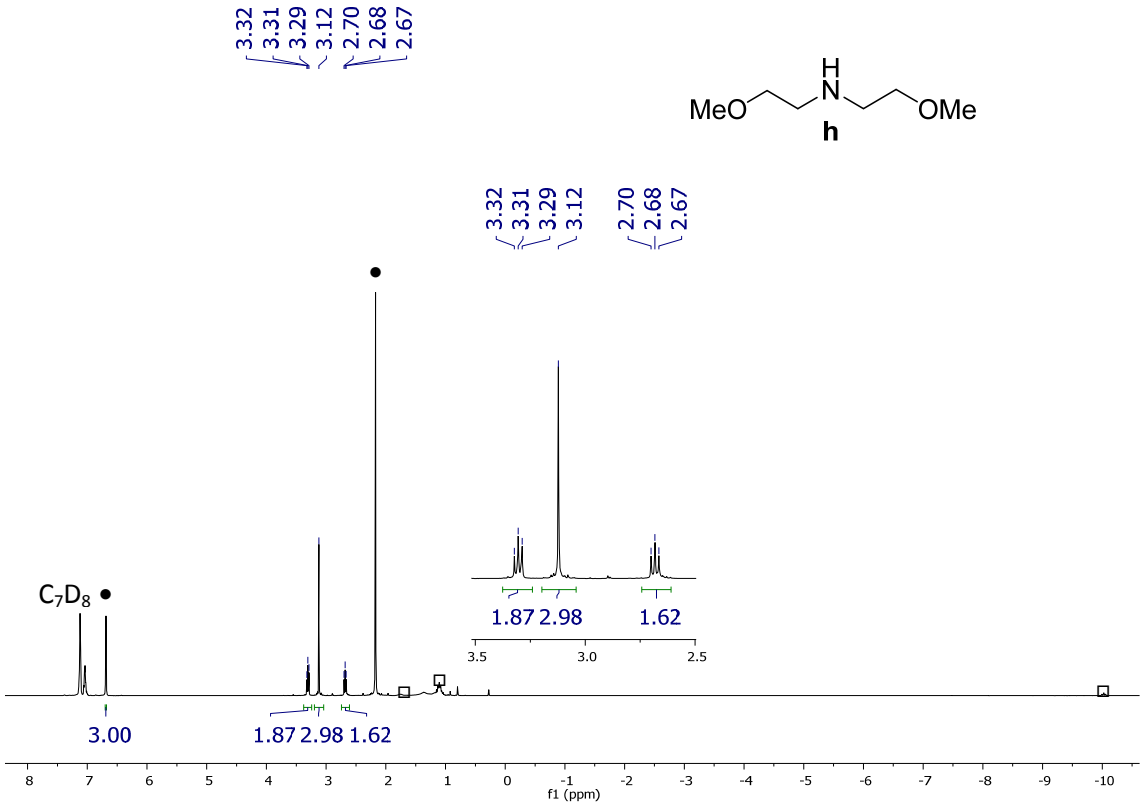

Figure S22. ^{1}H NMR (300.13 MHz, C_7D_8, 298 K) spectrum of reaction mixture of the hydrogenation of 2-methoxyacetonitrile: formation of bis(2-methoxyethyl)amine (**h**)[17]. • Mesitylene. □ $OsH_6(P^iPr_3)_2$ (**1**).

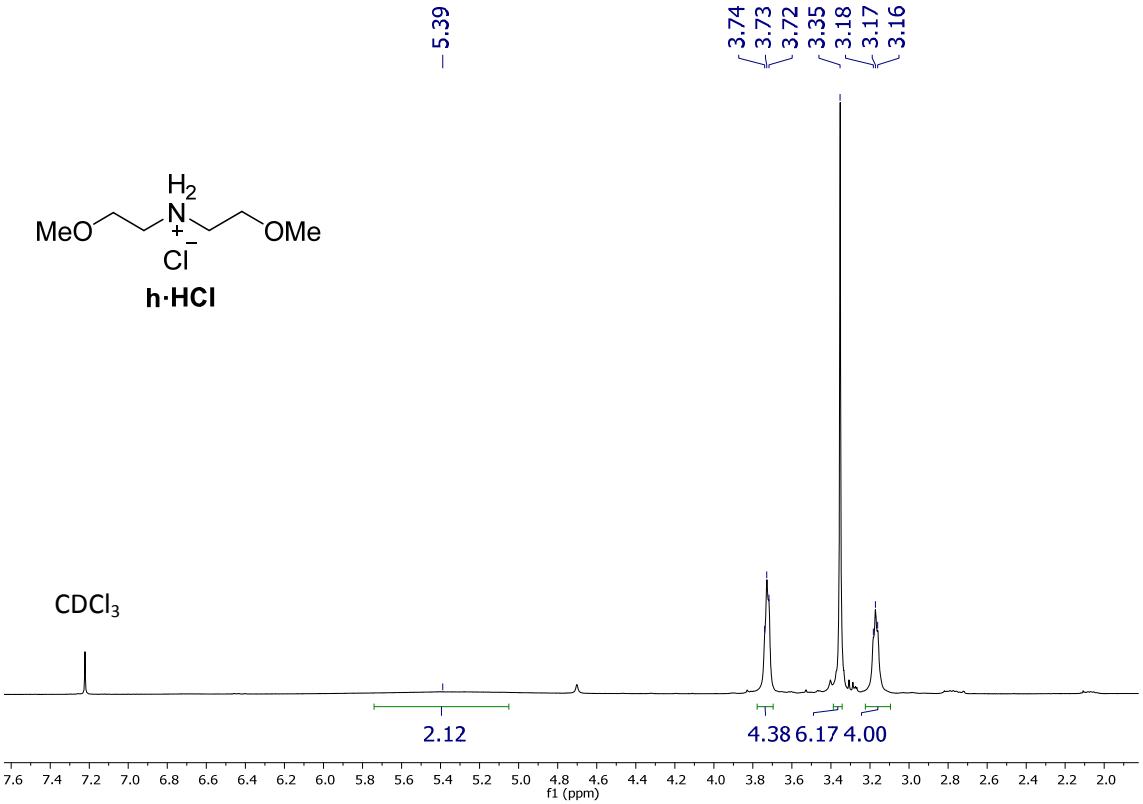

Figure S23. ^{1}H NMR (400.16 MHz, $CDCl_3$, 298 K) spectrum of **h·HCl**.

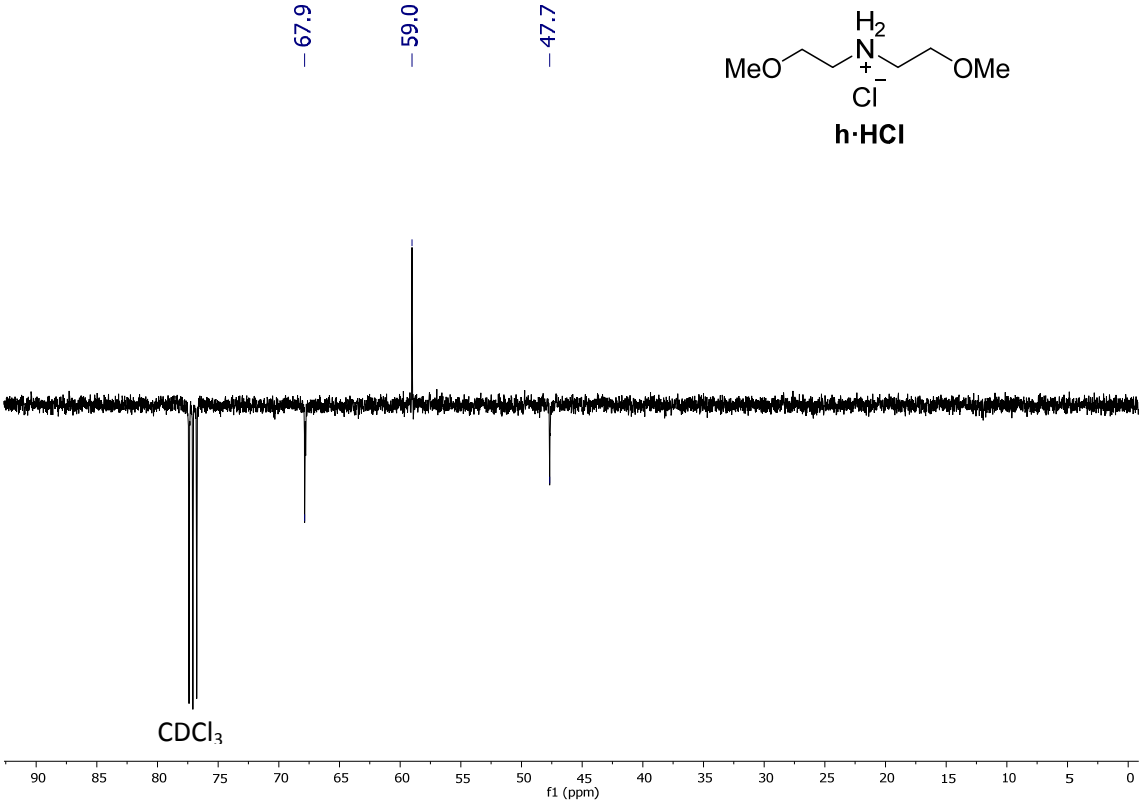

Figure S24. ^{13}C{^{1}H} APT NMR (100.63 MHz, $CDCl_3$, 298 K) spectrum of **h·HCl**.

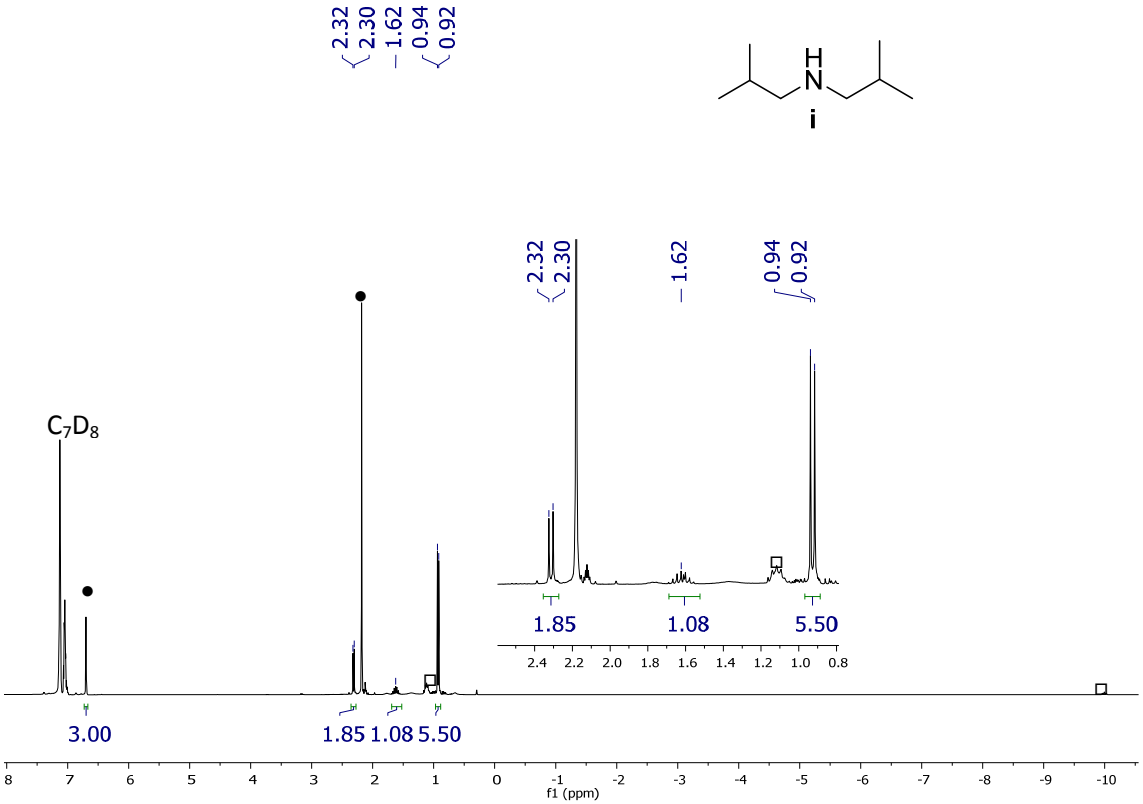

Figure S25. ^{1}H NMR (300.13 MHz, C_7D_8, 298 K) spectrum of the reaction mixture of the hydrogenation of isobutyronitrile: formation of diisobutylamine (**i**). • Mesitylene. □ $OsH_6(P^iPr_3)_2$ (**1**).

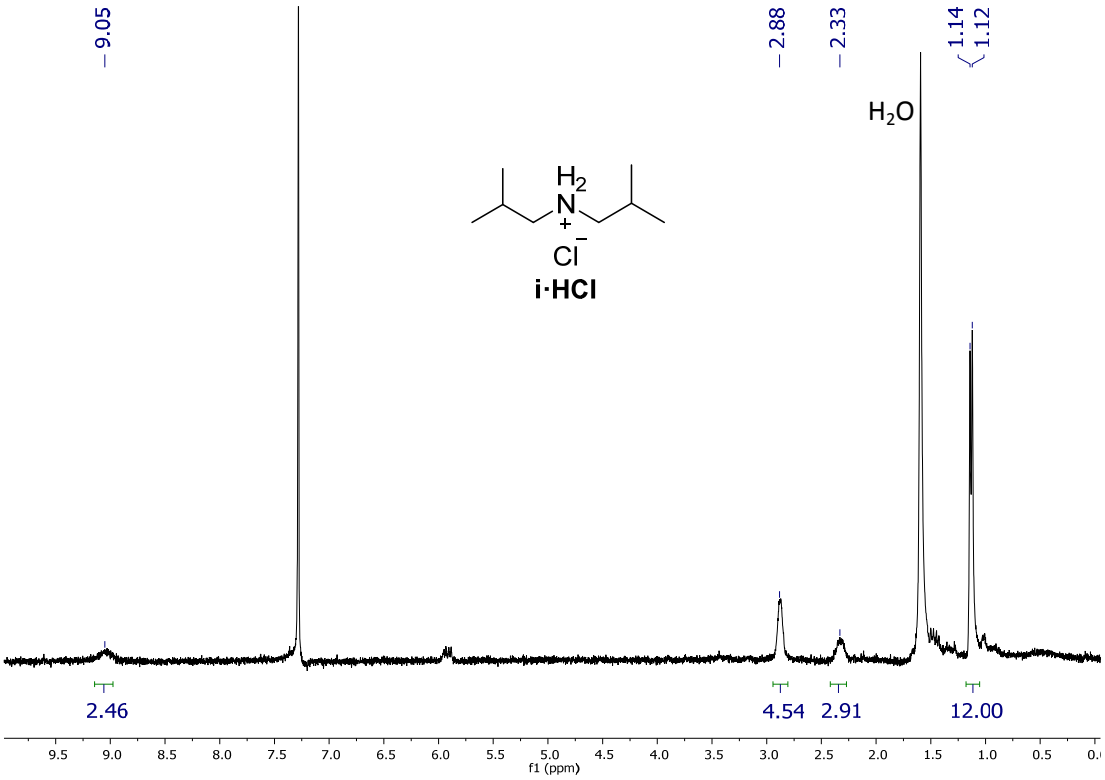

Figure S26. ^{1}H NMR (300.13 MHz, $CDCl_3$, 298 K) spectrum of **i·HCl**.

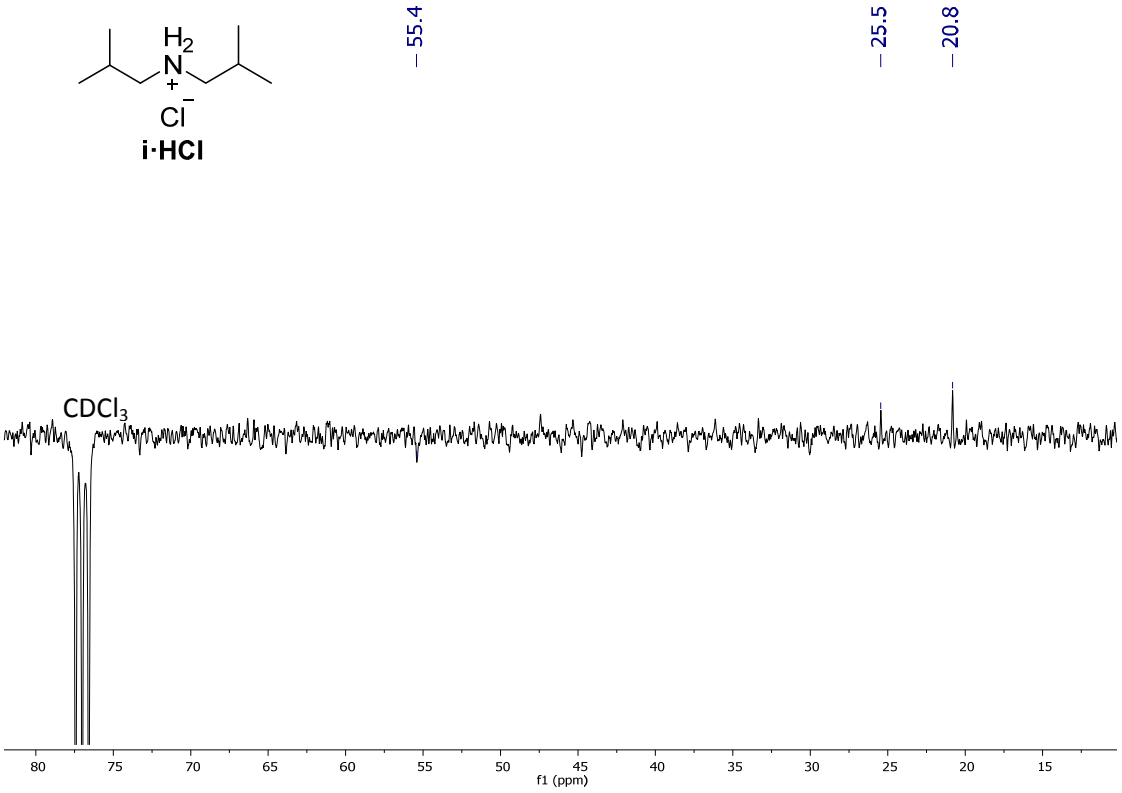

Figure S27. $^{13}C\{^{1}H\}$ APT NMR (75.48 MHz, $CDCl_3$, 298 K) spectrum of **i·HCl.**

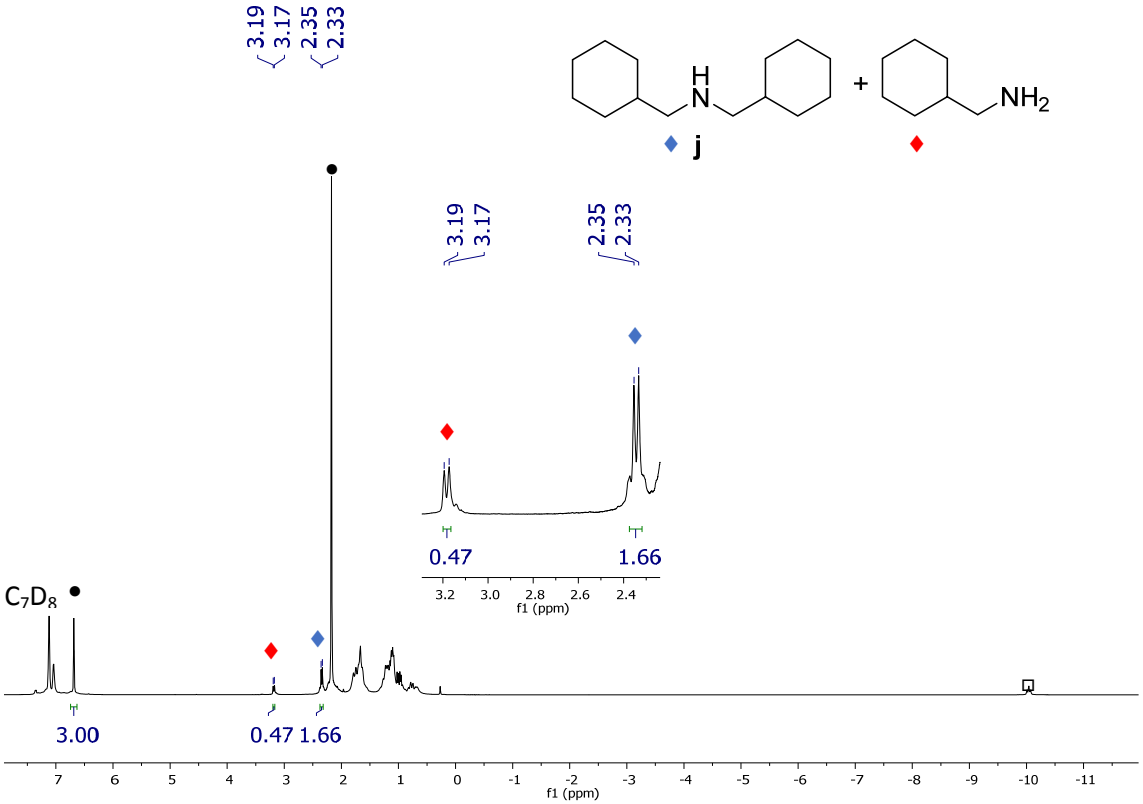

Figure S28. ^{1}H NMR (300.13 MHz, C_7D_8, 298 K) spectrum of reaction mixture of the hydrogenation of cyclohexanecarbonitrile: formation of bis(cyclohexylmethyl)amine (**j**)[15] (♦) and cyclohexylmethanamine (♦). • Mesitylene. □ $OsH_6(P^iPr_3)_2$ (**1**).

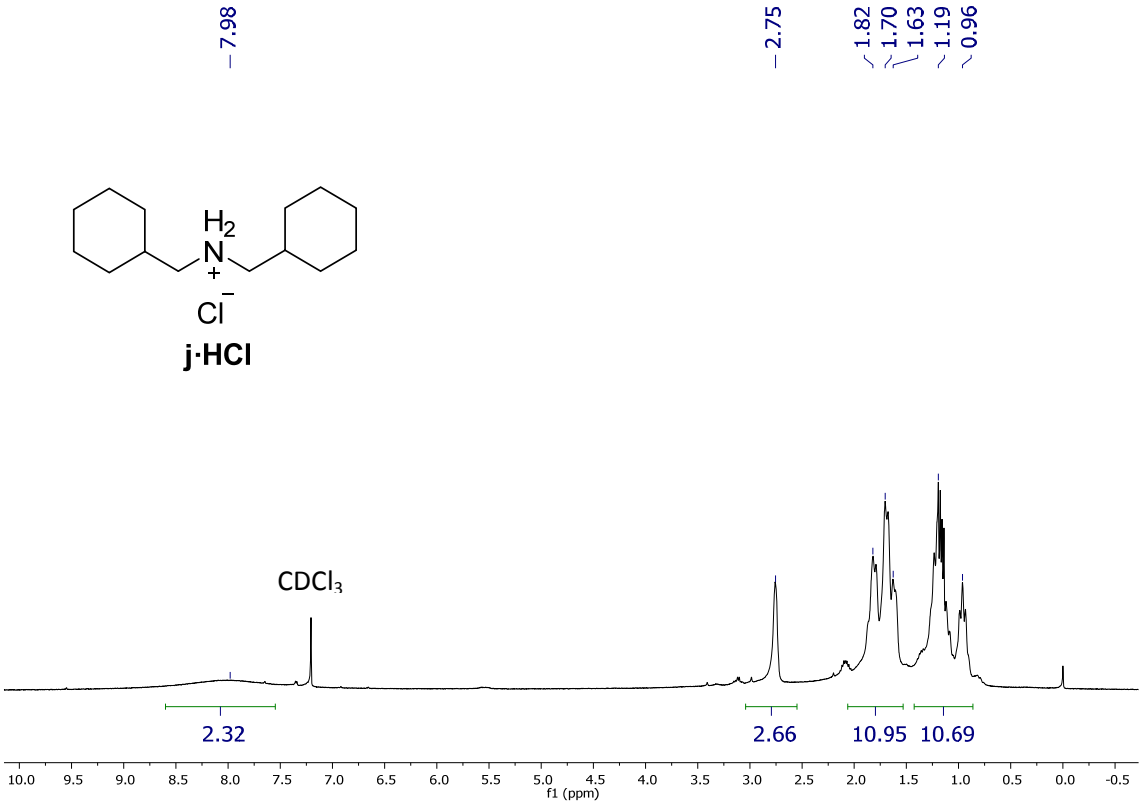

Figure S29. ^{1}H NMR (400.13 MHz, $CDCl_3$, 298 K) spectrum of **j·HCl**.

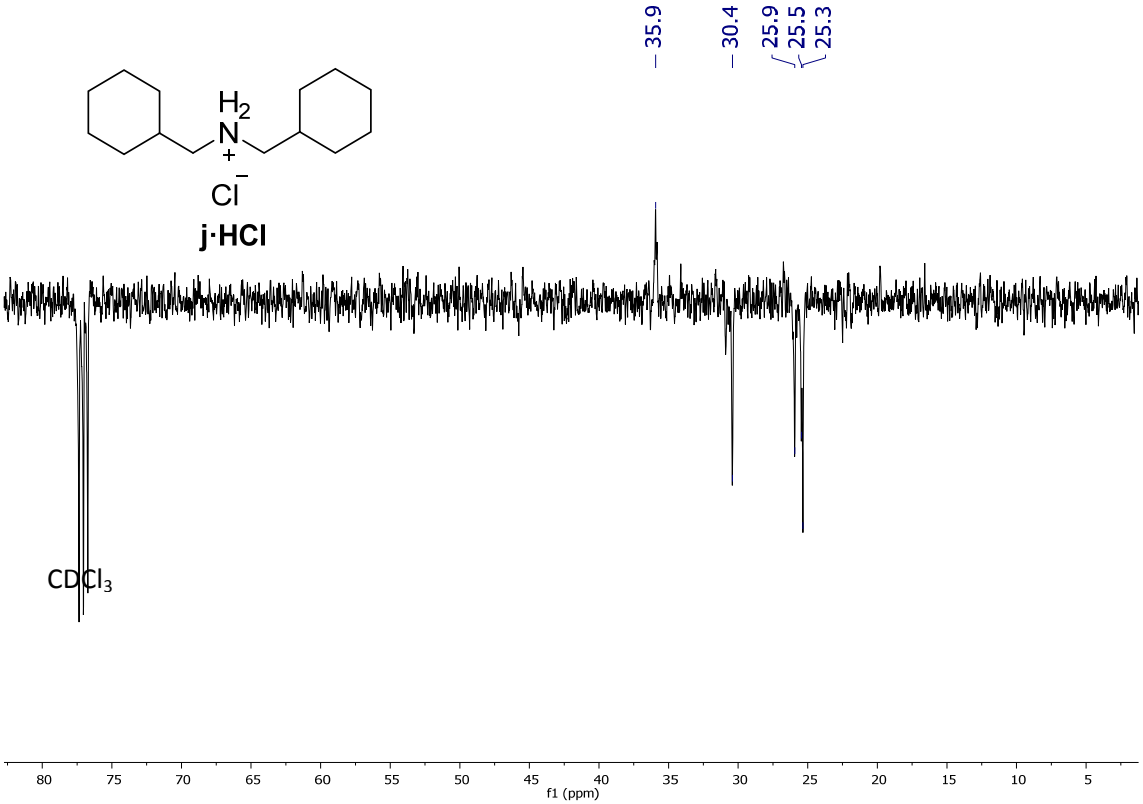

Figure S30. ^{13}C{^{1}H} APT NMR (100.63 MHz, $CDCl_3$, 298 K) spectrum of **j·HCl**.

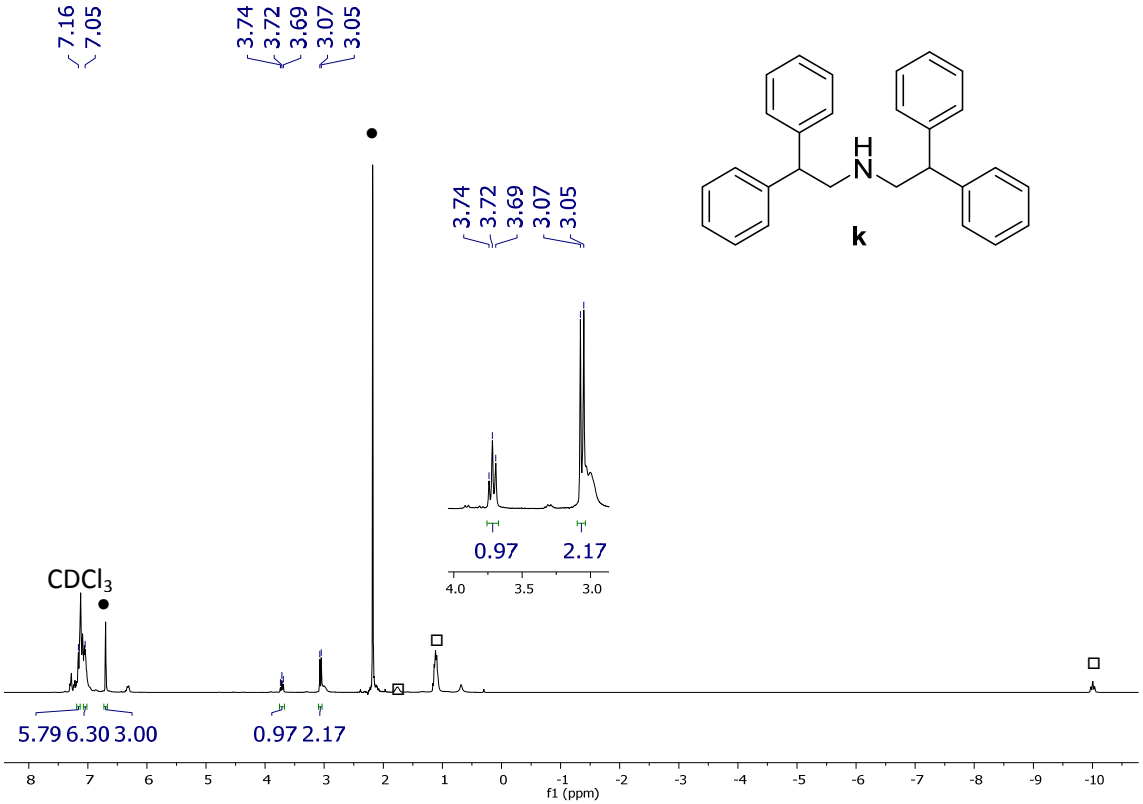

Figure S31. ^{1}H NMR (300.13 MHz, C_7D_8, 298 K) spectrum of the reaction mixture of the hydrogenation of 2,2-diphenylacetonitrile: formation of bis(2,2-diphenylethyl)amine (**k**). • Mesitylene. □ $OsH_6(P^iPr_3)_2$ (**1**).

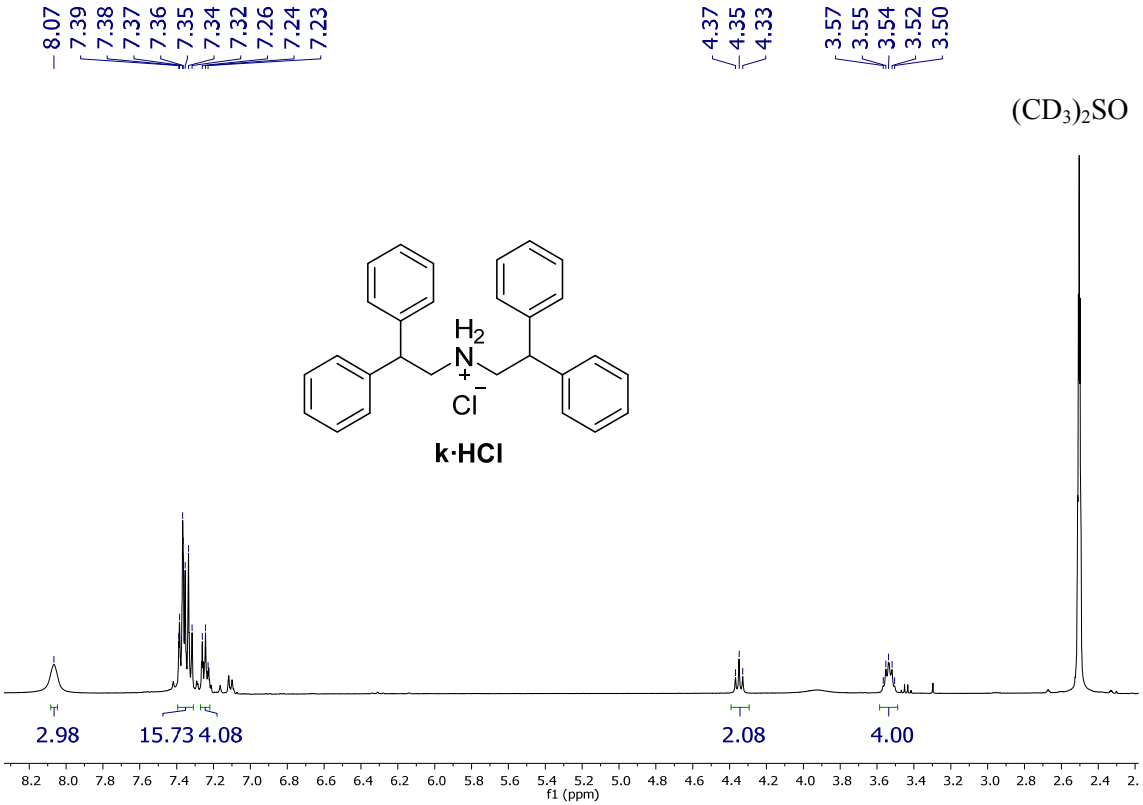

Figure S32. ^{1}H NMR (400.13 MHz, $(CD_3)_2SO$, 298 K) spectrum of **k·HCl**.

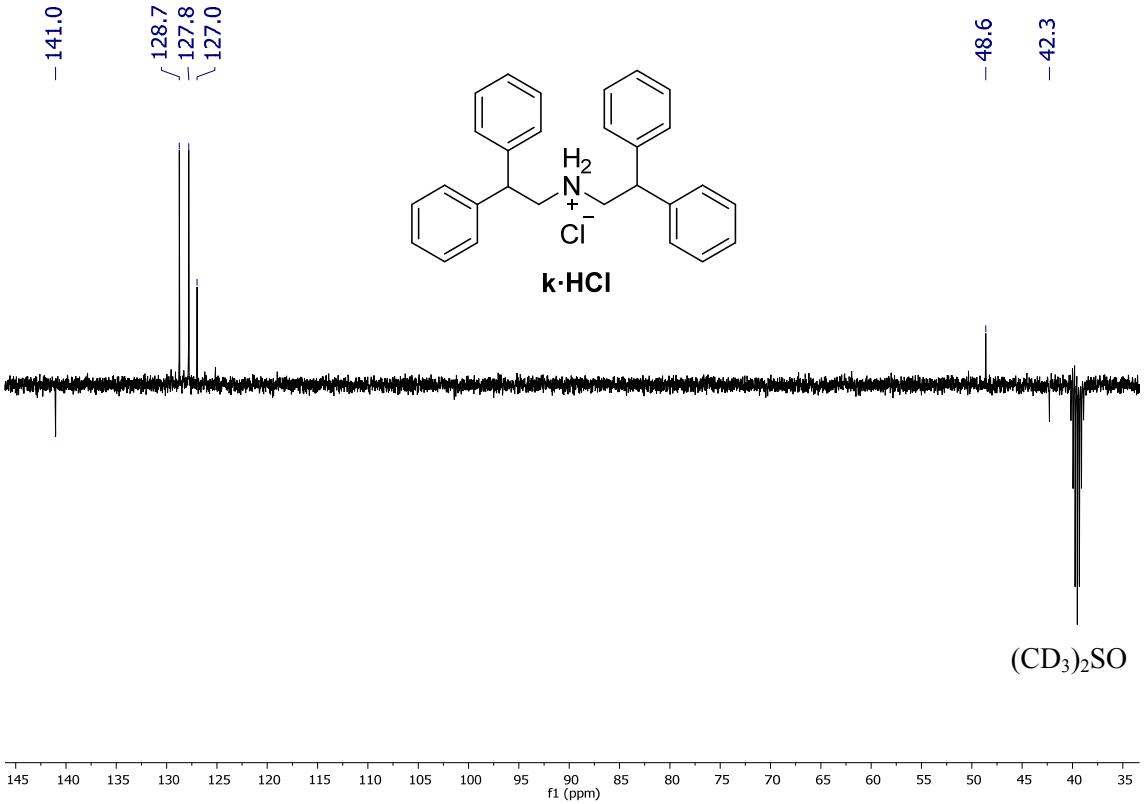

Figure S33. $^{13}C\{^{1}H\}$ APT NMR (100.63 MHz, $(CD_3)_2SO$, 298 K) spectrum of **k·HCl**.

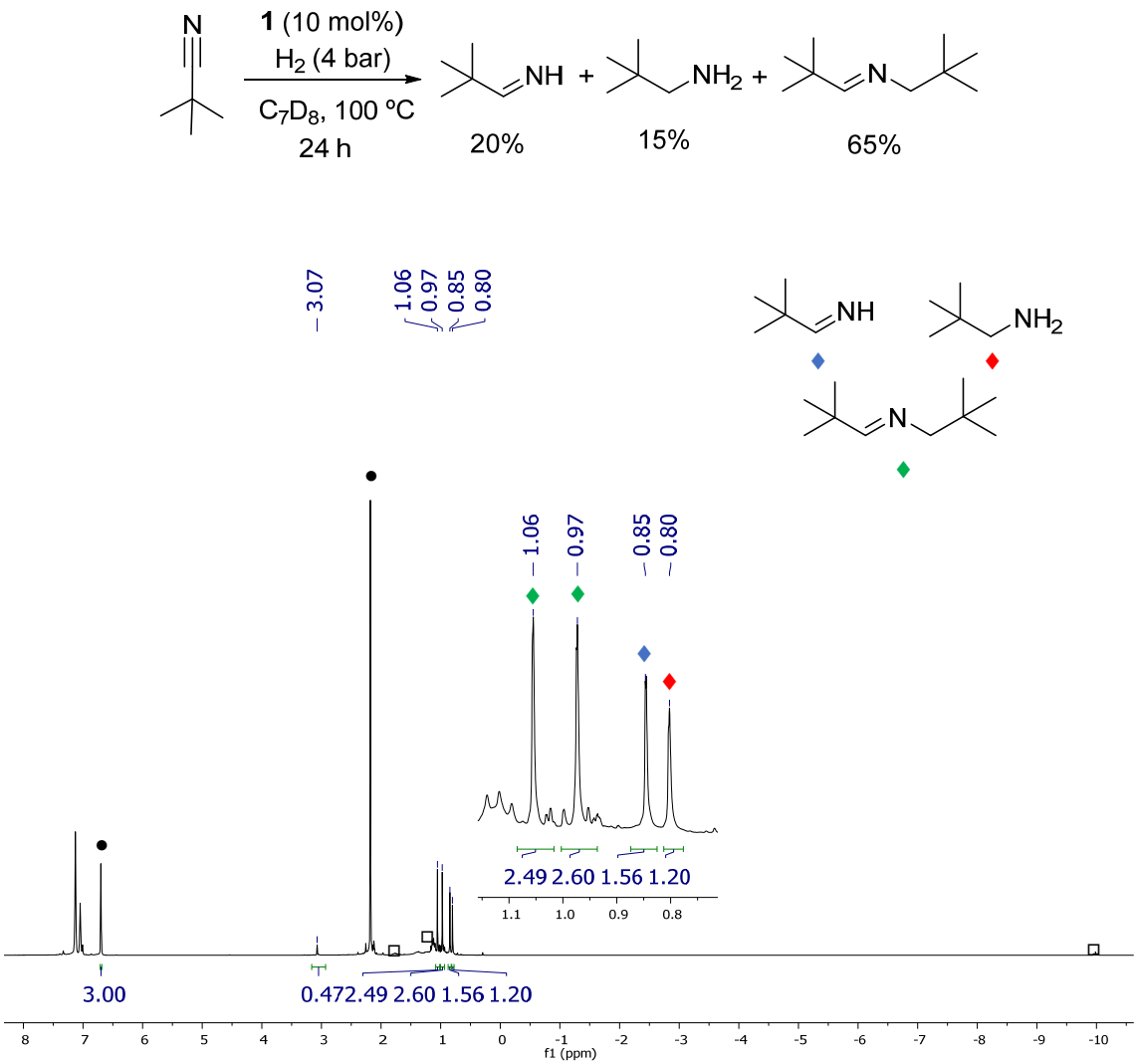

Figure S34. ^{1}H NMR (300.13 MHz, C_7D_8, 298 K) spectrum of the reaction mixture of the catalytic hydrogenation of pivalonitrile after 24 h at 100 ºC with 10% mol **1**: Formation of 2,2-dimethylpropan-1-amine (♦), 2,2-dimethylpropan-1-imine (♦) and 2,2-dimethyl-*N*-neopentylpropan-1-imine (♦). • Mesitylene. □ $OsH_6(P^iPr_3)_2$ (**1**).

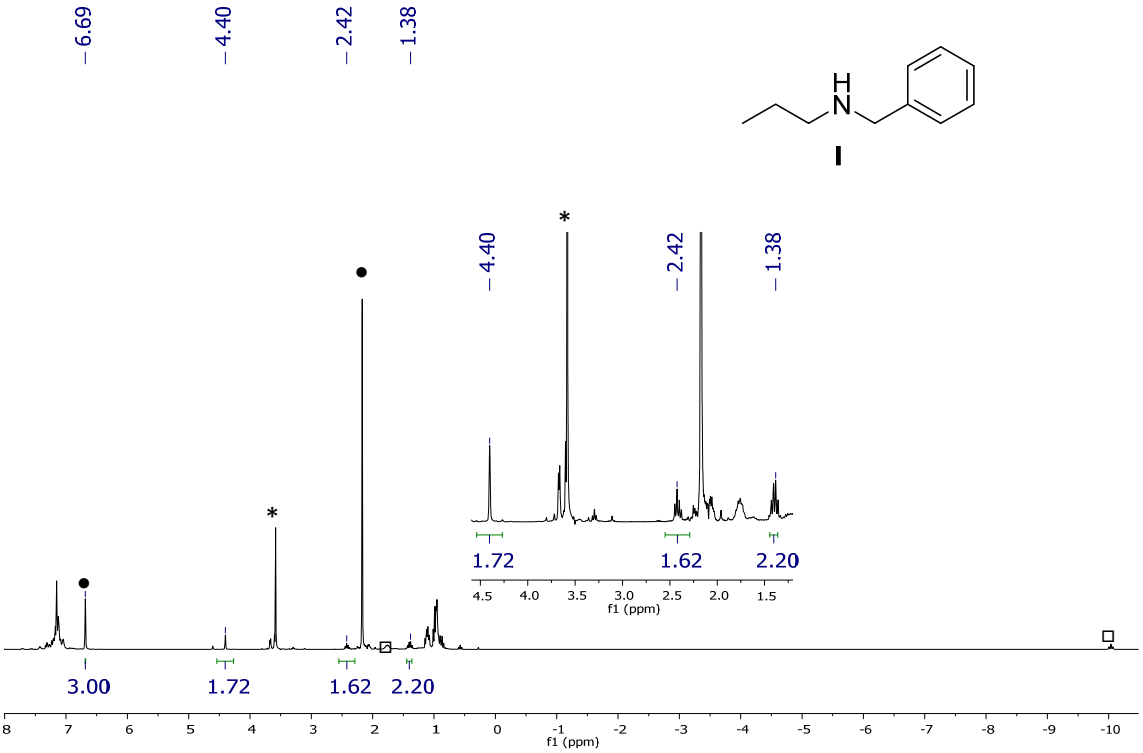

Figure S35. ^{1}H NMR (300.13 MHz, C_7D_8, 298 K) spectrum of the reaction mixture of the hydrogenation of propionitrile in the presence of benzylamine: formation of *N*-benzylpropan-1-amine (**l**).[18] • Mesitylene. □ $OsH_6(P^iPr_3)_2$ (**1**). * Excess of benzylamine.

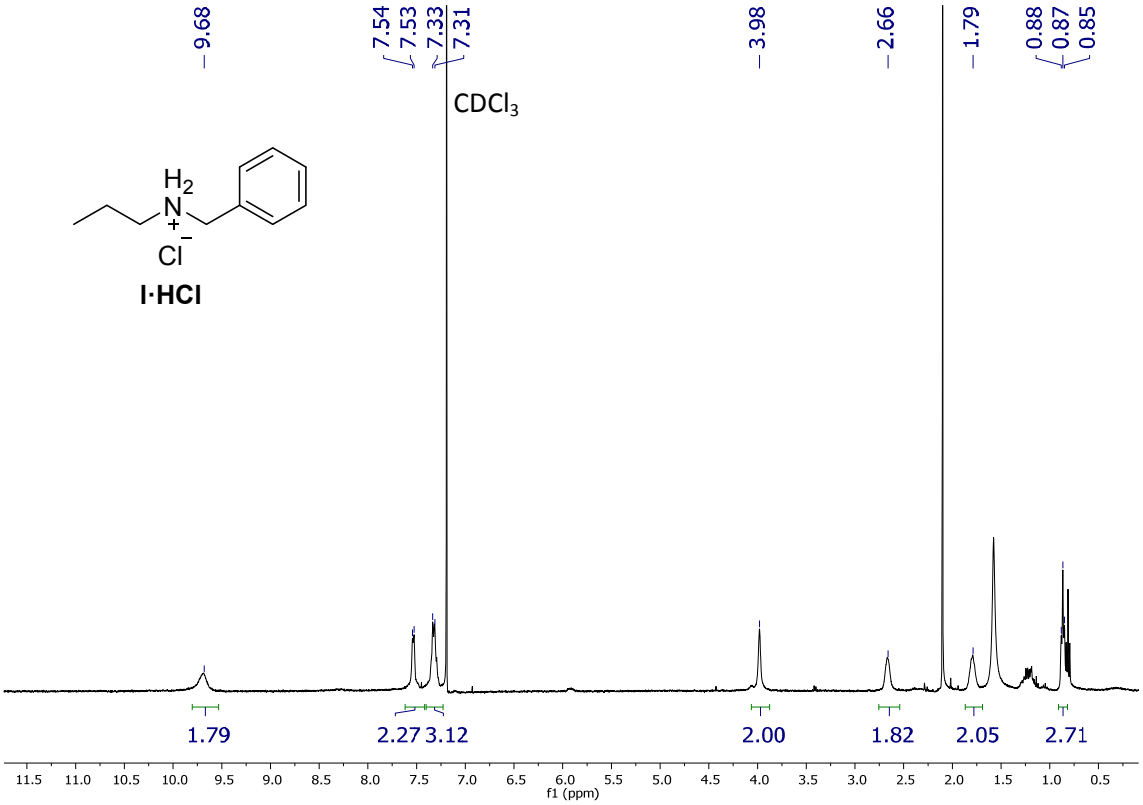

Figure S36. ^{1}H NMR (400.16 MHz, $CDCl_3$, 298 K) spectrum of **l·HCl**.

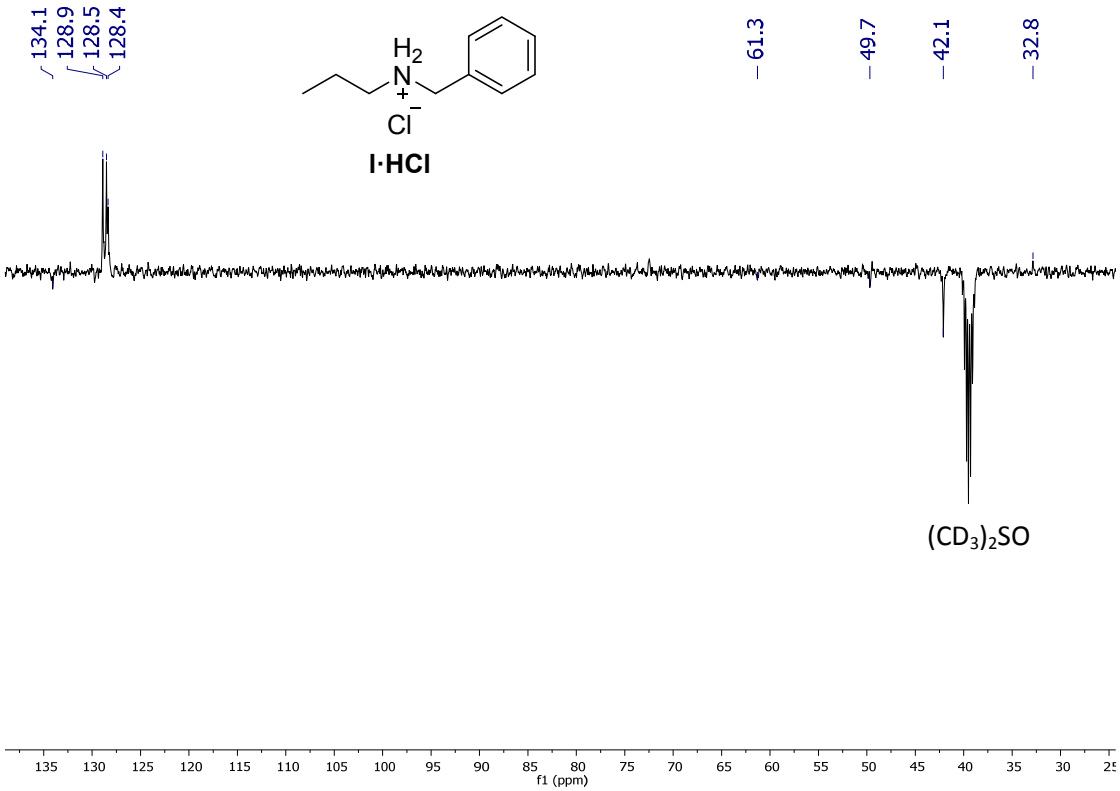

Figure S37. $^{13}C\{^{1}H\}$ APT NMR (100.63 MHz, $(CD_3)_2SO$, 298 K) spectrum of **l·HCl.**

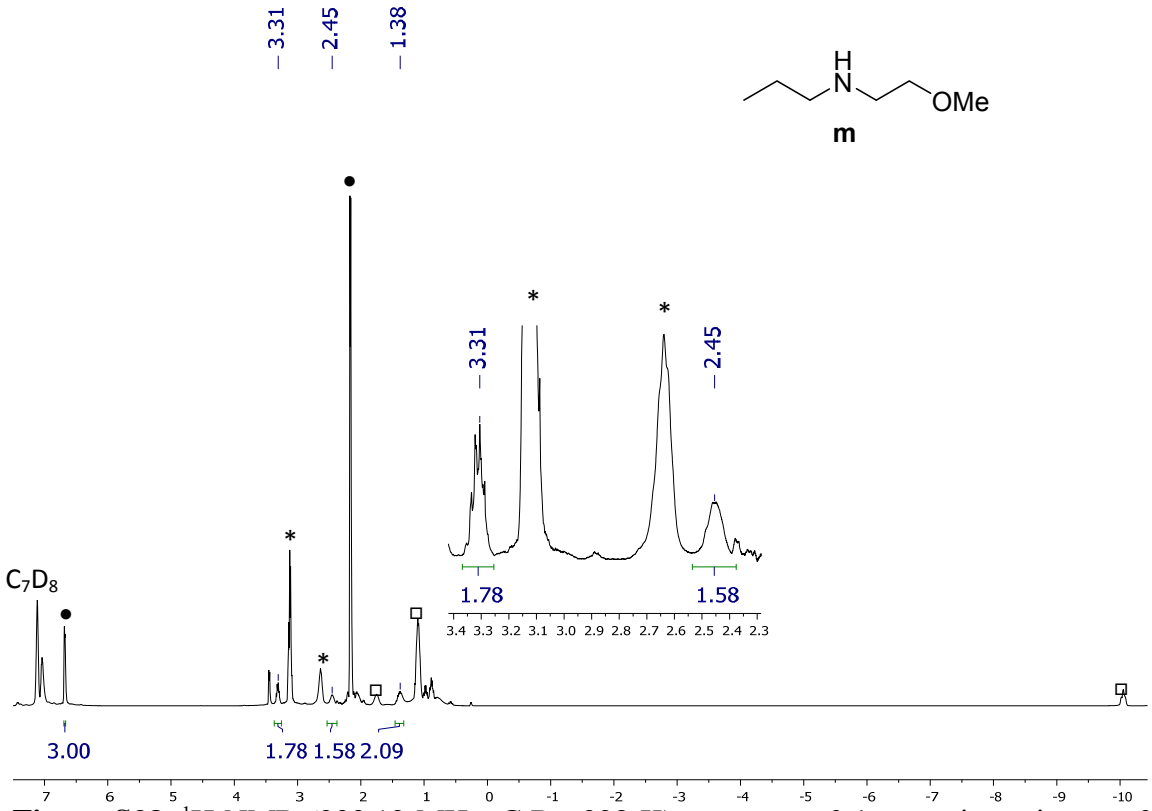

Figure S38. ^{1}H NMR (300.13 MHz, C_7D_8, 298 K) spectrum of the reaction mixture of the hydrogenation of propionitrile in the presence of 2-methoxyethan-1-amine: formation of *N*-(2-methoxyethyl)propan-1-amine (**m**). • Mesitylene. □ $OsH_6(P^iPr_3)_2$ (**1**). *Excess of 2-methoxyethan-1-amine.

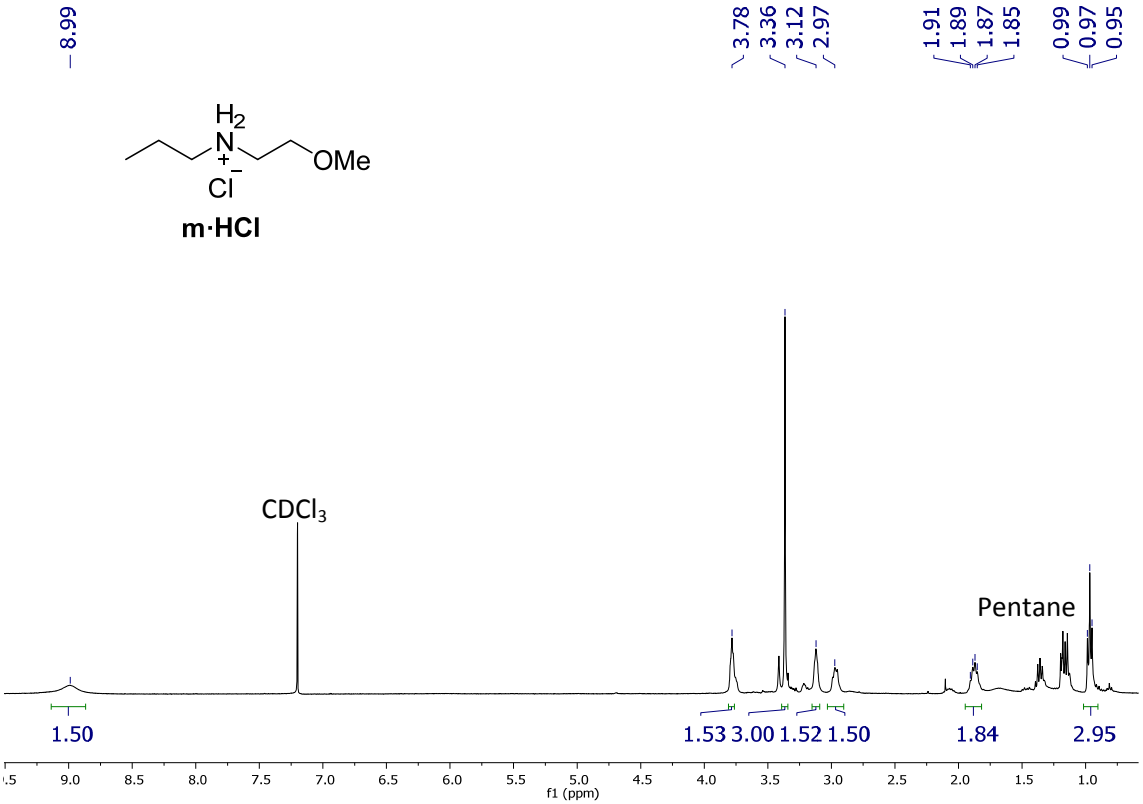

Figure S39. ^{1}H NMR (400.16 MHz, $CDCl_3$, 298 K) spectrum of **m·HCl**.

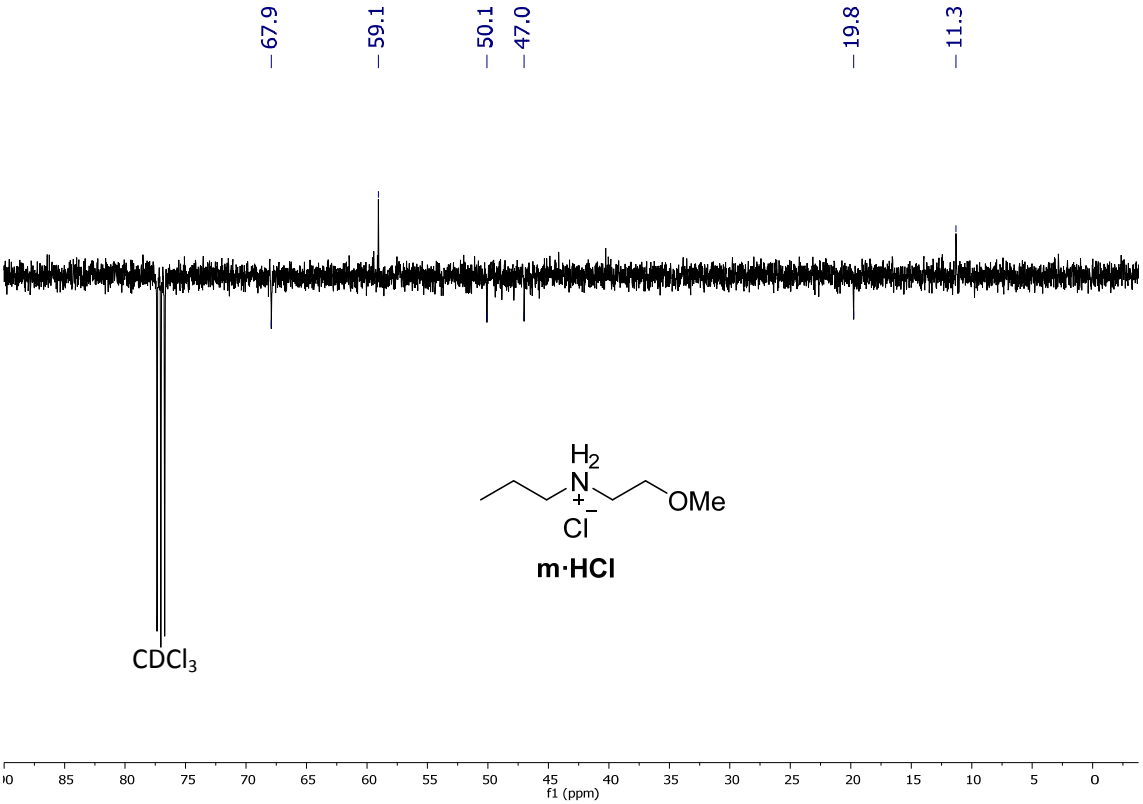

Figure S40. ^{13}C{^{1}H} APT NMR (100.63 MHz, $CDCl_3$, 298 K) spectrum of **m·HCl**.

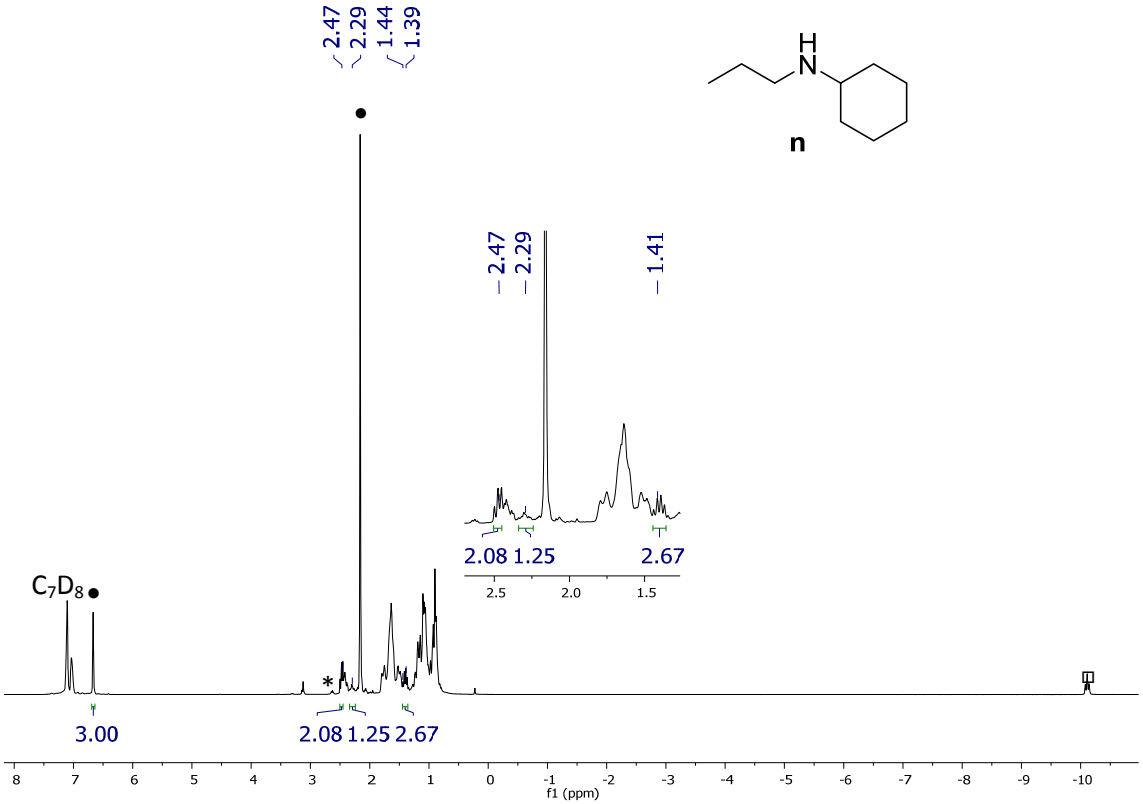

Figure S41. ^{1}H NMR (300.13 MHz, C_7D_8, 298 K) spectrum of the reaction mixture of the hydrogenation of butyronitrile in the presence of cyclohexylamine: formation of *N*-propylcyclohexanamine (**n**).[19] • Mesitylene. □ $OsH_6(P^iPr_3)_2$ (**1**). *Excess of cyclohexylamine.

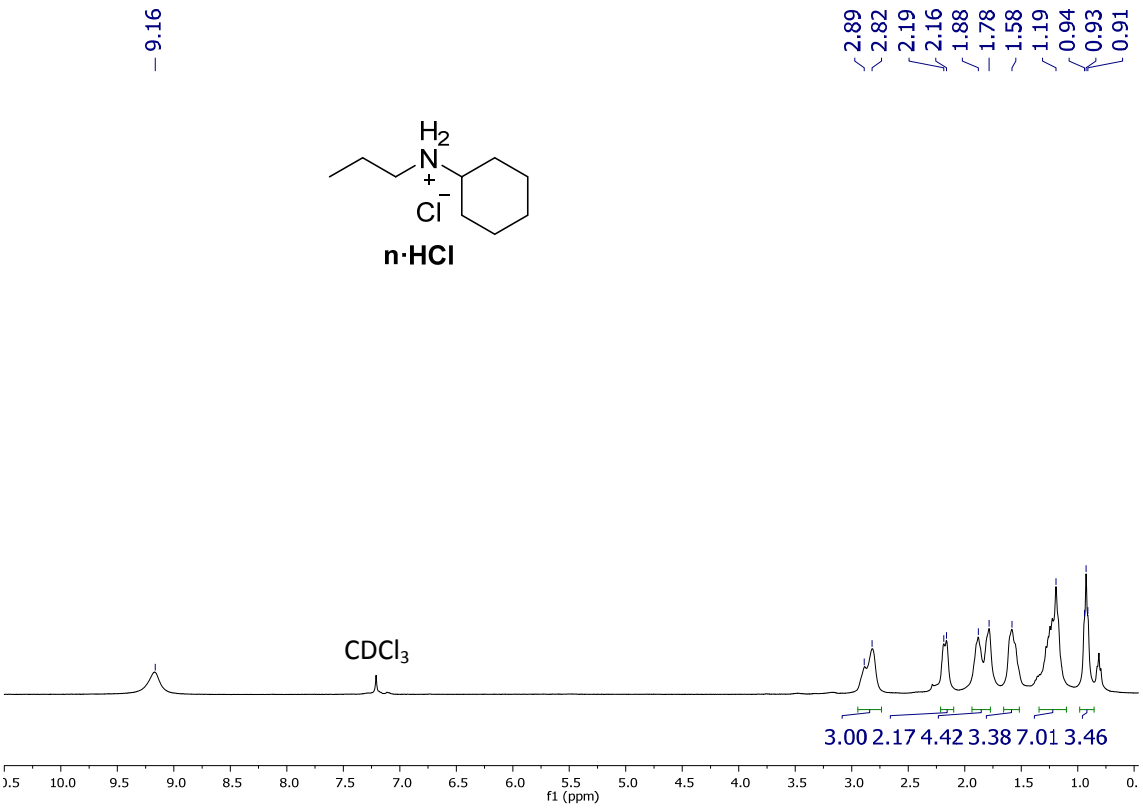

Figure S42. ^{1}H NMR (400.16 MHz, $CDCl_3$, 298 K) spectrum of **n·HCl**.

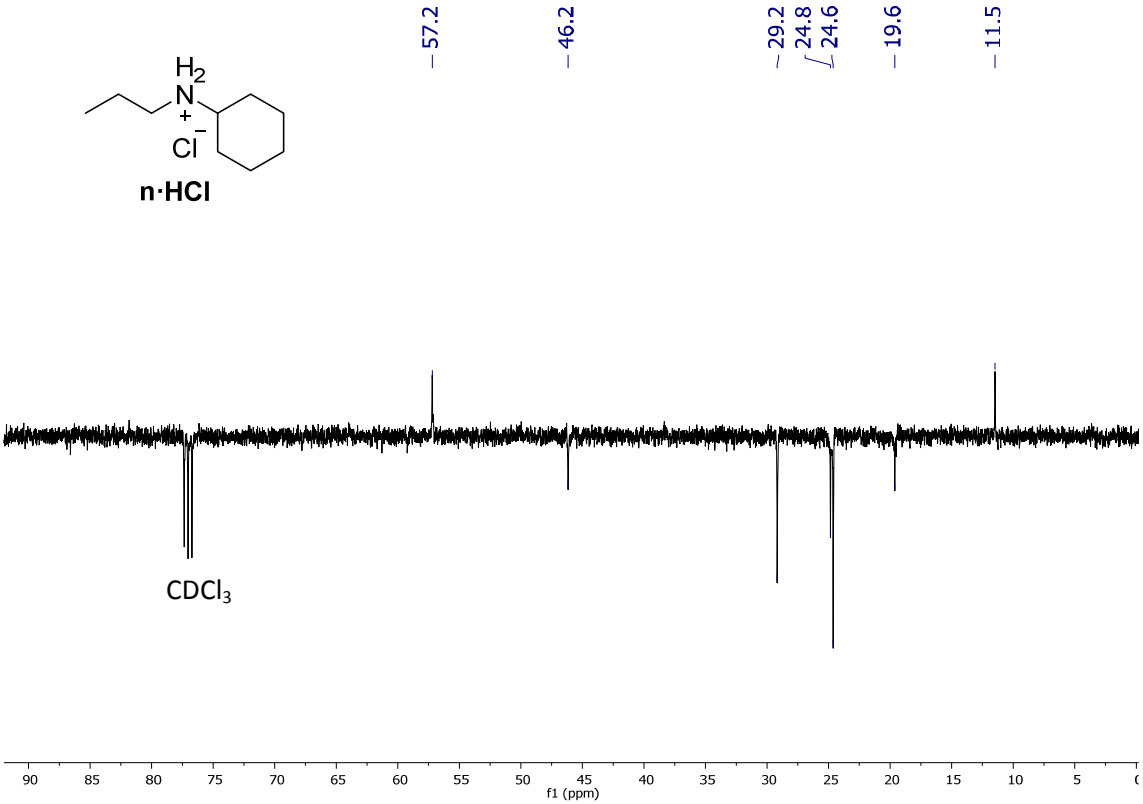

Figure S43. $^{13}C\{^{1}H\}$ APT NMR (100.63 MHz, $CDCl_3$, 298 K) spectrum for **n·HCl.**

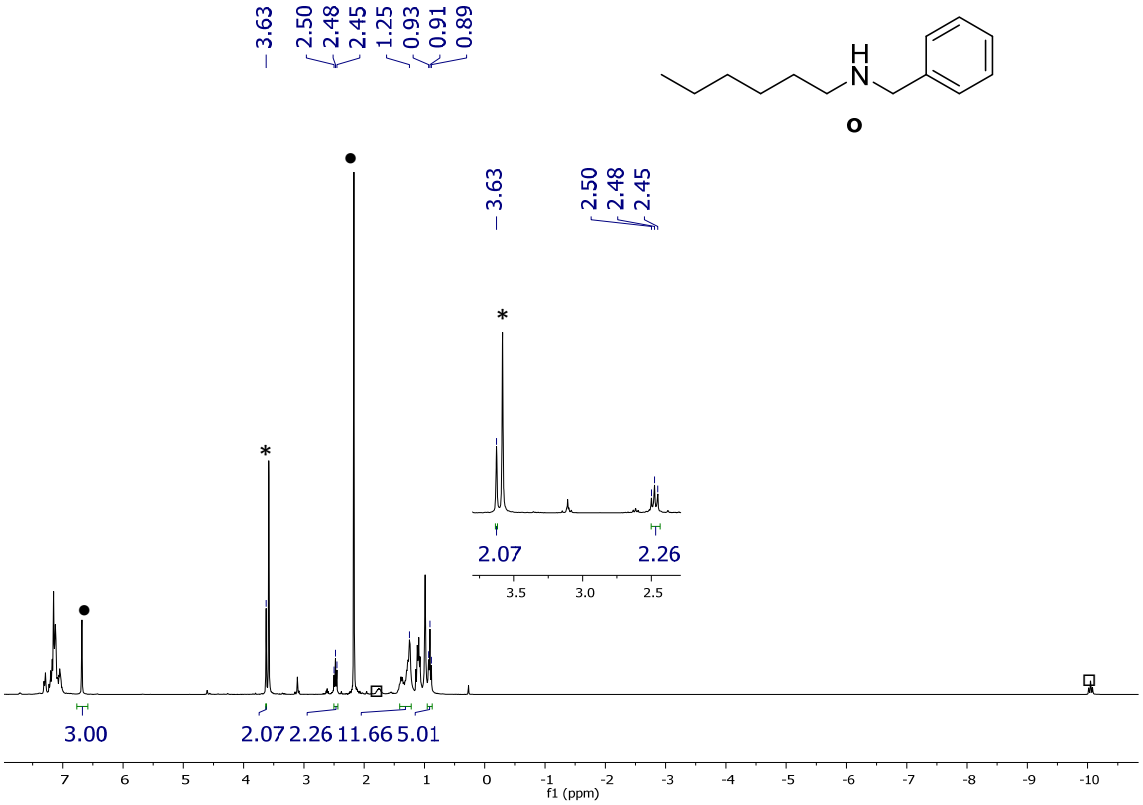

Figure S44. ^{1}H NMR (300.13 MHz, C_7D_8, 298 K) spectrum of the reaction mixture of the hydrogenation of hexanenitrile in the presence of benzylamine: formation of ***N***-benzylhexan-1-amine (**o**).[20] • Mesitylene. □ $OsH_6(P^iPr_3)_2$ (**1**). * Excess of benzylamine.

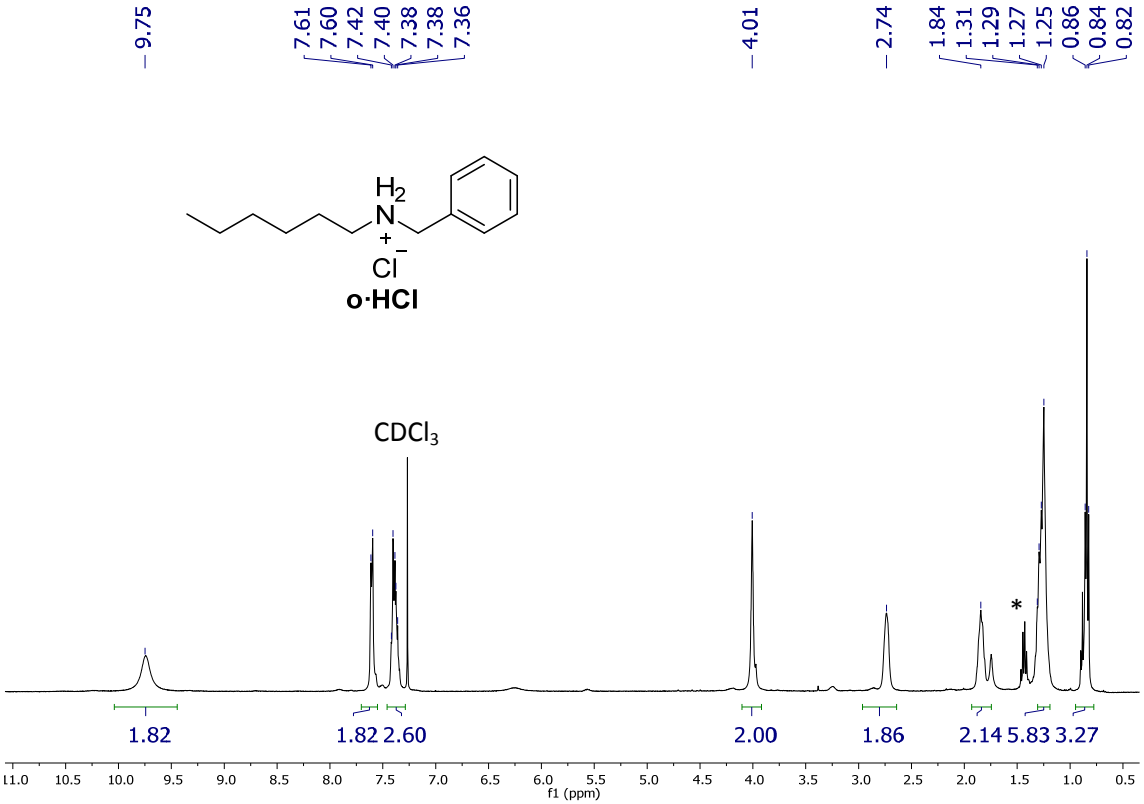

Figure S45. ^{1}H NMR (400.16 MHz, $CDCl_3$, 298 K) spectrum of **o·HCl**. *Pentane

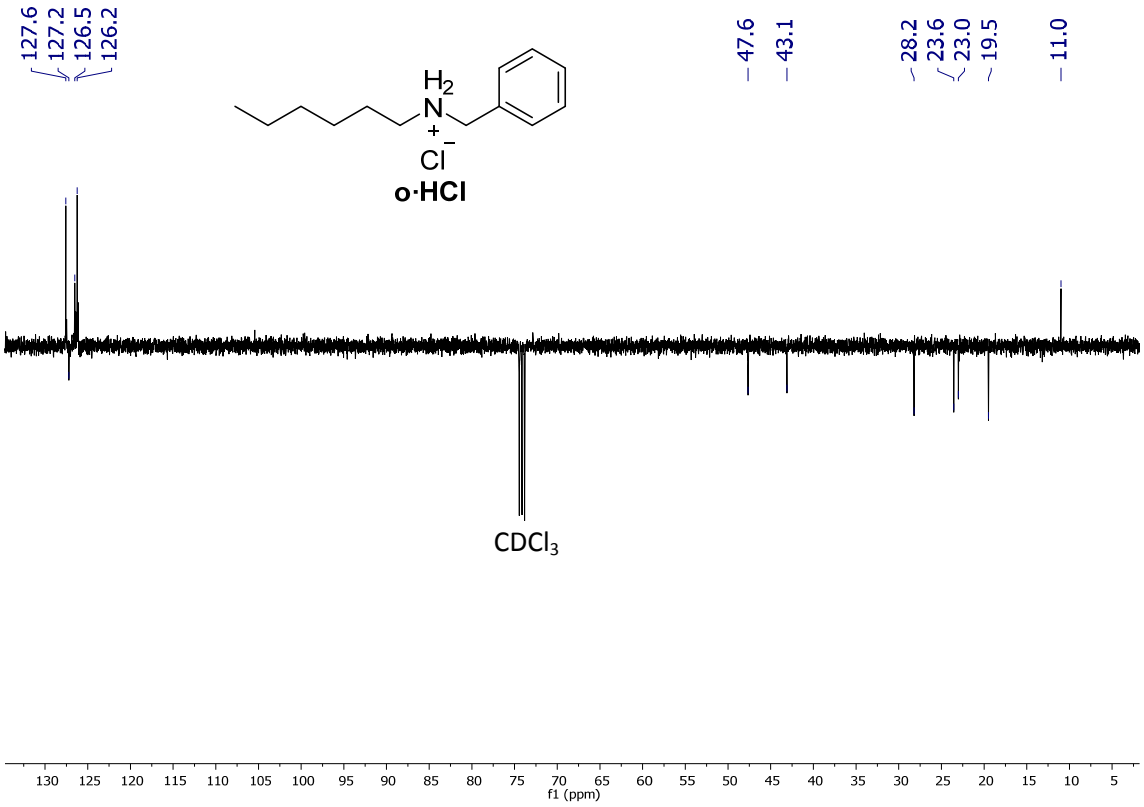

Figure S46. ^{13}C{^{1}H} APT NMR (100.63 MHz, $CDCl_3$, 298 K) spectrum of **o·HCl.**

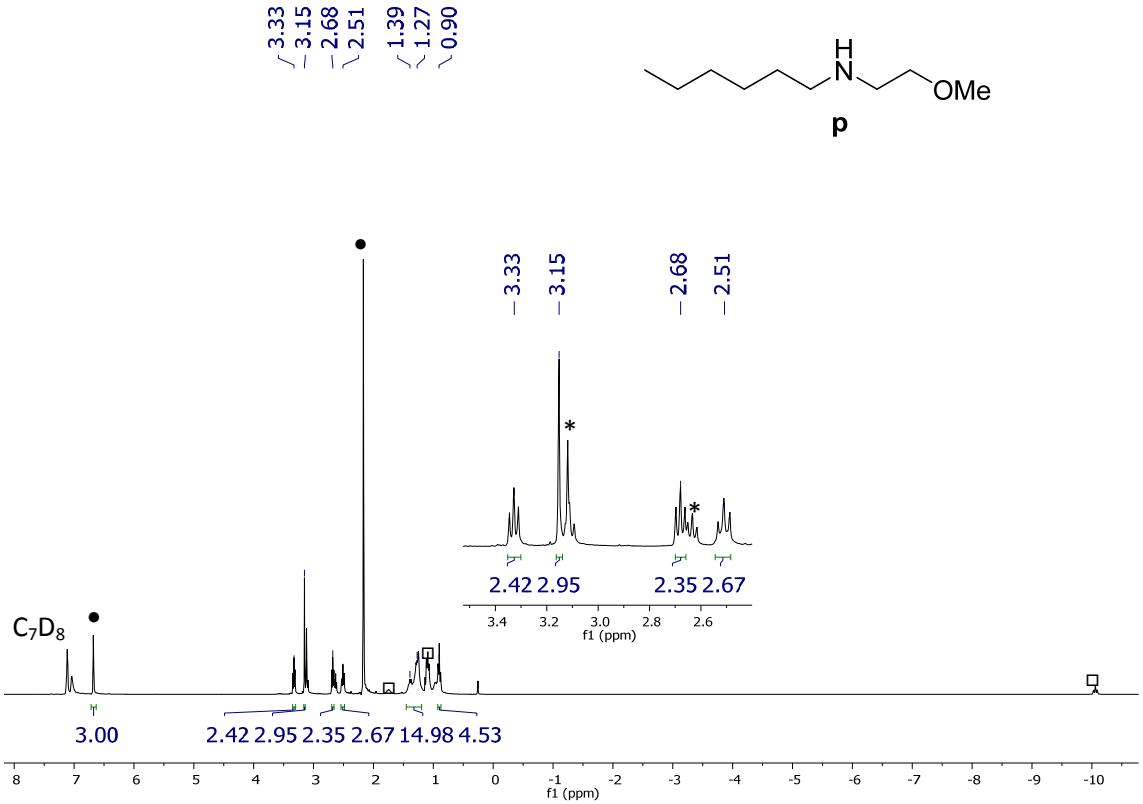

Figure S47. ^{1}H NMR (300.13 MHz, C_7D_8, 298 K) spectrum of the reaction mixture of the hydrogenation of hexanenitrile in the presence of 2-methoxyethan-1-amine: formation of *N*-(2-methoxyethyl)hexan-1-amine (**p**). • Mesitylene. □ $OsH_6(P^iPr_3)_2$ (**1**). * Excess of 2-methoxyethan-1-amine.

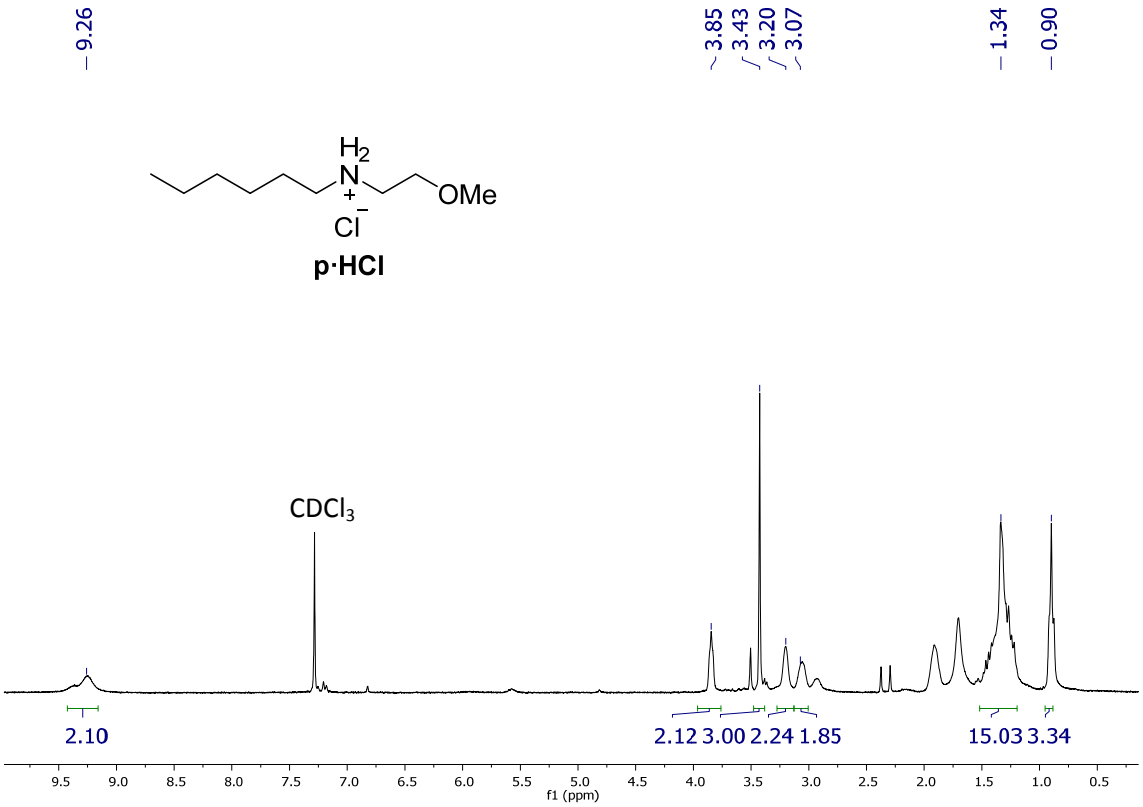

Figure S48. ^{1}H NMR (300.13 MHz, $CDCl_3$, 298 K) spectrum of **p·HCl**.

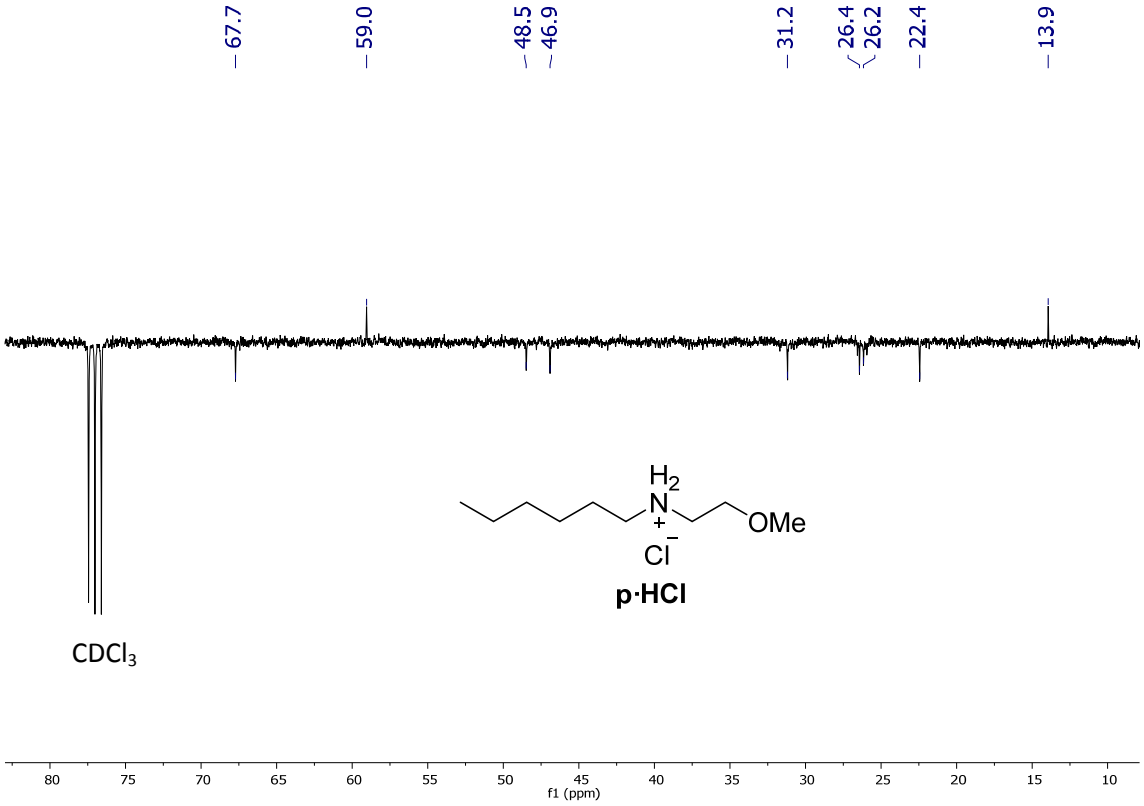

Figure S49. $^{13}C\{^{1}H\}$ APT NMR (75.48 MHz, $CDCl_3$, 298 K) spectrum for **p·HCl.**

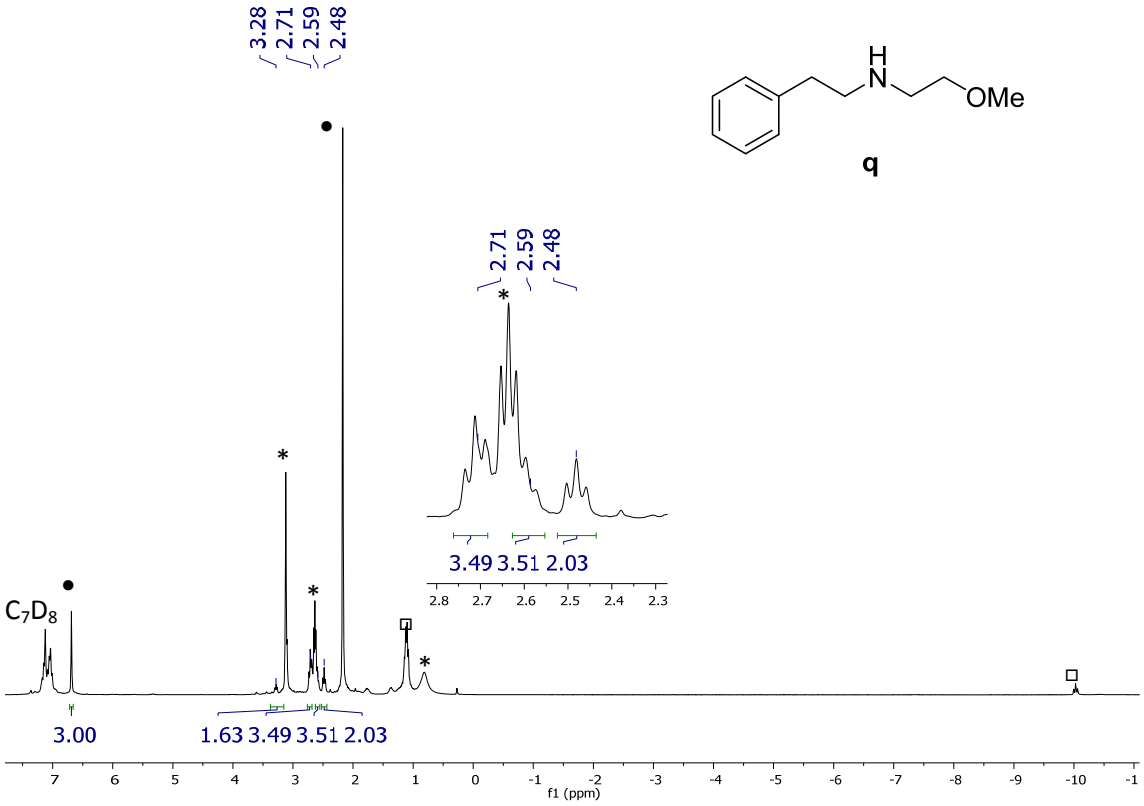

Figure S50. ^{1}H NMR (300.13 MHz, C_7D_8, 298 K) spectrum of the reaction mixture of the hydrogenation of 2-phenylacetonitrile in the presence of 2-methoxyethan-1-amine: formation of 2-methoxy-*N*-phenethylethan-1-amine (**q**). • Mesitylene. □ $OsH_6(P^iPr_3)_2$ (**1**). * Excess of 2-methoxyethan-1-amine.

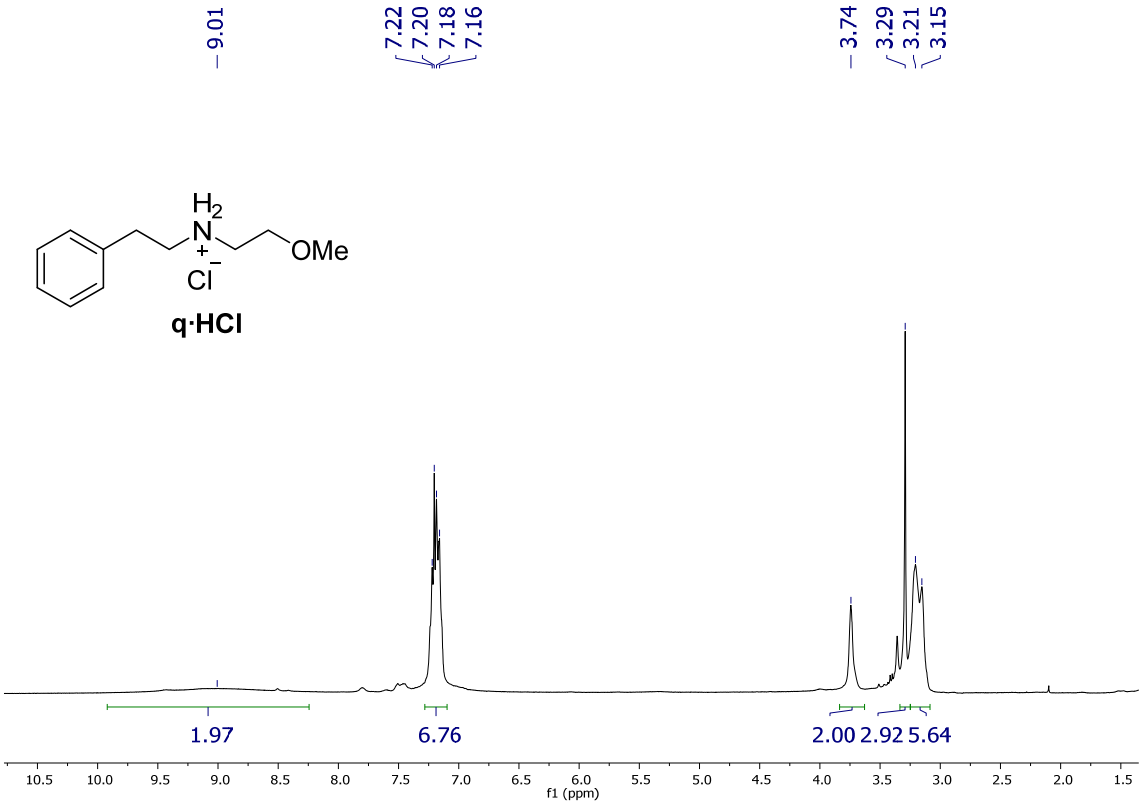

Figure S51. ^{1}H NMR (400.16 MHz, $CDCl_3$, 298 K) spectrum of **q·HCl**.

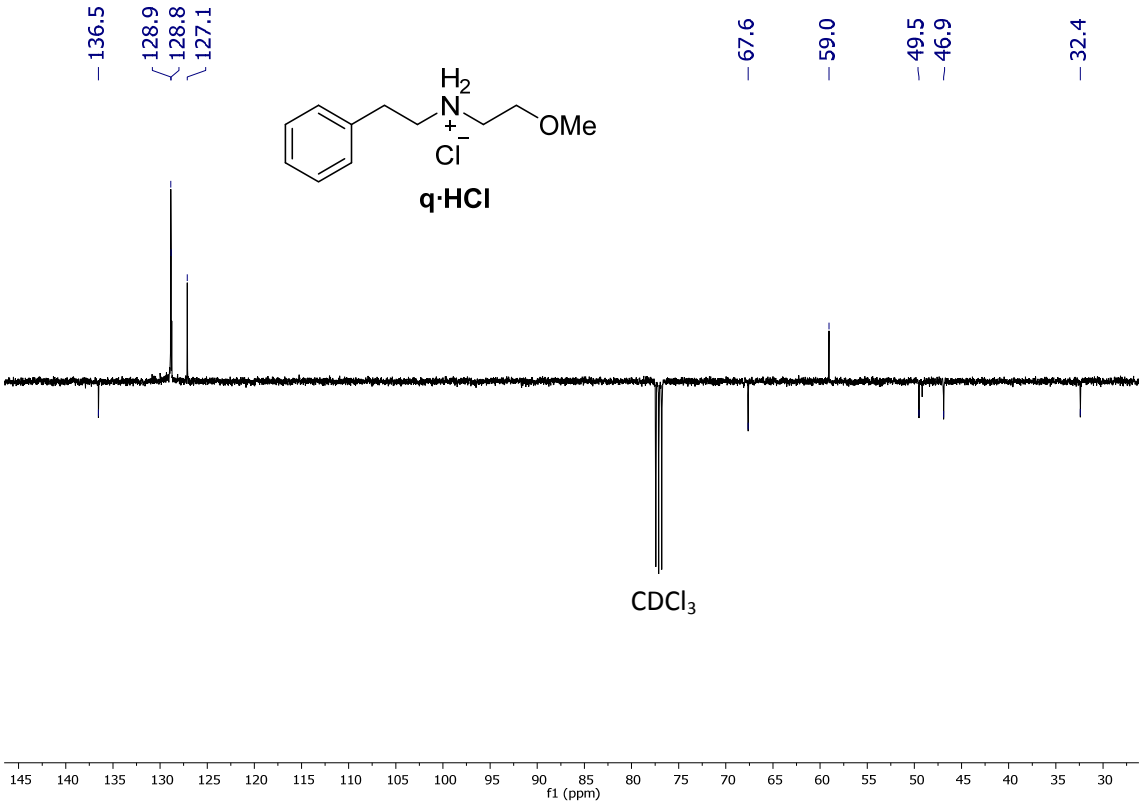

Figure S52. ^{13}C{^{1}H} APT NMR (100.63 MHz, $CDCl_3$, 298 K) spectrum of **q·HCl.**

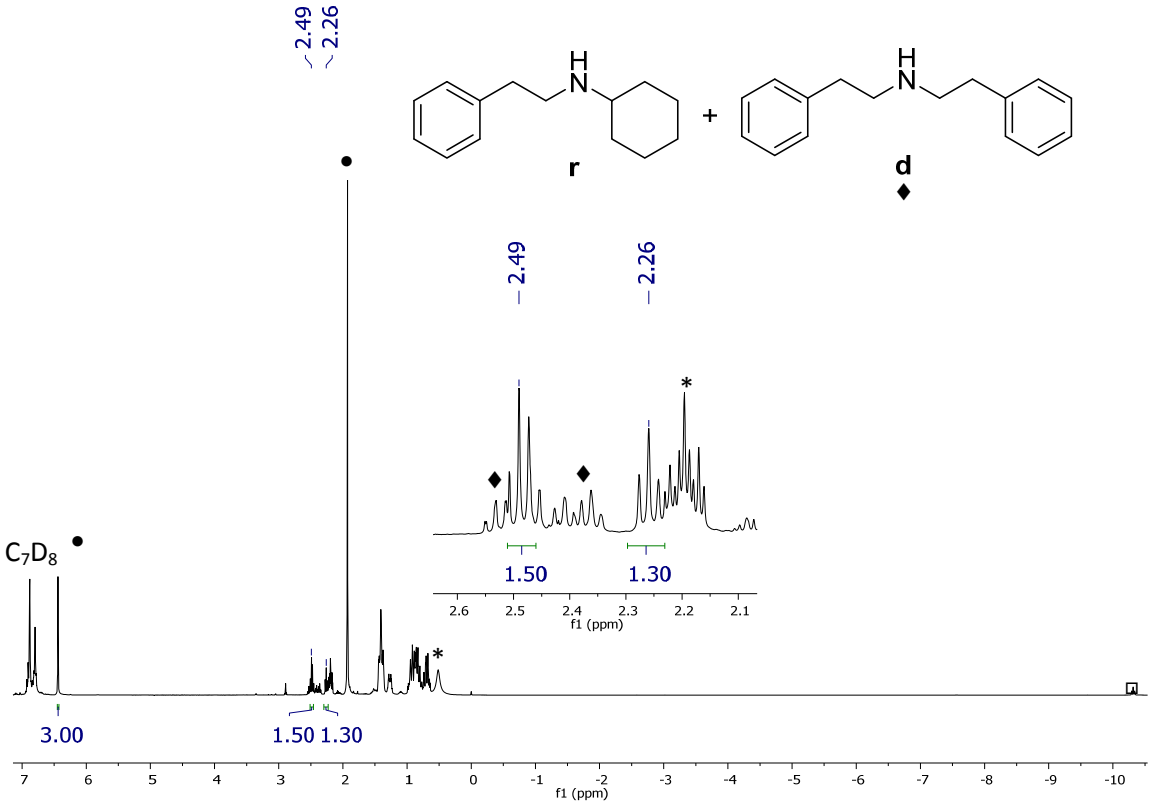

Figure S53. ^{1}H NMR (300.13 MHz, C_7D_8, 298 K) spectrum of the reaction mixture of the hydrogenation of 2-phenylacetonitrile in the presence of cyclohexylamine: formation of *N*-phenethylcyclohexanamine (**r**) and symmetrical secondary amine **d** (♦). • Mesitylene. □ $OsH_6(P^iPr_3)_2$ (**1**). * Excess of cyclohexylamine.

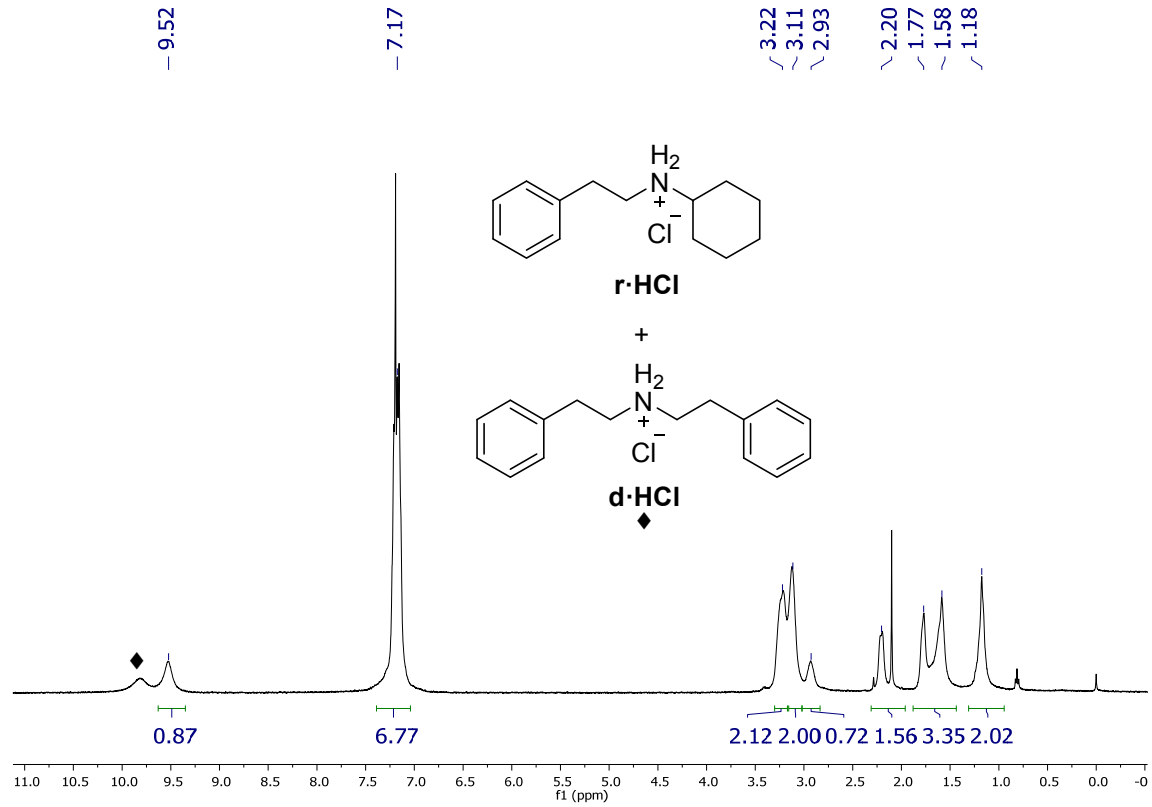

Figure S54. ^{1}H NMR (400.16 MHz, $CDCl_3$, 298 K) spectrum of **r·HCl** and **d·HCl** (♦).

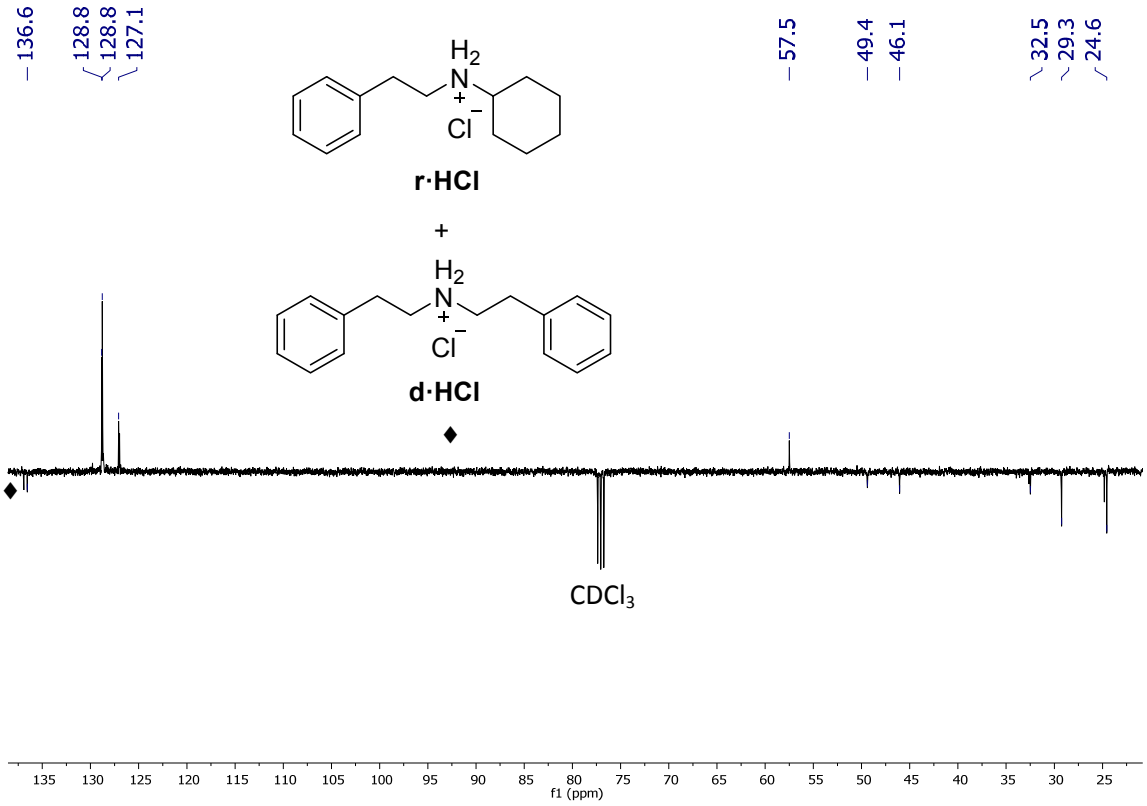

Figure S55. $^{13}C\{^{1}H\}$ APT NMR (100.63 MHz, $CDCl_3$, 298 K) spectrum of **r·HCl** and **d·HCl** (♦).

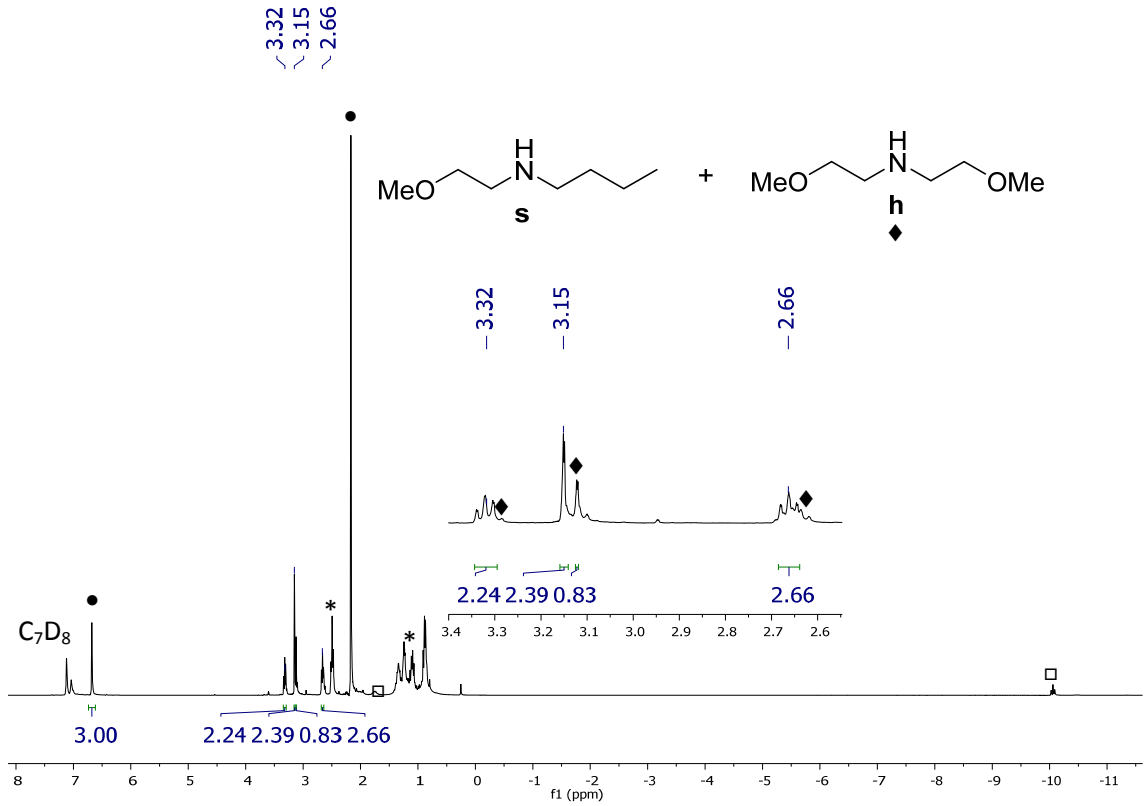

Figure S56. ^{1}H NMR (300.13 MHz, C_7D_8, 298 K) spectrum of the reaction mixture of the hydrogenation of 2-methoxyacetonitrile in the presence of butan-1-amine: formation of *N*-(2-methoxyethyl)butan-1-amine (**s**)[21] and symmetrical secondary amine **h** (♦). • Mesitylene. □ $OsH_6(P^iPr_3)_2$ (**1**). * Excess of butan-1-amine.

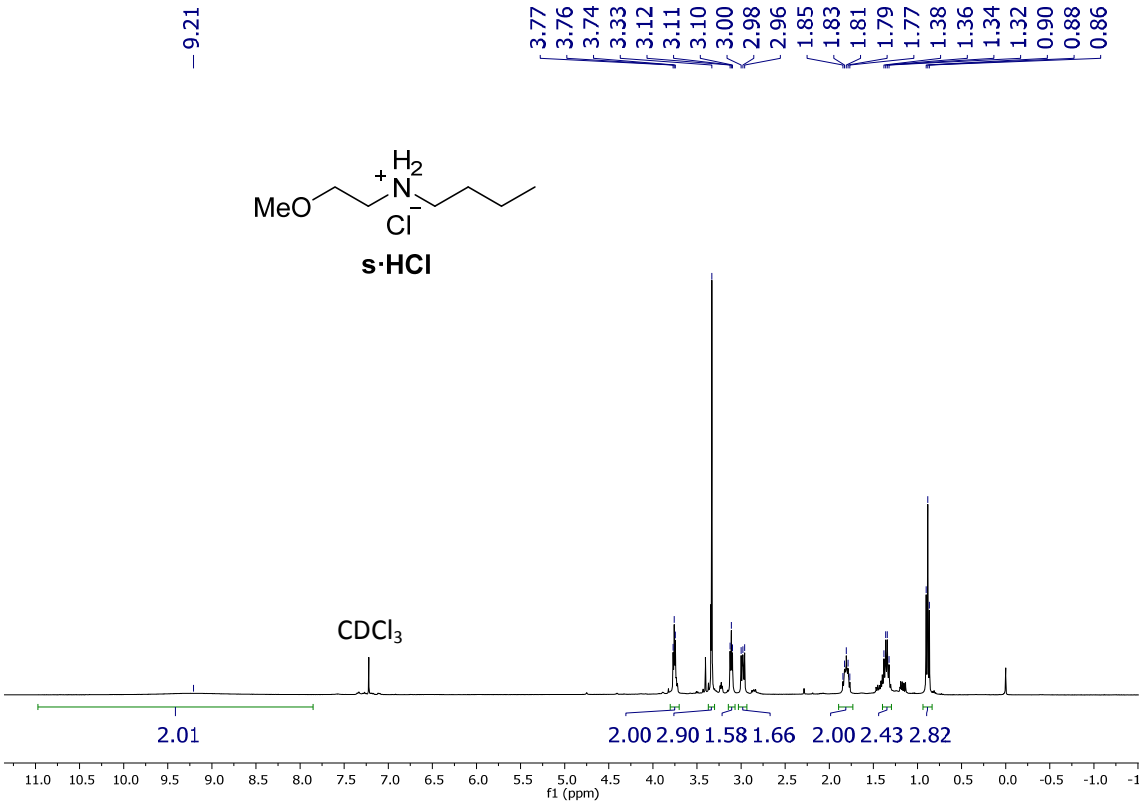

Figure S57. ^{1}H NMR (400.16 MHz, $CDCl_3$, 298 K) spectrum of **s·HCl**.

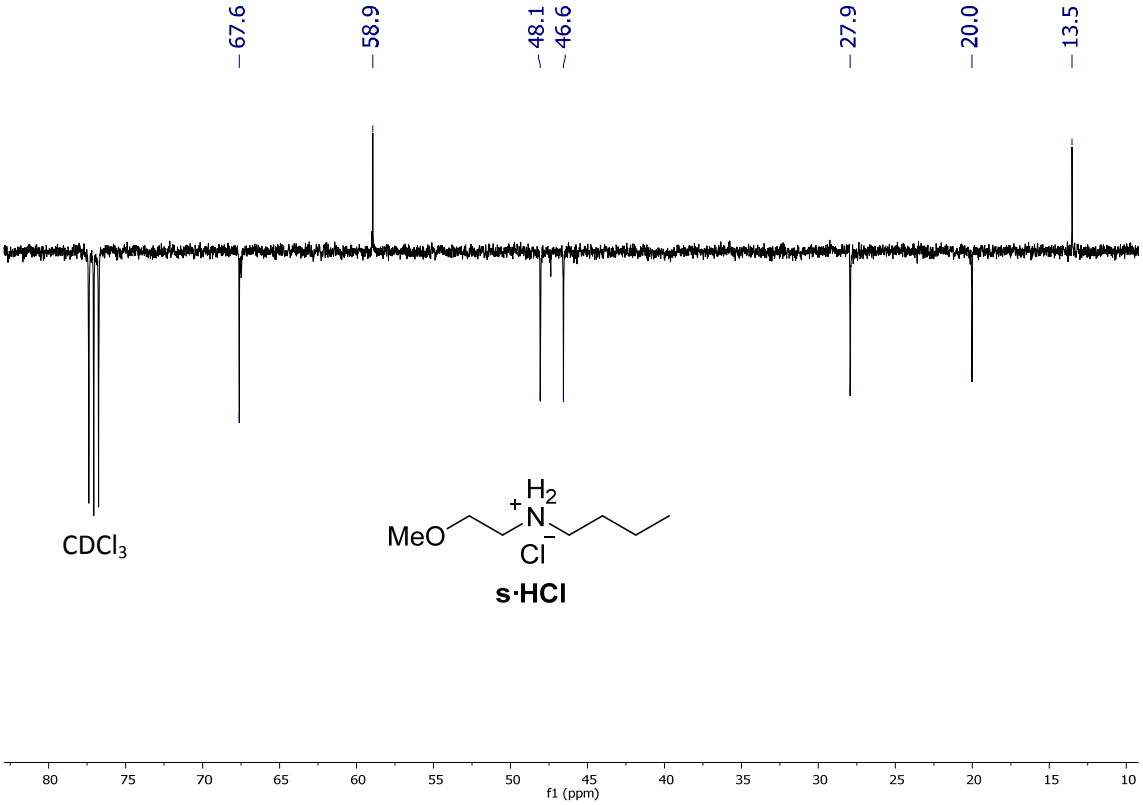

Figure S58. ^{13}C{^{1}H} APT NMR (100.63 MHz, $CDCl_3$, 298 K) spectrum for **s·HCl**.

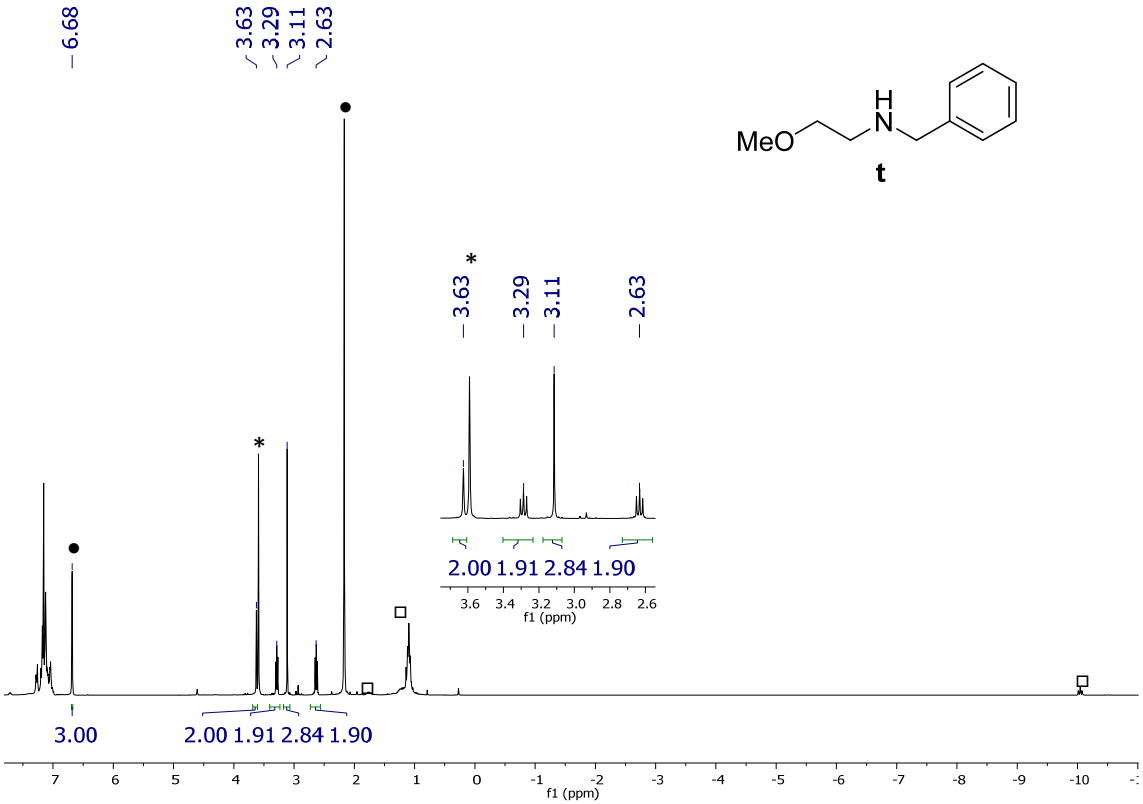

Figure S59. ^{1}H NMR (300.13 MHz, C_7D_8, 298 K) spectrum of the reaction mixture of the hydrogenation of 2-methoxyacetonitrile in the presence of benzylamine: formation of *N*-benzyl-2-methoxyethan-1-amine (**t**).[20] • Mesitylene. □ $OsH_6(P^iPr_3)_2$ (**1**). * Excess of benzylamine.

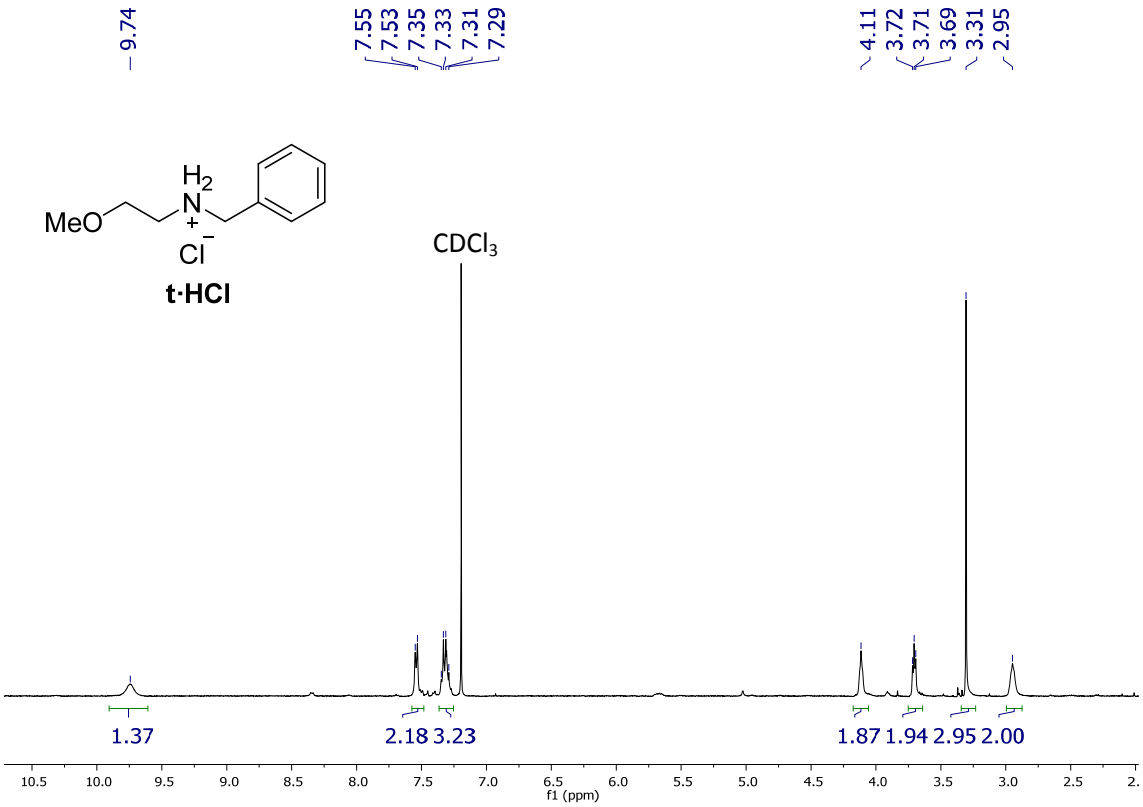

Figure S60. ^{1}H NMR (400.16 MHz, $CDCl_3$, 298 K) spectrum of **t·HCl**.

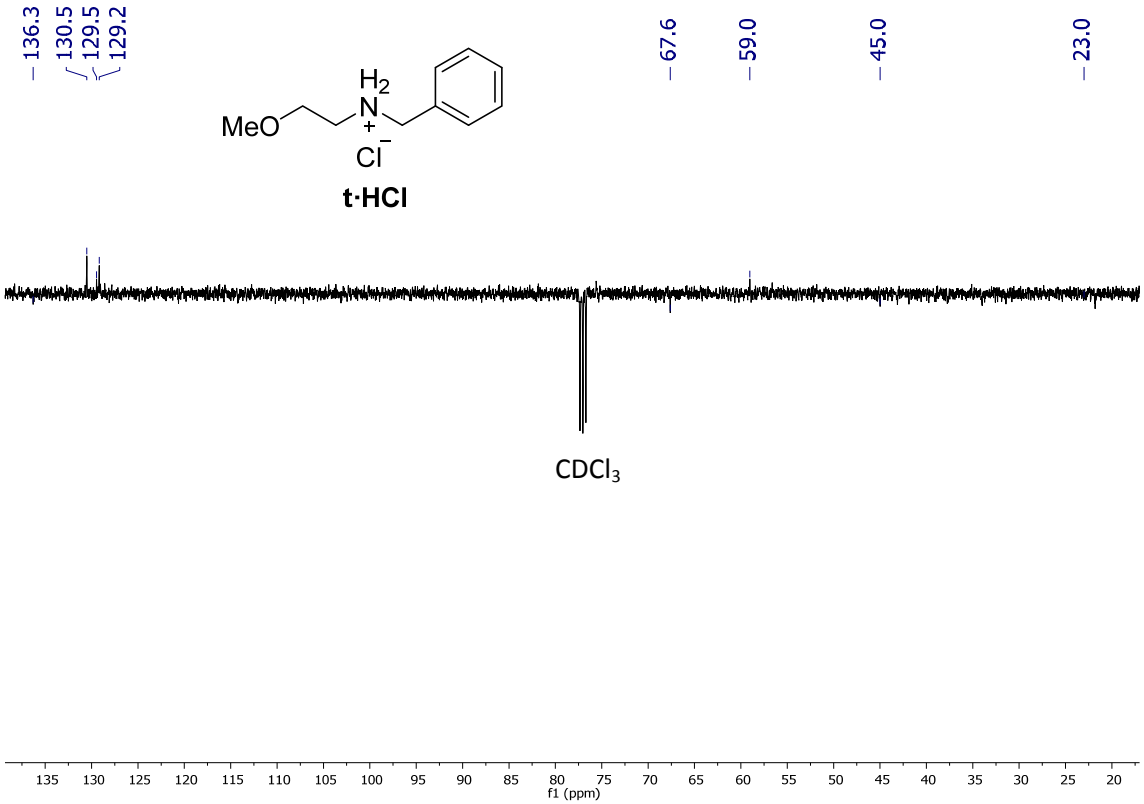

Figure S61. $^{13}C\{^{1}H\}$ APT NMR (100.63 MHz, $CDCl_3$, 298 K) spectrum of **t·HCl**.

NMR spectra of complexes of a mixture of complexes 2 and 3 (35:65 molar ratio).

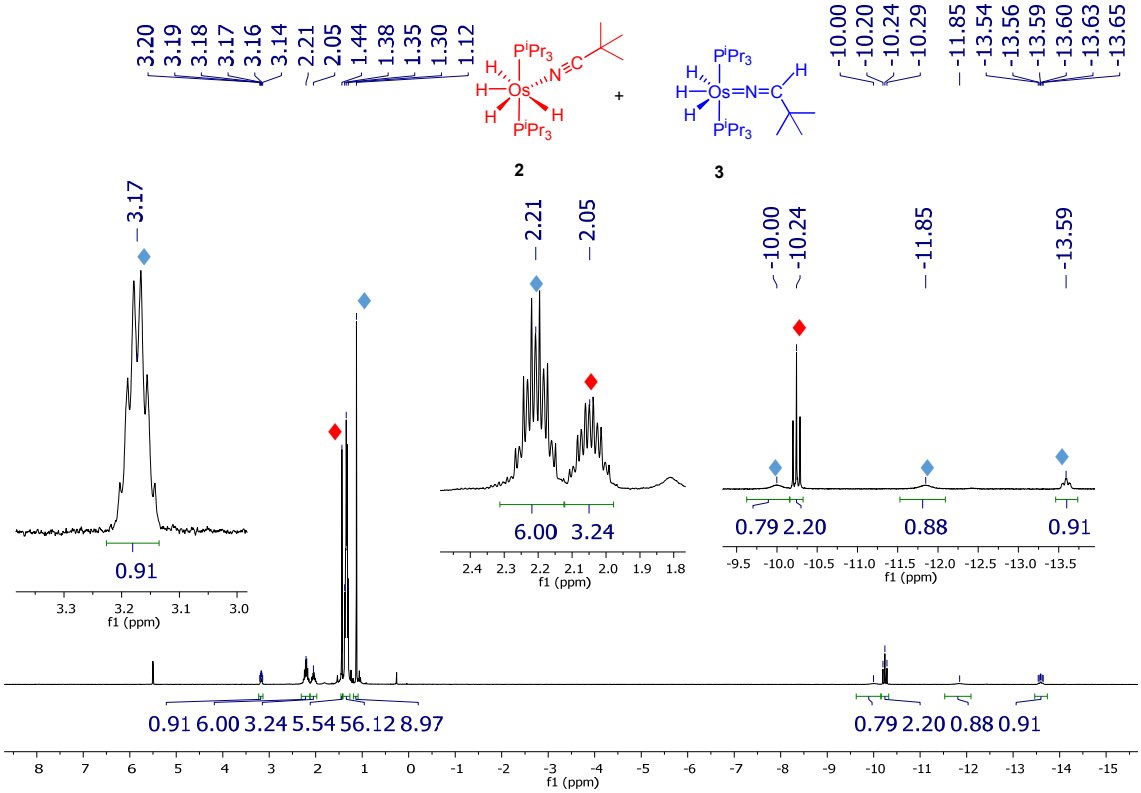

Figure S62. ^{1}H NMR (300.13 MHz, C_6D_6, 298 K) spectrum for mixture of complexes **2** (♦) and **3** (♦).

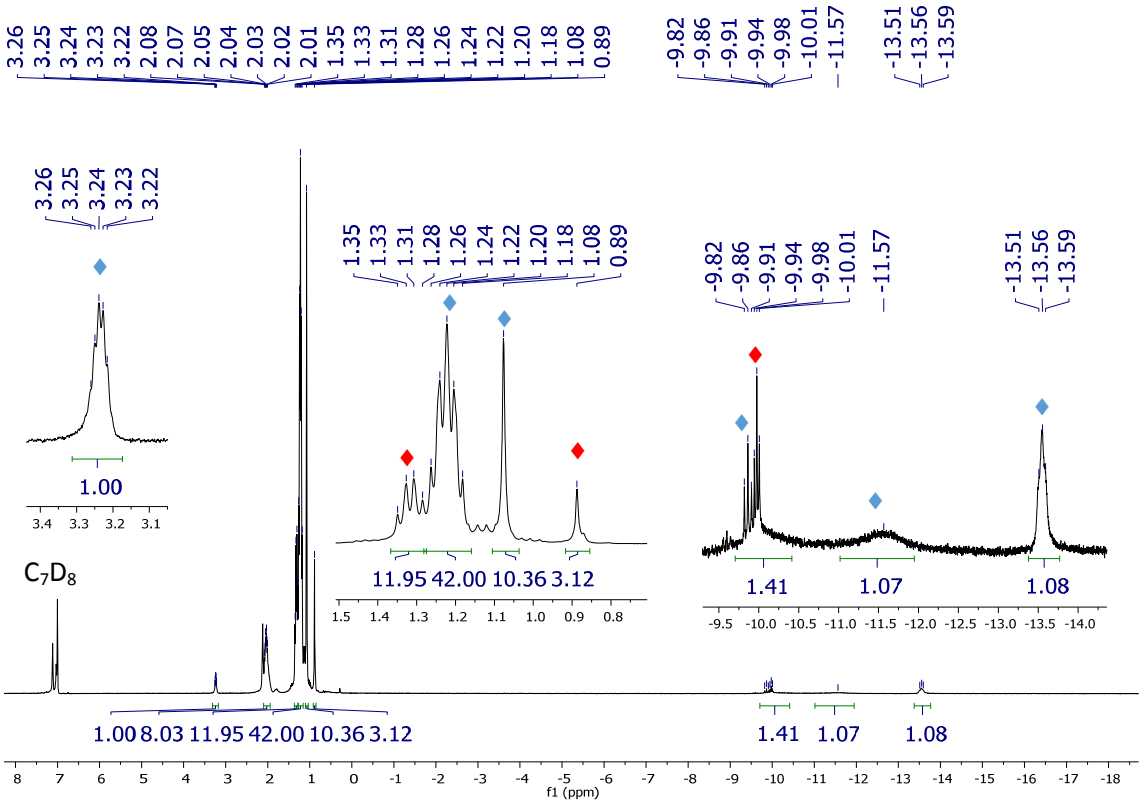

Figure S63. ^{1}H NMR (300.13 MHz, C_7D_8, 298 K) spectrum for mixture of complexes **2** (♦) and **3** (♦).

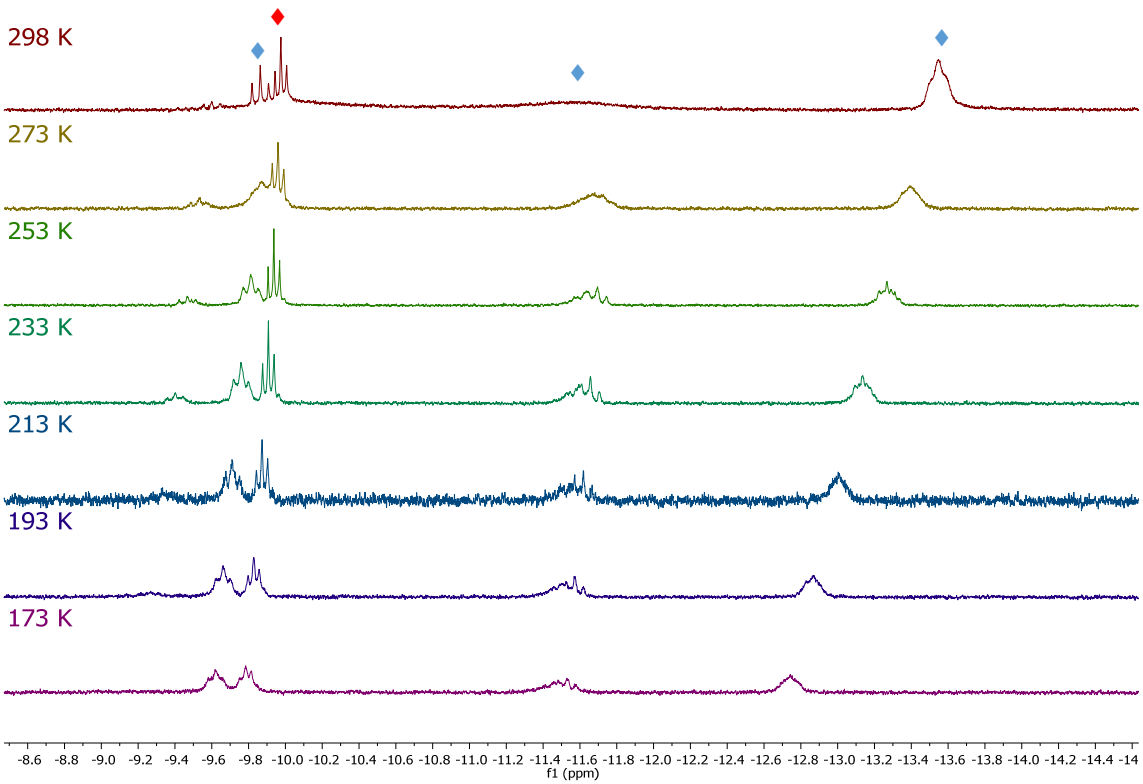

Figure S64. High-field region of the ^{1}H NMR (300.13 MHz, C_7D_8) spectrum for the mixture of complexes **2** (♦) and **3** (♦) between 298 and 173 K.

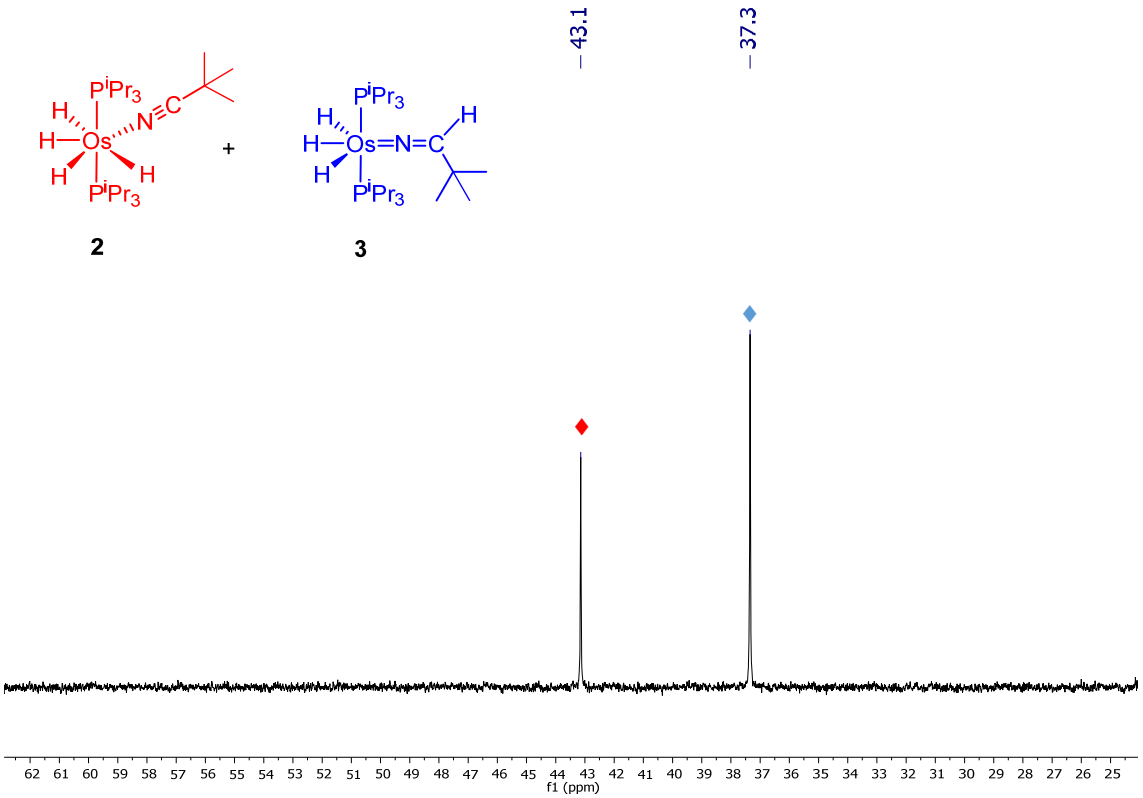

Figure S65. ^{31}P{^{1}H} NMR (121.49 MHz, C_7D_8, 298 K) spectrum for the mixture of complexes **2** (♦) and **3** (♦).

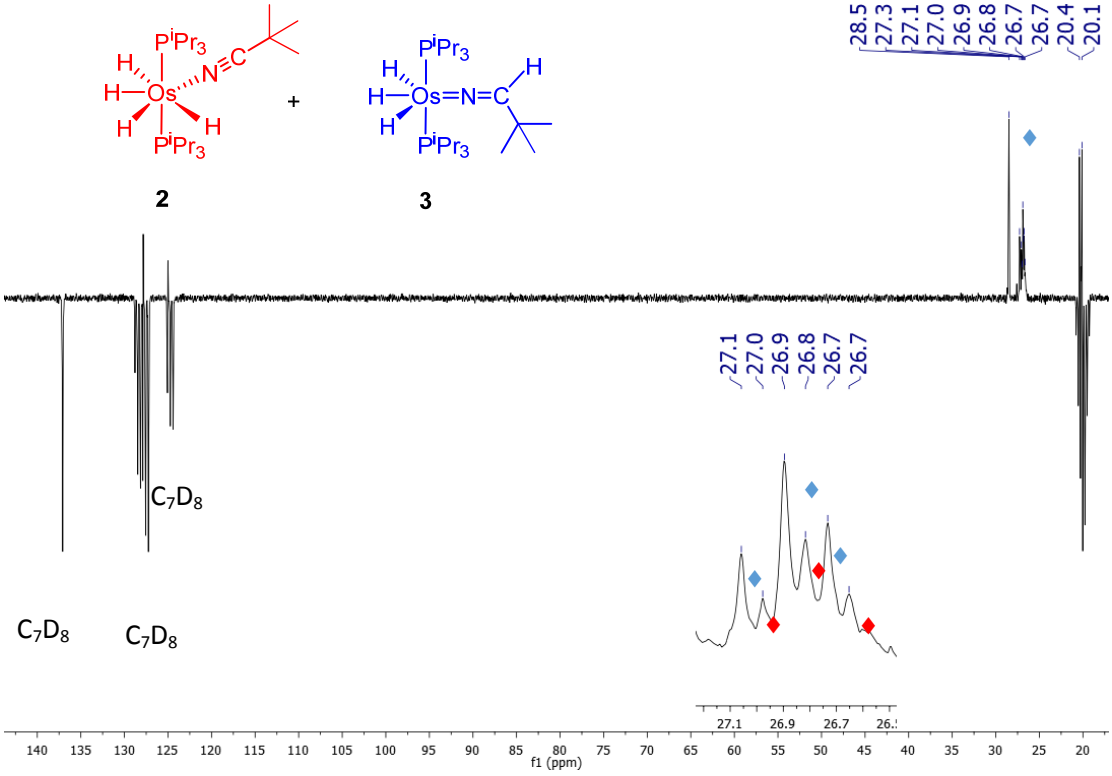

Figure S66. $^{13}C\{^{1}H\}$ APT NMR (75.48 MHz, C_7D_8, 298 K) spectrum for the mixture of complexes **2** (♦) and **3** (♦).

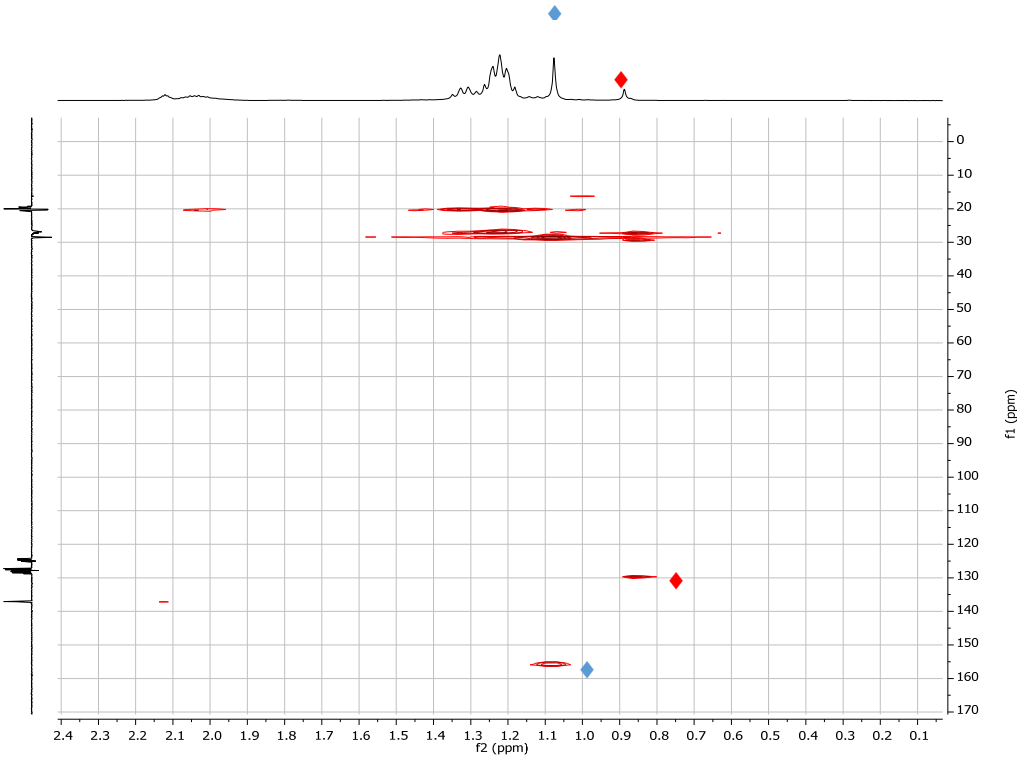

Figure S67. Region of the HMBC (^{1}H, ^{13}C) NMR (300.13, 75.48, C_7D_8, 298 K) spectrum for the mixture of complexes **2** (♦) and **3** (♦) showing the cross peaks between the N≡C and N=CH ^{13}C NMR signals and ^{1}H NMR signals of the corresponding ^{t}Bu groups.

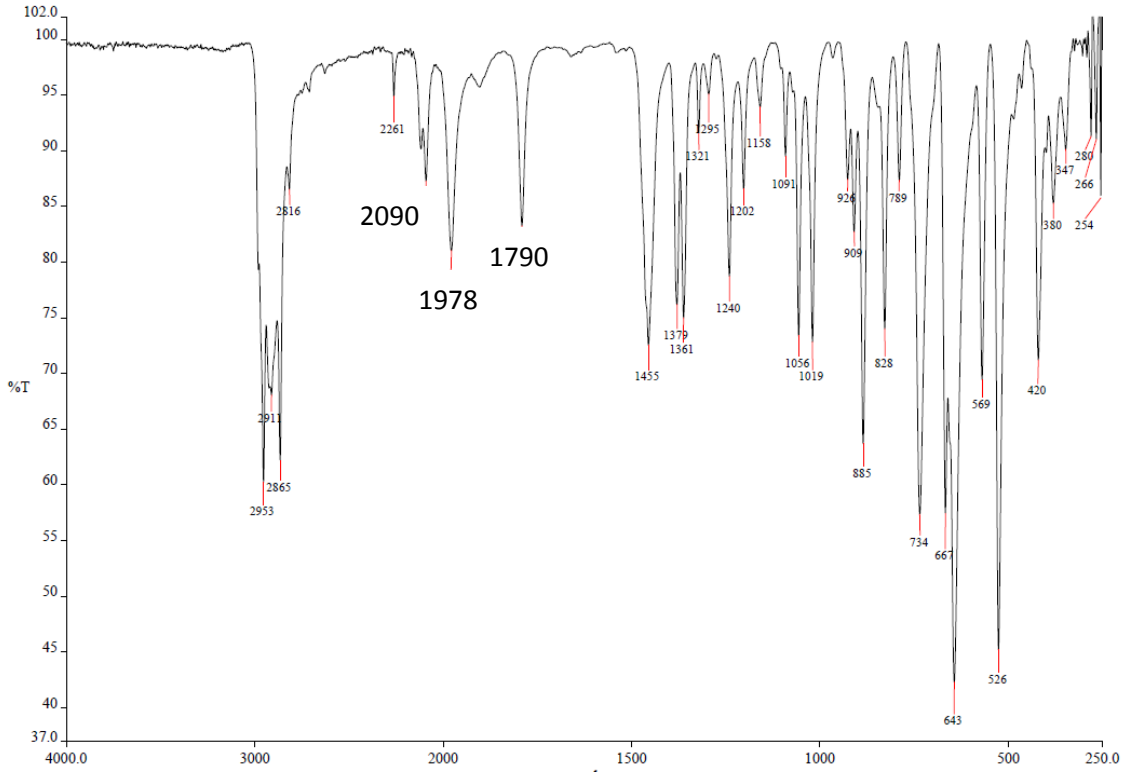

Figure S68. IR ATR spectrum for mixture of complexes **2** and **3**.

^{1}H NMR and ^{31}P{^{1}H}NMR spectra of reaction of a mixture of 2 and 3 in a 35:65 molar ratio with H_2

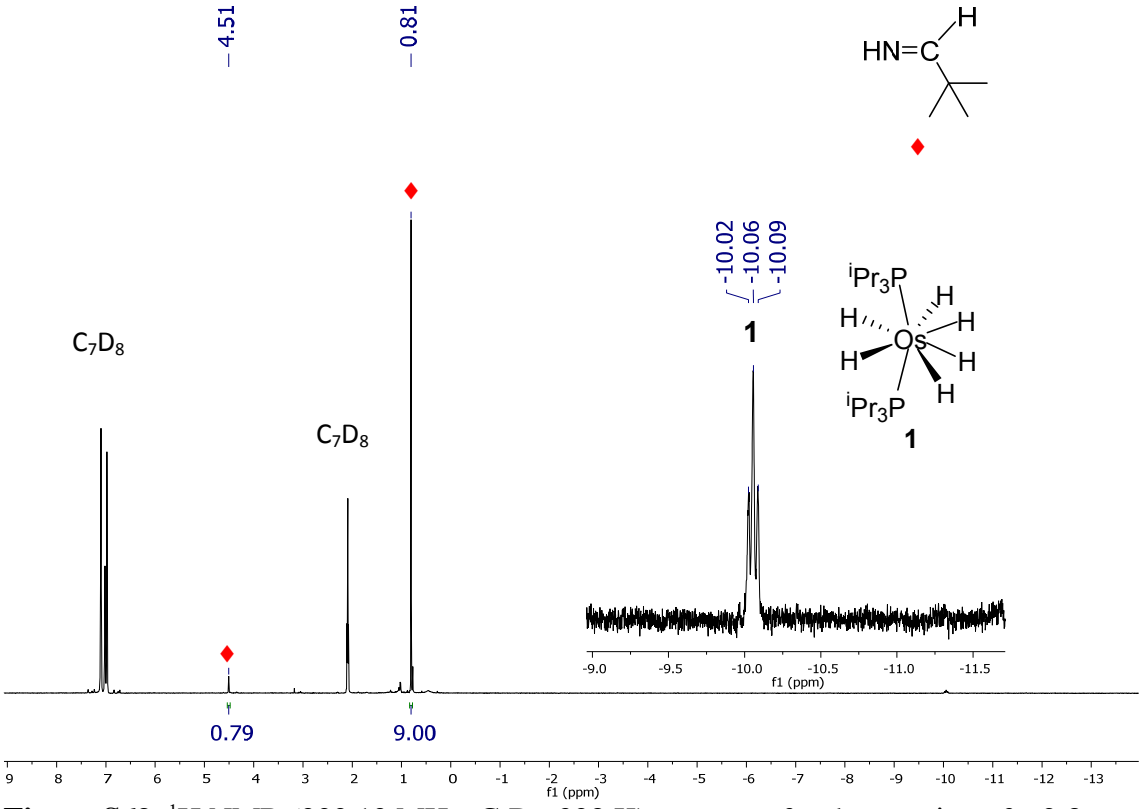

Figure S69. ^{1}H NMR (300.13 MHz, C_6D_6, 298 K) spectrum for the reaction of a **2**:**3** mixture (35:65) with H_2 (1 bar, 10 min, 100 ºC). 3,3-dimethylbutan-2-imine (♦)

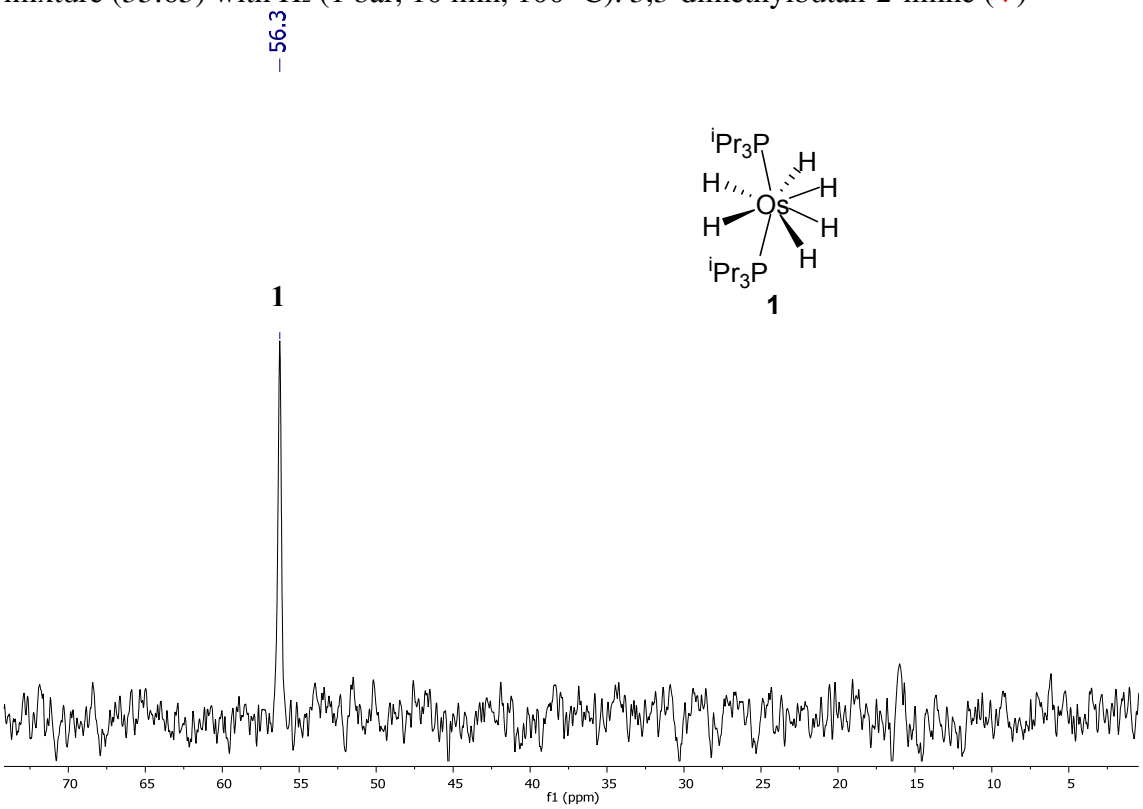

Figure S70. ^{31}P{^{1}H} NMR (121.49 MHz, C_7D_8, 298 K) spectrum for the reaction of a **2**:**3** mixture (35:65) with H_2 (1 bar, 10 min, 100 ºC).

Monitoring of the reaction of 1 with 2-methoxyacetonitrile (1:1 molar ratio; both 0.1 M) by ^{1}H NMR and ^{31}P{^{1}H}NMR

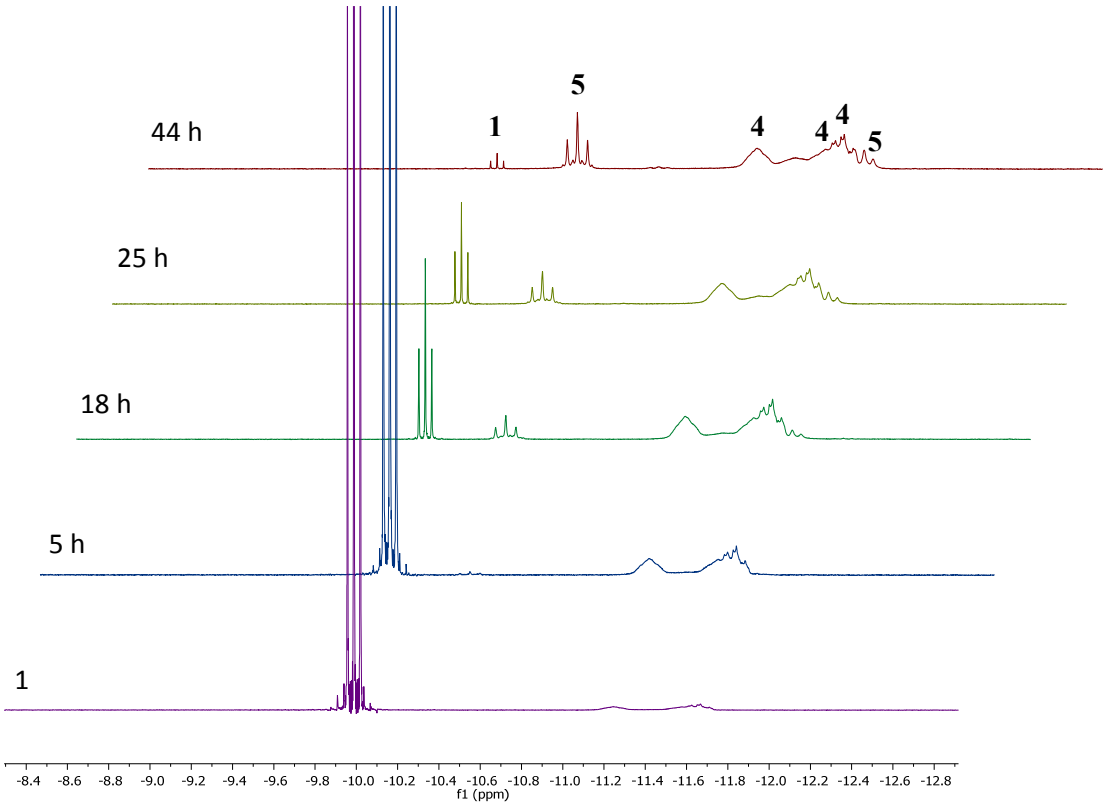

Figure S71. High field region of the ^{1}H NMR (300.13 MHz, C_7D_8, 298 K) spectrum for the reaction of complex **1** with 2-methoxyacetonitrile (1:1; both 0.1 M) at 50 ºC.

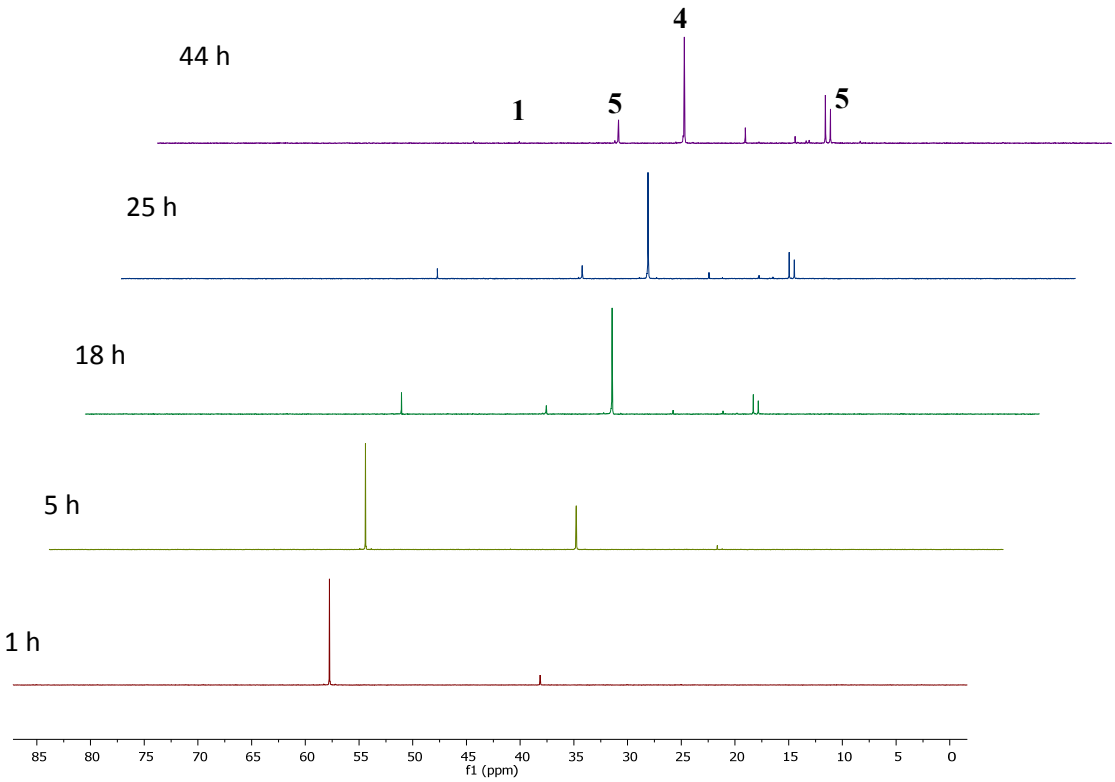

Figure S72. ^{31}P{^{1}H} NMR (121.49 MHz, C_7D_8, 298 K) spectrum for the reaction of complex **1** with 2-methoxyacetonitrile (1:1; both 0.1 M) at 50 ºC.

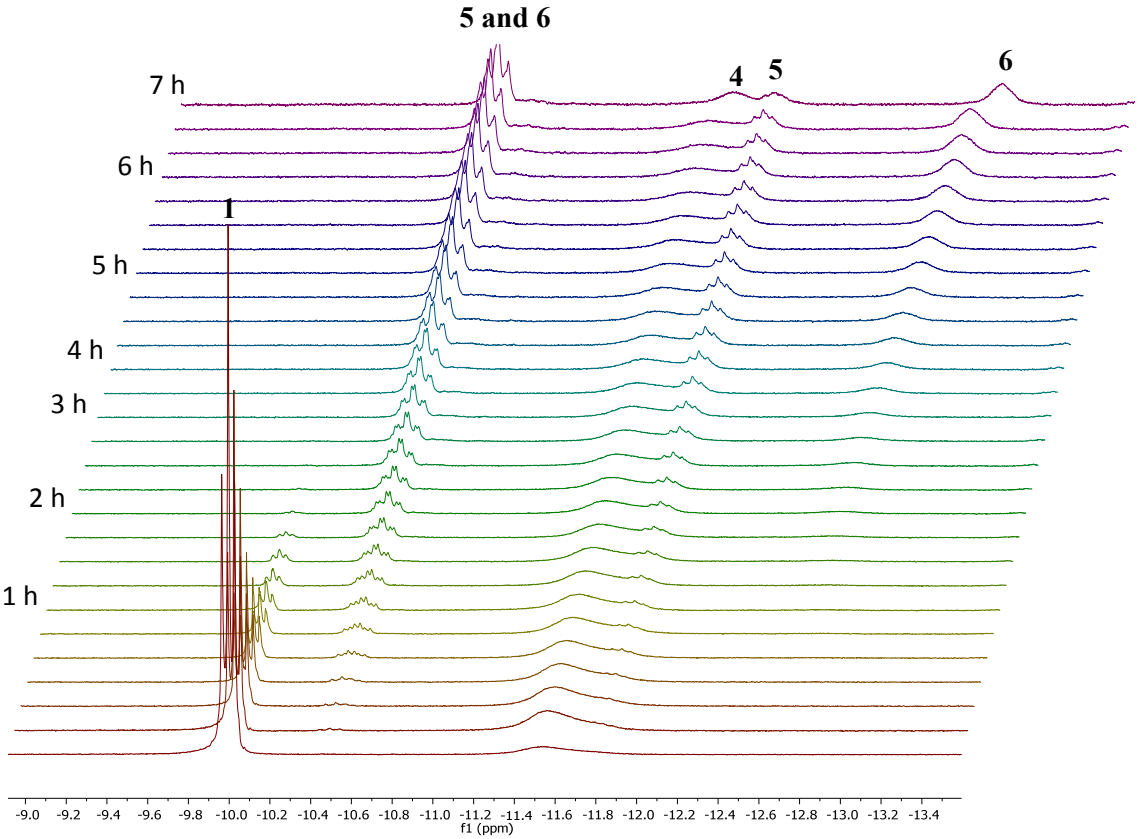

Figure S73. High field region of the ^{1}H NMR (300.13 MHz, C_7D_8, 298 K) spectrum for the reaction of complex **1** with 2-methoxyacetonitrile (1:1; both 0.1 M) at 80 ºC.

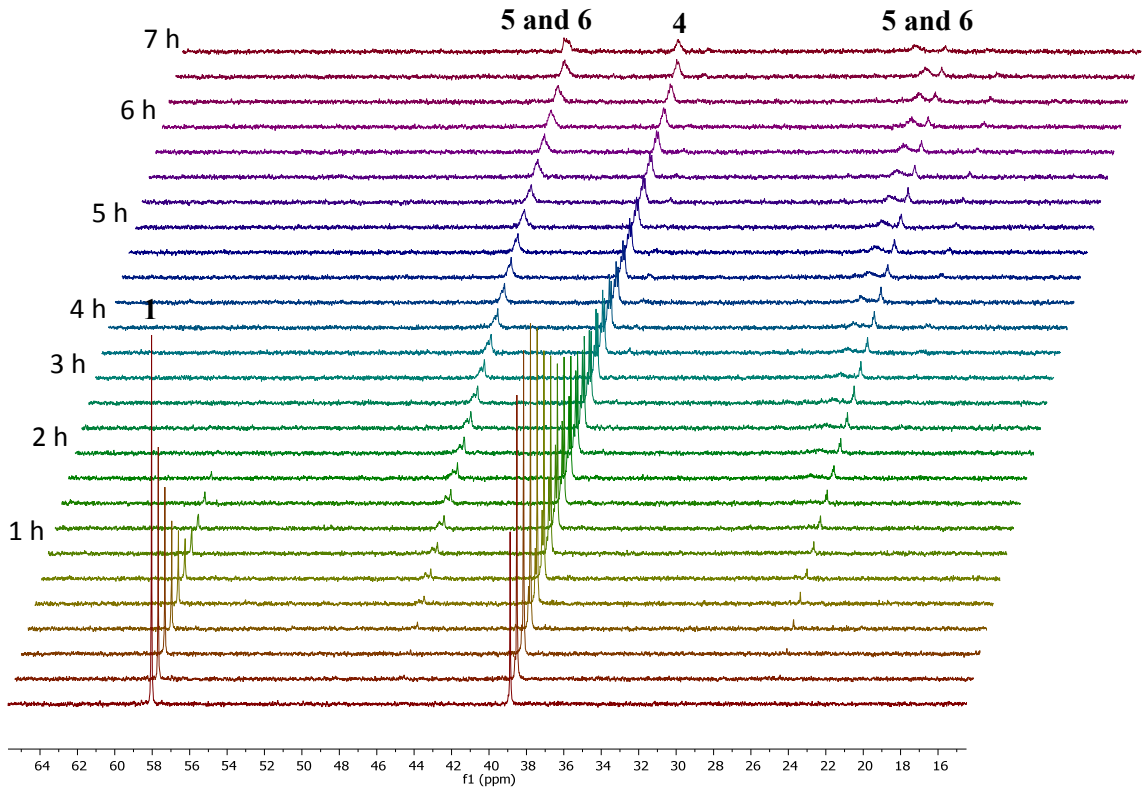

Figure S74. ^{31}P{^{1}H} NMR (121.49 MHz, C_7D_8, 298 K) spectrum for the reaction of complex **1** with 2-methoxyacetonitrile (1:1; both 0.1 M) at 80 ºC.

^{1}H NMR, ^{31}P{^{1}H}NMR, and ^{13}C{^{1}H} APT NMR spectra of complexes 4-6

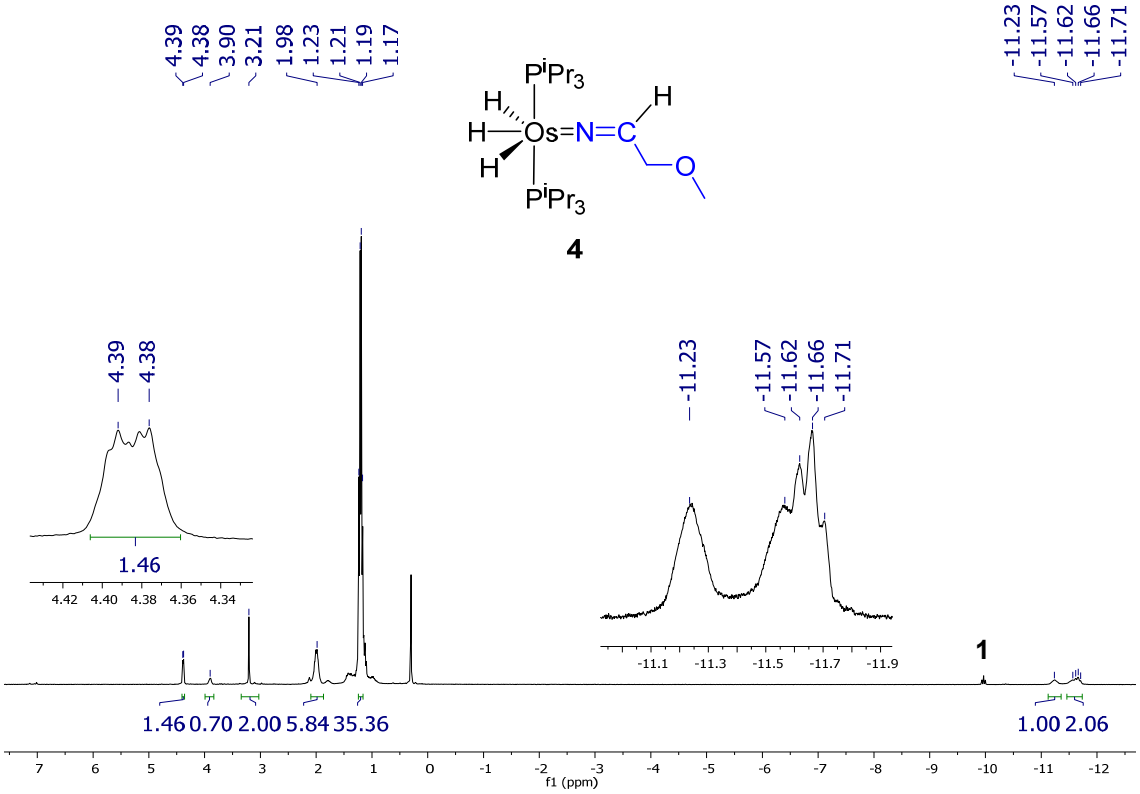

Figure S75. ^{1}H NMR (300.13 MHz, C_7D_8, 298 K) spectrum for complex **4**.

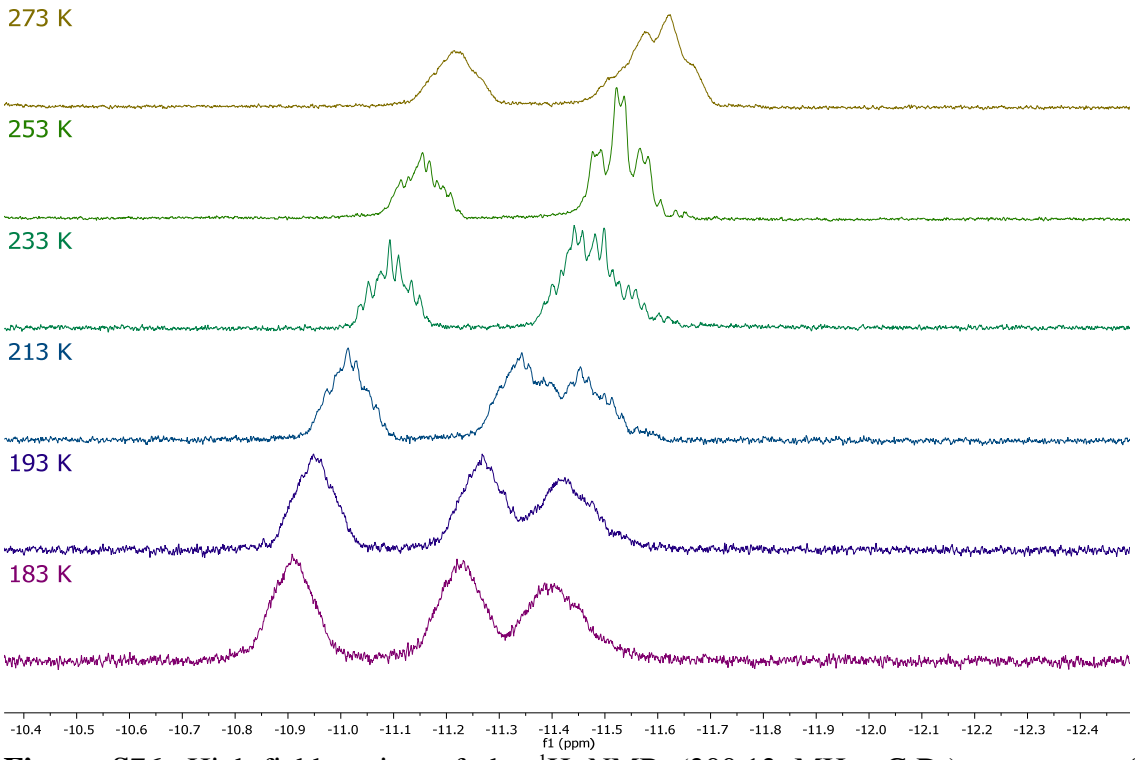

Figure S76. High-field region of the ^{1}H NMR (300.13 MHz, C_7D_8) spectrum of complex **4** between 273 K and 183 K.

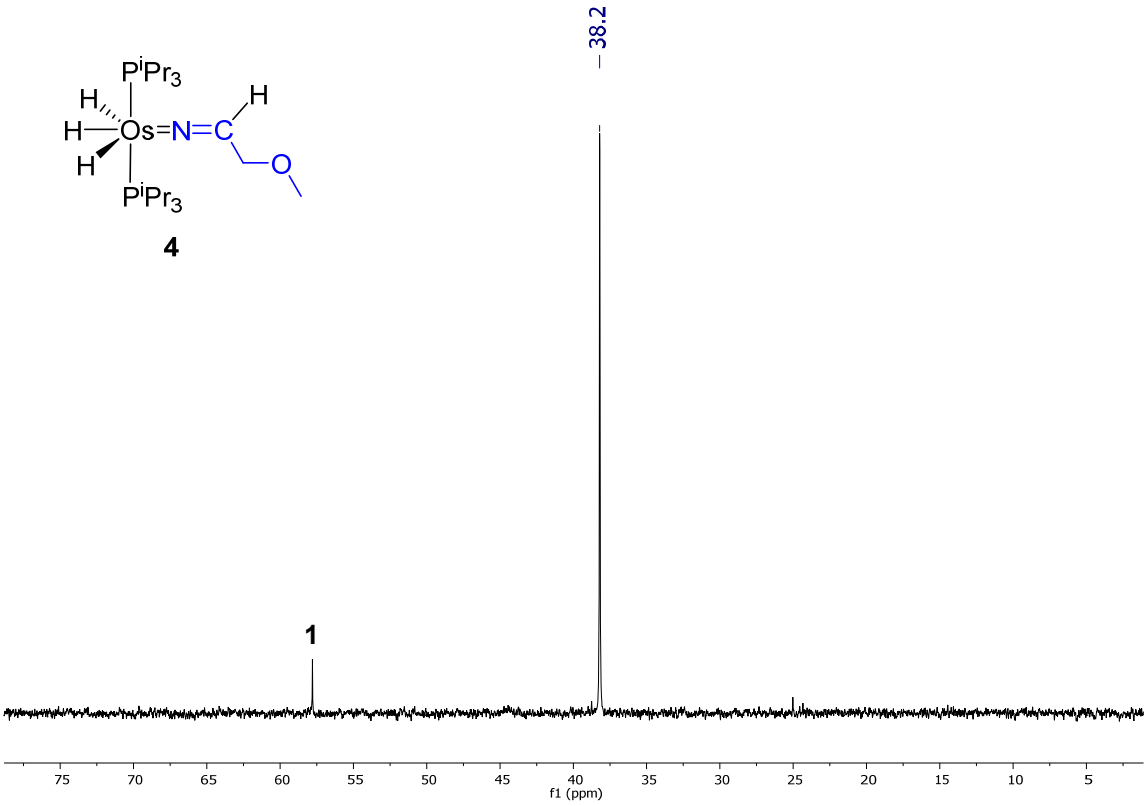

Figure S77. $^{31}P\{^{1}H\}$ NMR (121.49 MHz, C_7D_8, 298 K) spectrum for complex **4**.

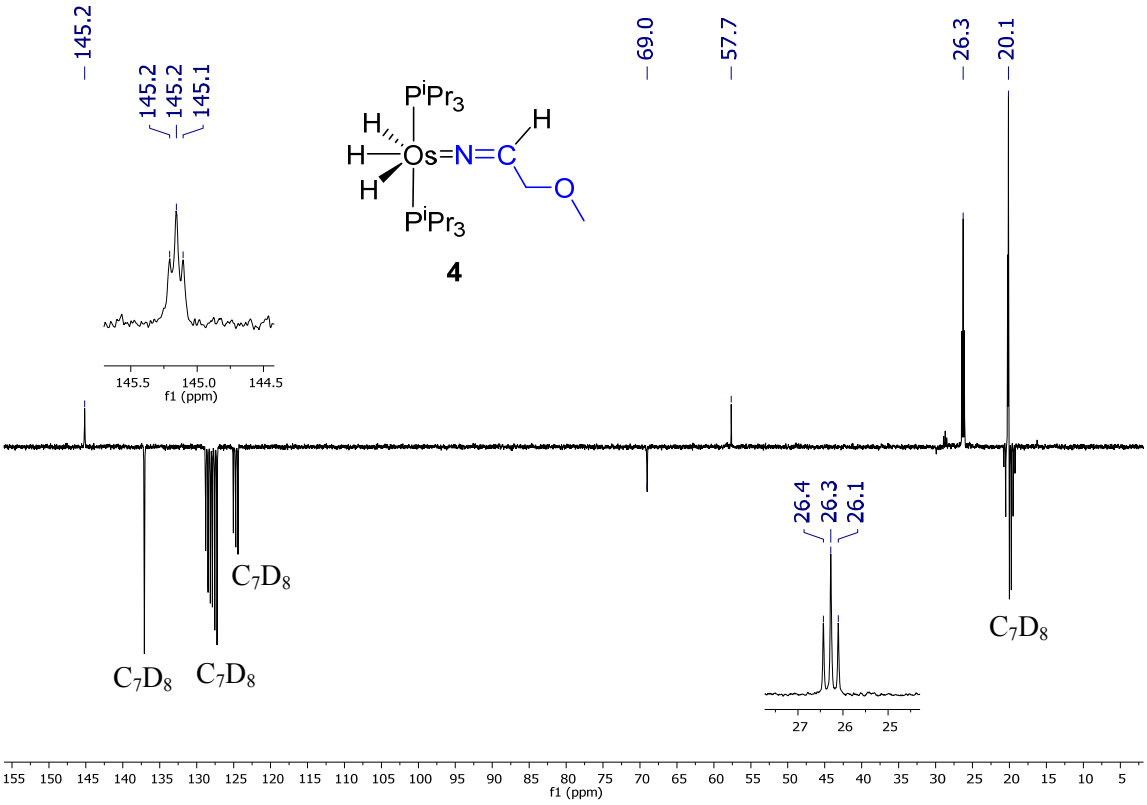

Figure S78. $^{13}C\{^{1}H\}$ APT NMR (75.48 MHz, C_7D_8, 298 K) spectrum for complex **4**.

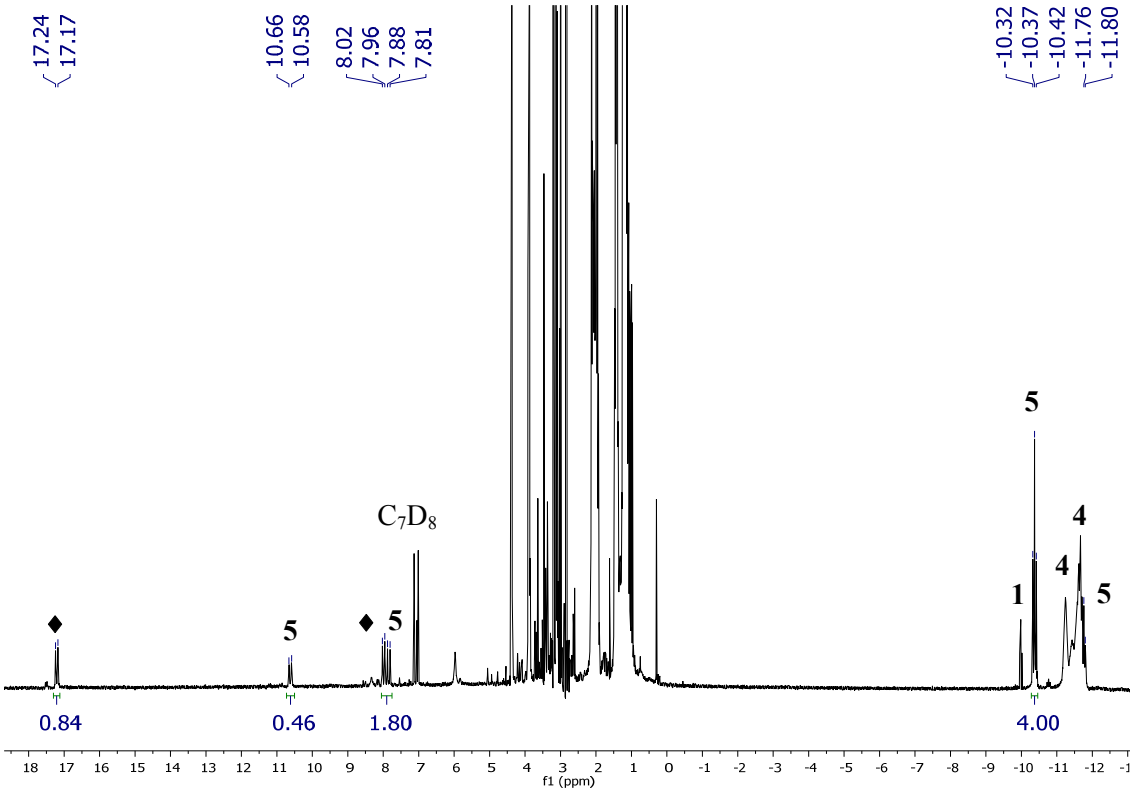

Figure S79. ^{1}H NMR (300.13 MHz, C_7D_8, 298 K) spectrum for reaction mixture of **1** with 2-methoxyacetonitrile (44 h, 50 ºC). Free 2-methoxyethan-1-imine (♦)

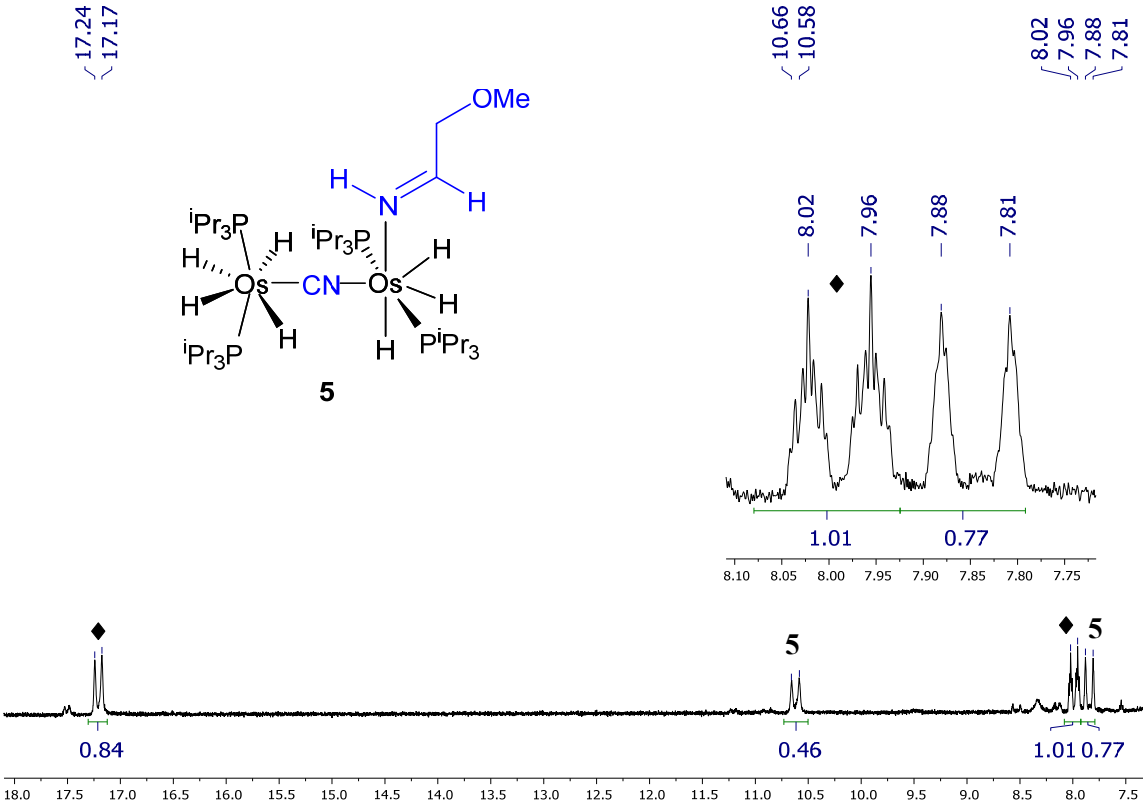

Figure S80. Low field region of ^{1}H NMR (300.13 MHz, C_7D_8, 298 K) spectrum for reaction mixture of **1** with 2-methoxyacetonitrile (44 h, 50 ºC). Free 2-methoxyethan-1-imine (♦)

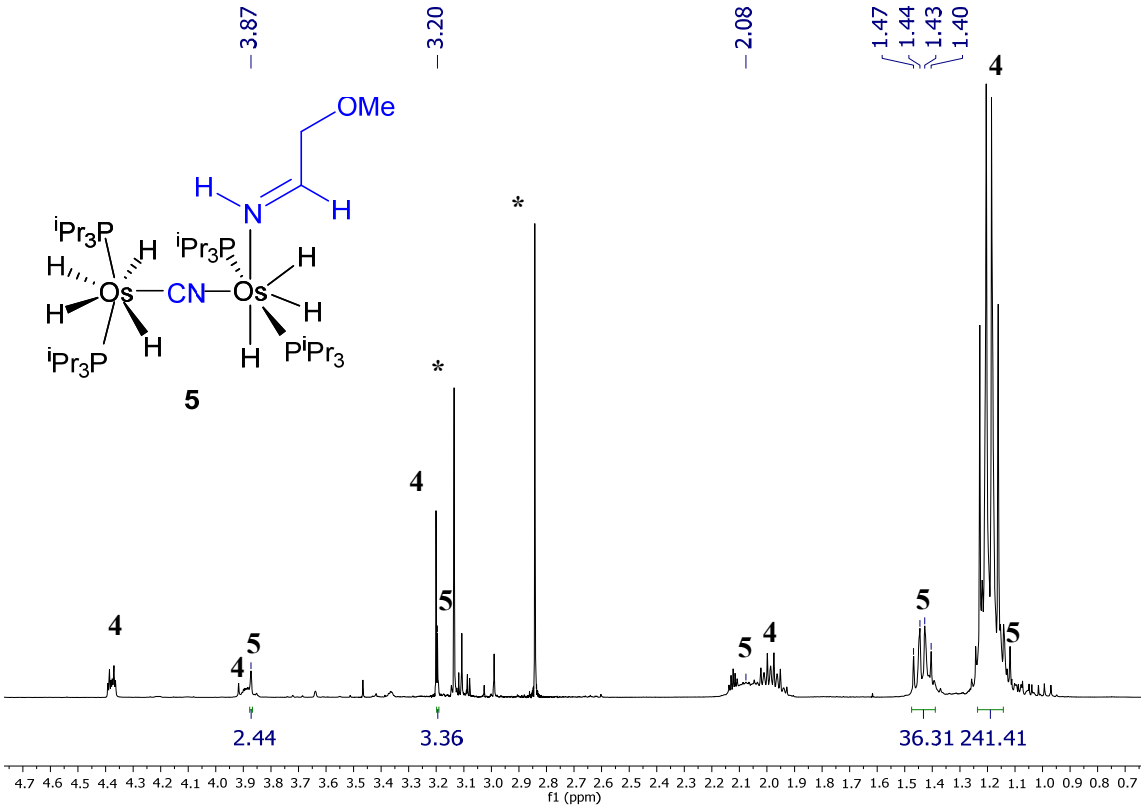

Figure S81. Mid field region of ^{1}H NMR (300.13 MHz, C_7D_8, 298 K) spectrum for reaction mixture of **1** with 2-methoxyacetonitrile (44 h, 50 ºC). *Excess of 2-methoxyacetonitrile.

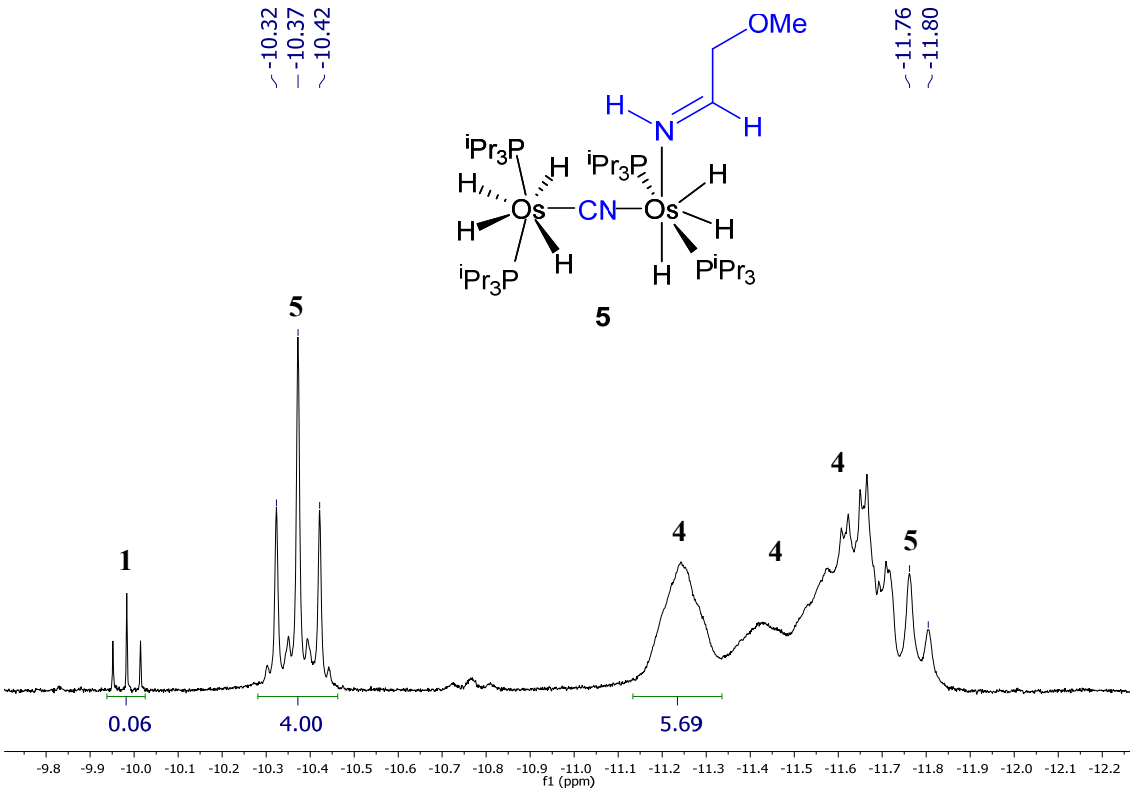

Figure S82. High field region of ^{1}H NMR (300.13 MHz, C_7D_8, 298 K) spectrum for the reaction mixture of **1** with 2-methoxyacetonitrile (44 h, 50 ºC).

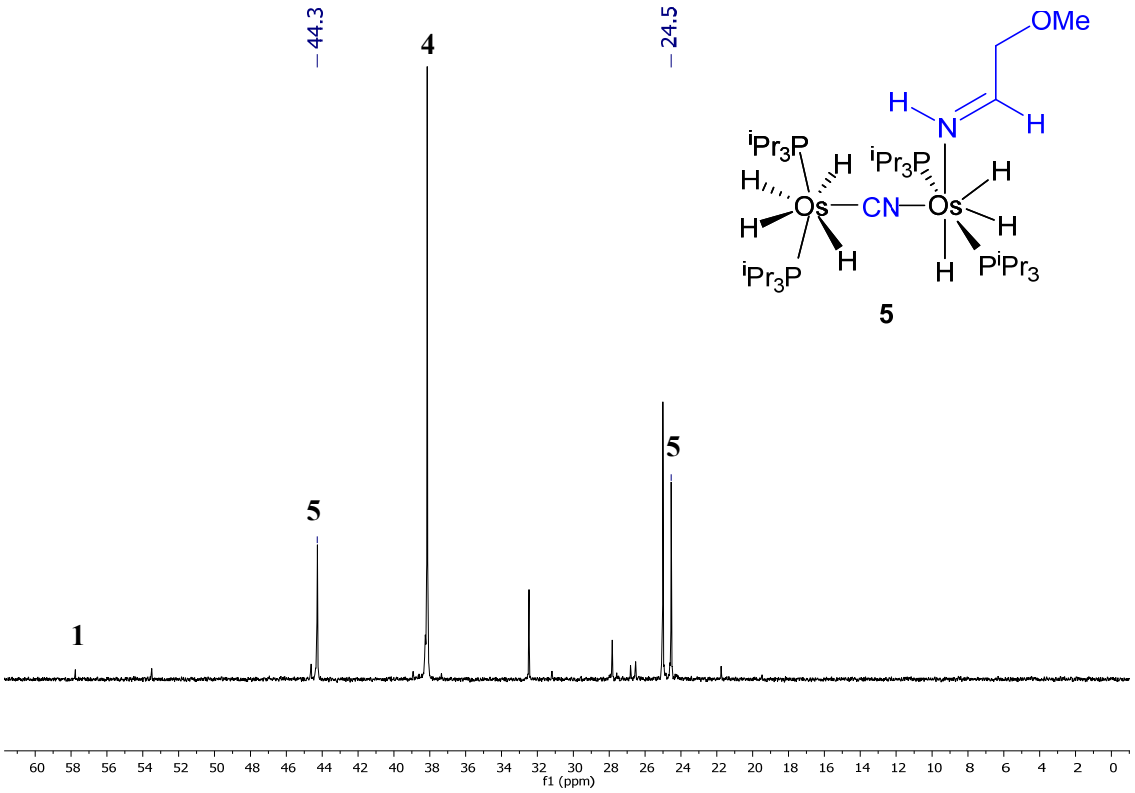

Figure S83. $^{31}P\{^{1}H\}$ NMR (121.49 MHz, C_7D_8, 298 K) spectrum for reaction mixture of **1** with 2-methoxyacetonitrile (44 h, 50 ºC).

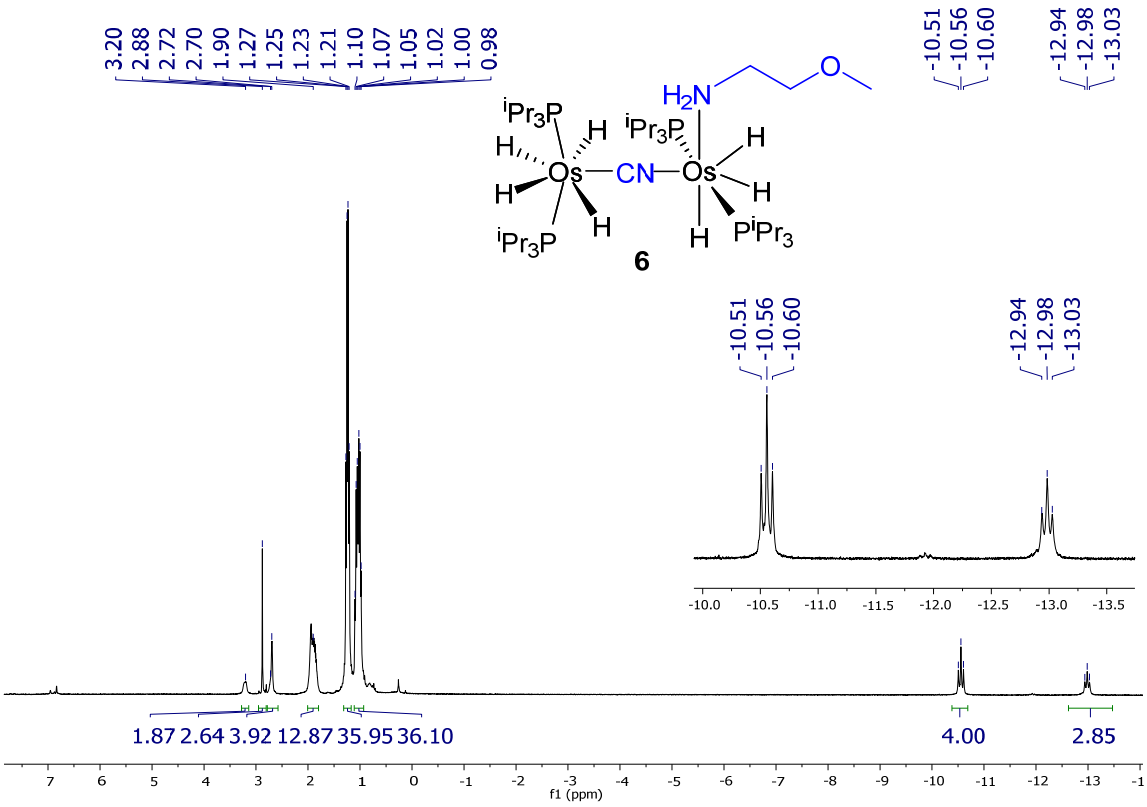

Figure S84. ^{1}H NMR (300.13 MHz, C_7D_8, 298 K) spectrum for complex **6**.

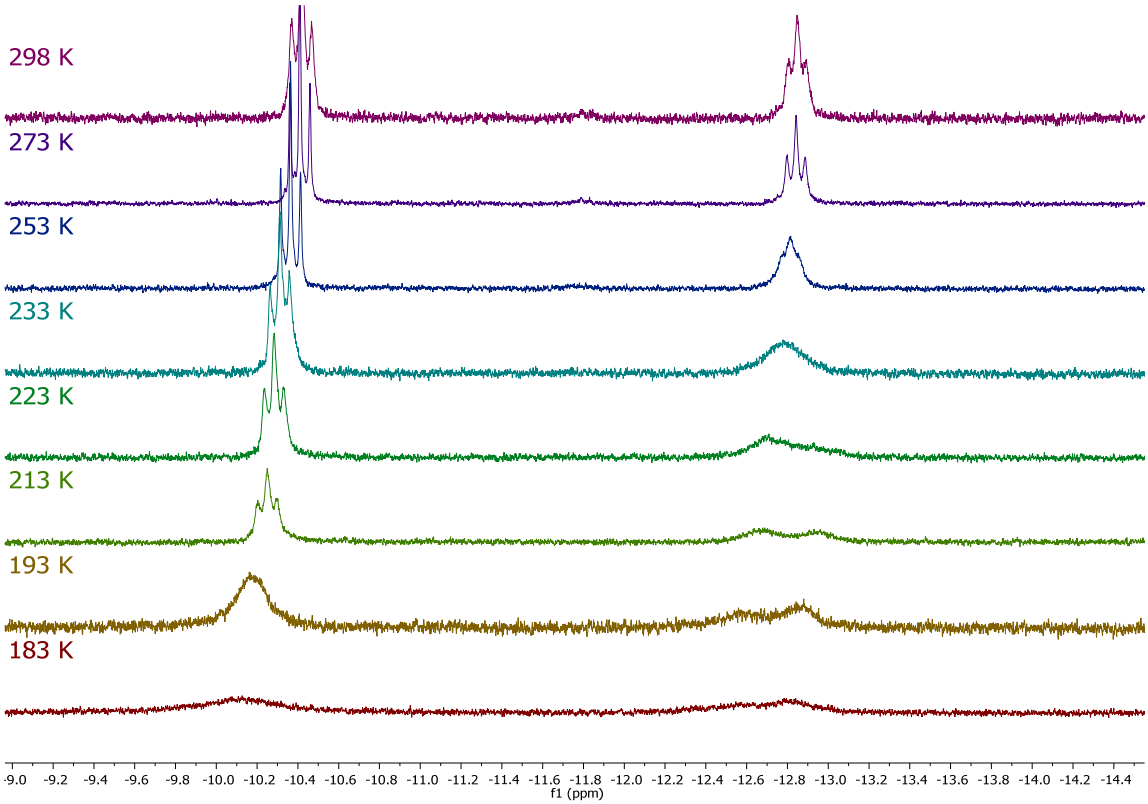

Figure S85. High-field region of the ^{1}H NMR (300.13 MHz, C_7D_8) spectrum of complex **6** between 298 and 183 K.

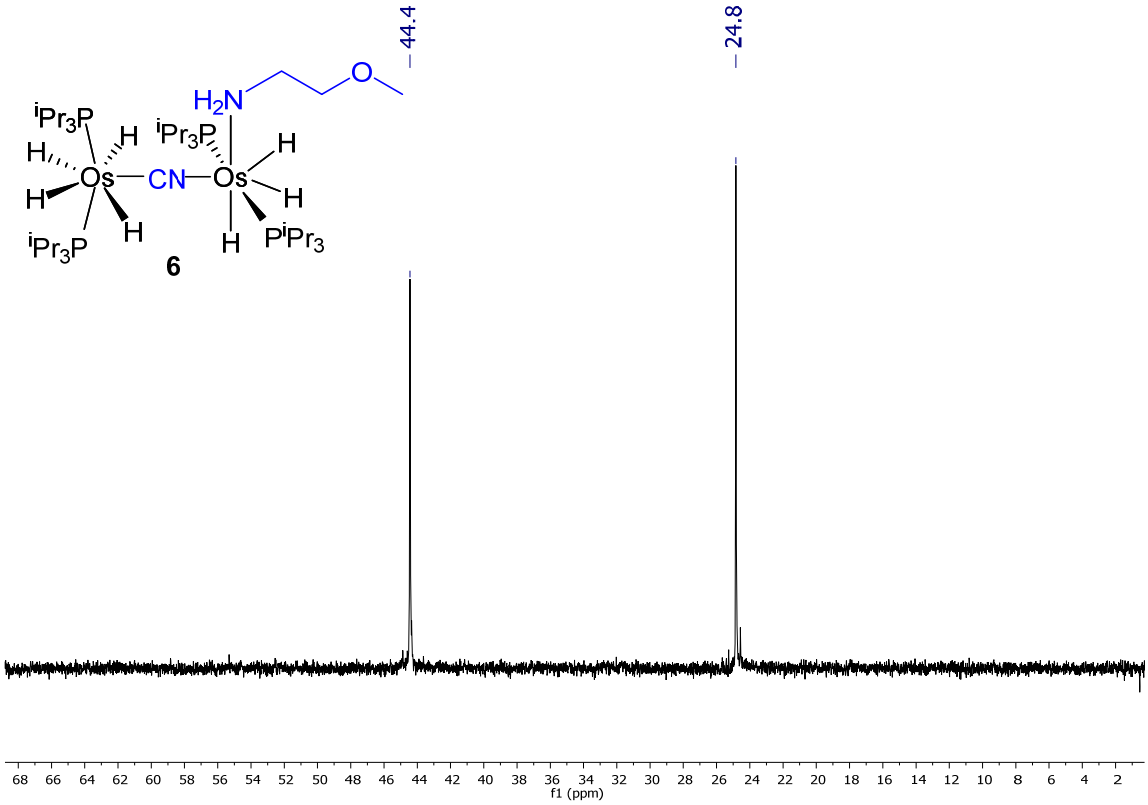

Figure S86. ^{31}P{^{1}H} NMR (121.49 MHz, C_7D_8, 298 K) spectrum for complex **6**.

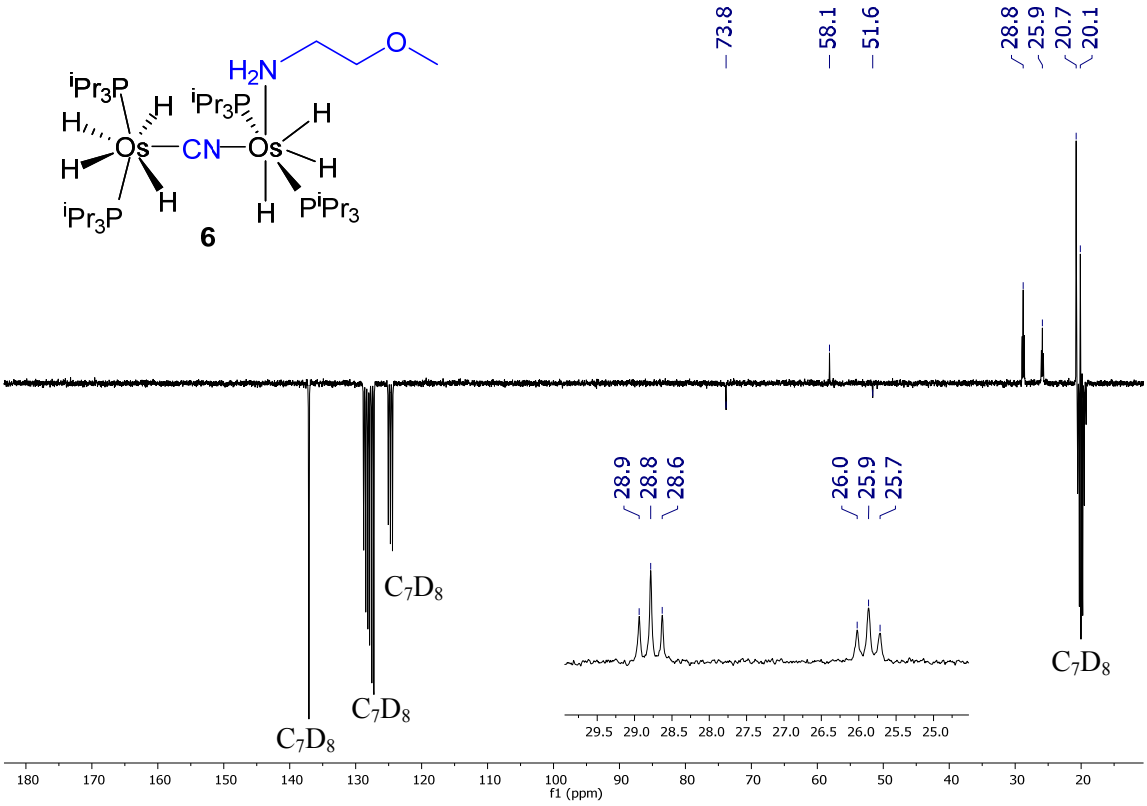

Figure S87. $^{13}C\{^{1}H\}$ APT NMR (75.48 MHz, C_7D_8, 298 K) spectrum for complex **6**.

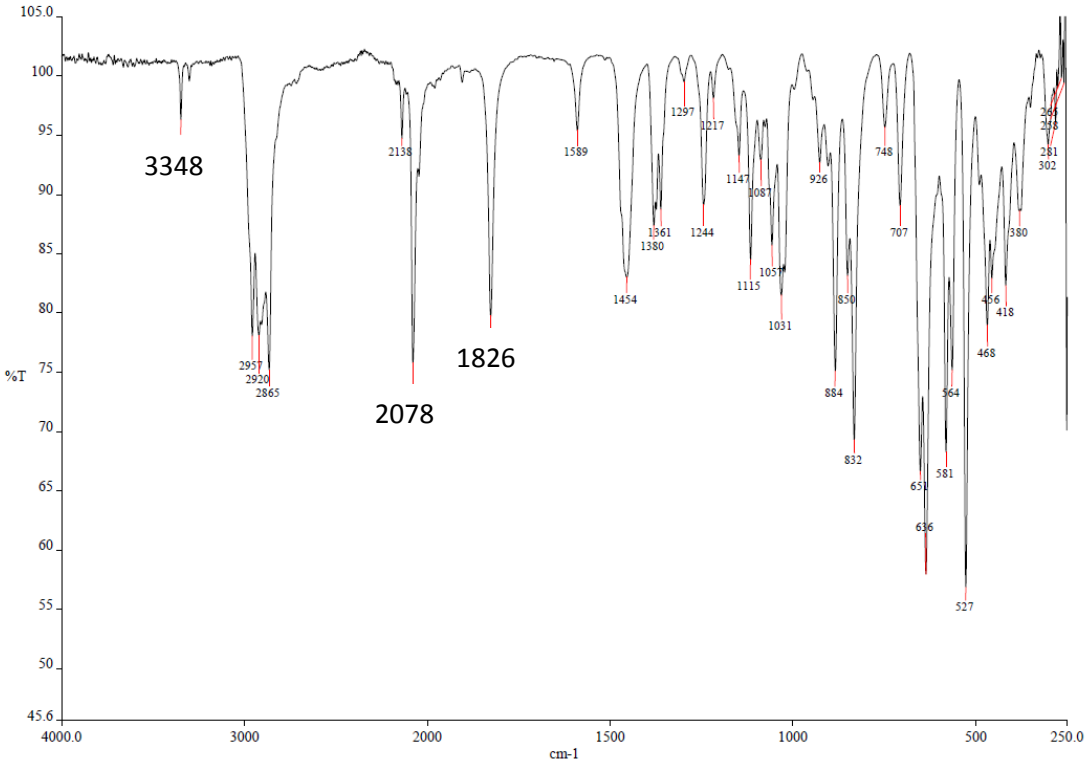

Figure S88. IR ATR spectrum for complex **6**.

Energy values of the computed structures included in the mechanistic studies (B3LYPD3/SDD/6-31G** level): the calculated complexes can be viewed with the xyz file with a free software as Mercury (CCDC) following the nomenclature given in the manuscript (Figures 5-8 of the manuscript and Figures S87-S90).

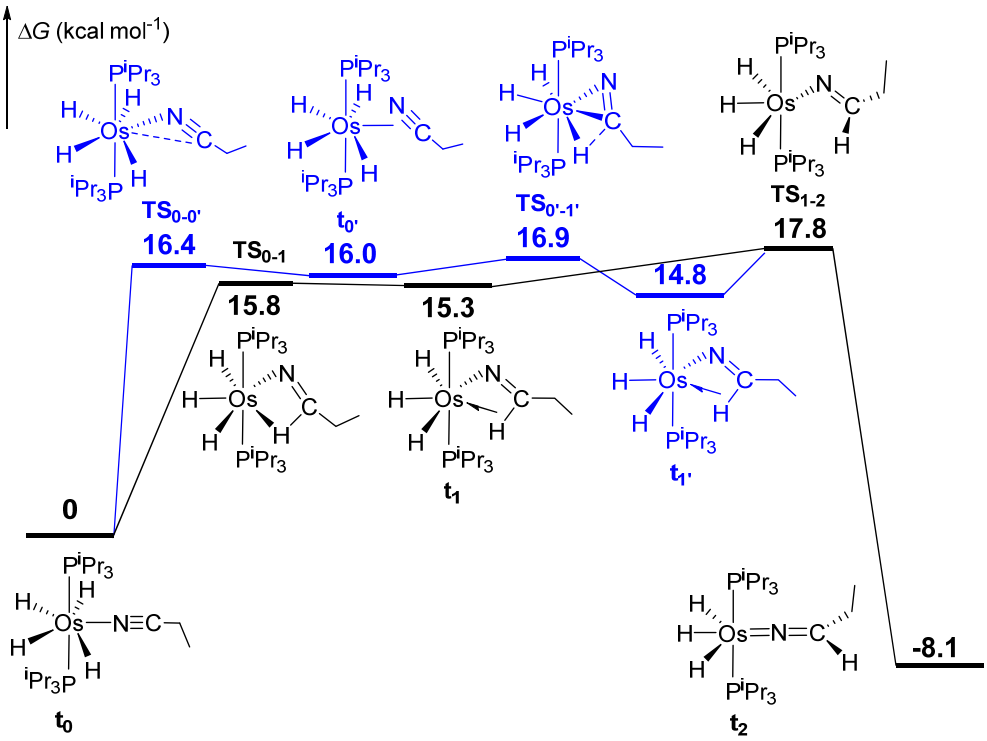

Figure S89. Computed energy profile for the formation of the azavinylidene intermediate $\mathbf{t_2}$ via 1,3-hydrogen shift (▬) or via 1,2-hydrogen migration on a η^2-CN intermediate (▬).

t_0

Zero-point correction= 0.684220 (Hartree/Particle)
Thermal correction to Energy= 0.722454
Thermal correction to Enthalpy= 0.723398
Thermal correction to Gibbs Free Energy= 0.615599
Sum of electronic and zero-point Energies= -1658.715169
Sum of electronic and thermal Energies= -1658.676936
Sum of electronic and thermal Enthalpies= -1658.675991
Sum of electronic and thermal Free Energies= -1658.783791

TS_{0-1}

Zero-point correction= 0.682197 (Hartree/Particle)
Thermal correction to Energy= 0.720014
Thermal correction to Enthalpy= 0.720959
Thermal correction to Gibbs Free Energy= 0.614952
Sum of electronic and zero-point Energies= -1658.691444
Sum of electronic and thermal Energies= -1658.653626
Sum of electronic and thermal Enthalpies= -1658.652682
Sum of electronic and thermal Free Energies= -1658.758689

t_1

Zero-point correction= 0.685477 (Hartree/Particle)
Thermal correction to Energy= 0.723259
Thermal correction to Enthalpy= 0.724203
Thermal correction to Gibbs Free Energy= 0.617697
Sum of electronic and zero-point Energies= -1658.691602
Sum of electronic and thermal Energies= -1658.653820
Sum of electronic and thermal Enthalpies= -1658.652876
Sum of electronic and thermal Free Energies= -1658.759382

$TS_{1\text{-}2}$

Zero-point correction= 0.685137 (Hartree/Particle)
Thermal correction to Energy= 0.722862
Thermal correction to Enthalpy= 0.723806
Thermal correction to Gibbs Free Energy= 0.617142
Sum of electronic and zero-point Energies= -1658.687359
Sum of electronic and thermal Energies= -1658.649634
Sum of electronic and thermal Enthalpies= -1658.648689
Sum of electronic and thermal Free Energies= -1658.755353

t_2

Zero-point correction= 0.685912 (Hartree/Particle)
Thermal correction to Energy= 0.724532
Thermal correction to Enthalpy= 0.725477
Thermal correction to Gibbs Free Energy= 0.614620
Sum of electronic and zero-point Energies= -1658.725459
Sum of electronic and thermal Energies= -1658.686838
Sum of electronic and thermal Enthalpies= -1658.685894
Sum of electronic and thermal Free Energies= -1658.796751

$TS_{0\text{-}0'}$

Zero-point correction= 0.683371 (Hartree/Particle)
Thermal correction to Energy= 0.721118
Thermal correction to Enthalpy= 0.722063
Thermal correction to Gibbs Free Energy= 0.616380
Sum of electronic and zero-point Energies= -1658.690629
Sum of electronic and thermal Energies= -1658.652881
Sum of electronic and thermal Enthalpies= -1658.651937
Sum of electronic and thermal Free Energies= -1658.757620

$t_{0'}$

Zero-point correction= 0.683414 (Hartree/Particle)
Thermal correction to Energy= 0.721919
Thermal correction to Enthalpy= 0.722863

Thermal correction to Gibbs Free Energy= 0.615858
Sum of electronic and zero-point Energies= -1658.690737
Sum of electronic and thermal Energies= -1658.652232
Sum of electronic and thermal Enthalpies= -1658.651288
Sum of electronic and thermal Free Energies= -1658.758293

$TS_{0'-1'}$

Zero-point correction= 0.682718 (Hartree/Particle)
Thermal correction to Energy= 0.720453
Thermal correction to Enthalpy= 0.721397
Thermal correction to Gibbs Free Energy= 0.615716
Sum of electronic and zero-point Energies= -1658.689800
Sum of electronic and thermal Energies= -1658.652064
Sum of electronic and thermal Enthalpies= -1658.651120
Sum of electronic and thermal Free Energies= -1658.756801

$t_{1'}$

Zero-point correction= 0.684466 (Hartree/Particle)
Thermal correction to Energy= 0.722622
Thermal correction to Enthalpy= 0.723566
Thermal correction to Gibbs Free Energy= 0.615636
Sum of electronic and zero-point Energies= -1658.691440
Sum of electronic and thermal Energies= -1658.653285
Sum of electronic and thermal Enthalpies= -1658.652341
Sum of electronic and thermal Free Energies= -1658.760270

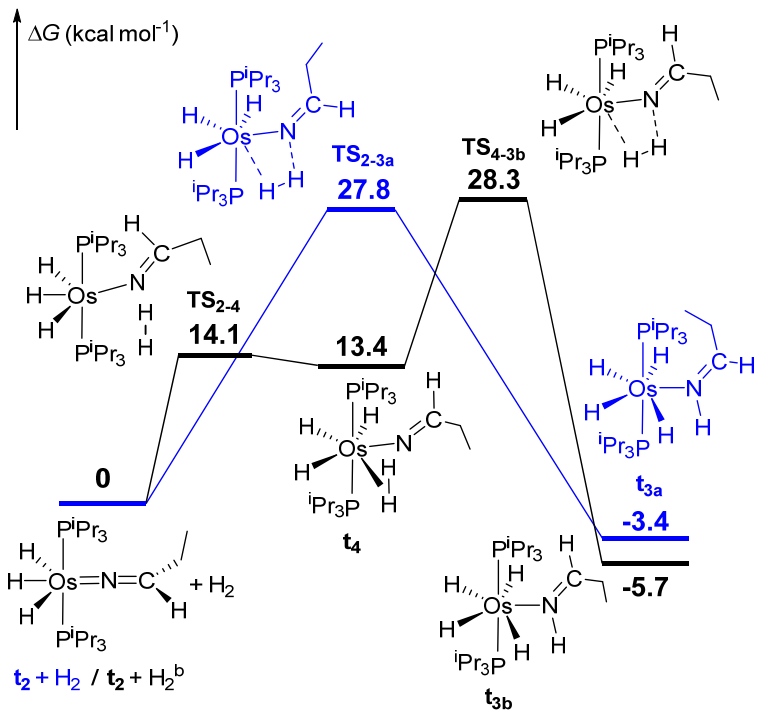

Figure S90. Computed energy profile for the reaction of the model azavinylidene **t₂** with H_2: outer sphere (◘) and inner sphere via a dihydogen intermediate.

t_2+H_2

Zero-point correction= 0.698377 (Hartree/Particle)
Thermal correction to Energy= 0.739681
Thermal correction to Enthalpy= 0.740625
Thermal correction to Gibbs Free Energy= 0.626411
Sum of electronic and zero-point Energies= -1659.893729
Sum of electronic and thermal Energies= -1659.852425
Sum of electronic and thermal Enthalpies= -1659.851481
Sum of electronic and thermal Free Energies= -1659.965695

$TS_{2\text{-}3a}$

Zero-point correction= 0.700884 (Hartree/Particle)
Thermal correction to Energy= 0.739404
Thermal correction to Enthalpy= 0.740348
Thermal correction to Gibbs Free Energy= 0.632350
Sum of electronic and zero-point Energies= -1659.852812
Sum of electronic and thermal Energies= -1659.814292
Sum of electronic and thermal Enthalpies= -1659.813348
Sum of electronic and thermal Free Energies= -1659.921347

t_{3a}

Zero-point correction= 0.709134 (Hartree/Particle)
Thermal correction to Energy= 0.747130
Thermal correction to Enthalpy= 0.748074
Thermal correction to Gibbs Free Energy= 0.642465

Sum of electronic and zero-point Energies= -1659.904496
Sum of electronic and thermal Energies= -1659.866500
Sum of electronic and thermal Enthalpies= -1659.865556
Sum of electronic and thermal Free Energies= -1659.971165

$7t_2+H_2^b$

Zero-point correction= 0.698727 (Hartree/Particle)
Thermal correction to Energy= 0.740020
Thermal correction to Enthalpy= 0.740965
Thermal correction to Gibbs Free Energy= 0.626739
Sum of electronic and zero-point Energies= -1659.894198
Sum of electronic and thermal Energies= -1659.852904
Sum of electronic and thermal Enthalpies= -1659.851960
Sum of electronic and thermal Free Energies= -1659.966185

$TS_{2\text{-}4}$

Zero-point correction= 0.700645 (Hartree/Particle)
Thermal correction to Energy= 0.739799
Thermal correction to Enthalpy= 0.740743
Thermal correction to Gibbs Free Energy= 0.632584
Sum of electronic and zero-point Energies= -1659.875713
Sum of electronic and thermal Energies= -1659.836559
Sum of electronic and thermal Enthalpies= -1659.835615
Sum of electronic and thermal Free Energies= -1659.943774

t_4

Zero-point correction= 0.704524 (Hartree/Particle)
Thermal correction to Energy= 0.742835
Thermal correction to Enthalpy= 0.743779
Thermal correction to Gibbs Free Energy= 0.637490
Sum of electronic and zero-point Energies= -1659.877883
Sum of electronic and thermal Energies= -1659.839572
Sum of electronic and thermal Enthalpies= -1659.838628
Sum of electronic and thermal Free Energies= -1659.944917

$TS_{4\text{-}3b}$

Zero-point correction= 0.700630 (Hartree/Particle)
Thermal correction to Energy= 0.739254
Thermal correction to Enthalpy= 0.740198
Thermal correction to Gibbs Free Energy= 0.631625
Sum of electronic and zero-point Energies= -1659.852043
Sum of electronic and thermal Energies= -1659.813419
Sum of electronic and thermal Enthalpies= -1659.812475
Sum of electronic and thermal Free Energies= -1659.921048

t_{3b}

Zero-point correction= 0.708140 (Hartree/Particle)
Thermal correction to Energy= 0.746567
Thermal correction to Enthalpy= 0.747512
Thermal correction to Gibbs Free Energy= 0.639566
Sum of electronic and zero-point Energies= -1659.906635
Sum of electronic and thermal Energies= -1659.868208
Sum of electronic and thermal Enthalpies= -1659.867264
Sum of electronic and thermal Free Energies= -1659.975209

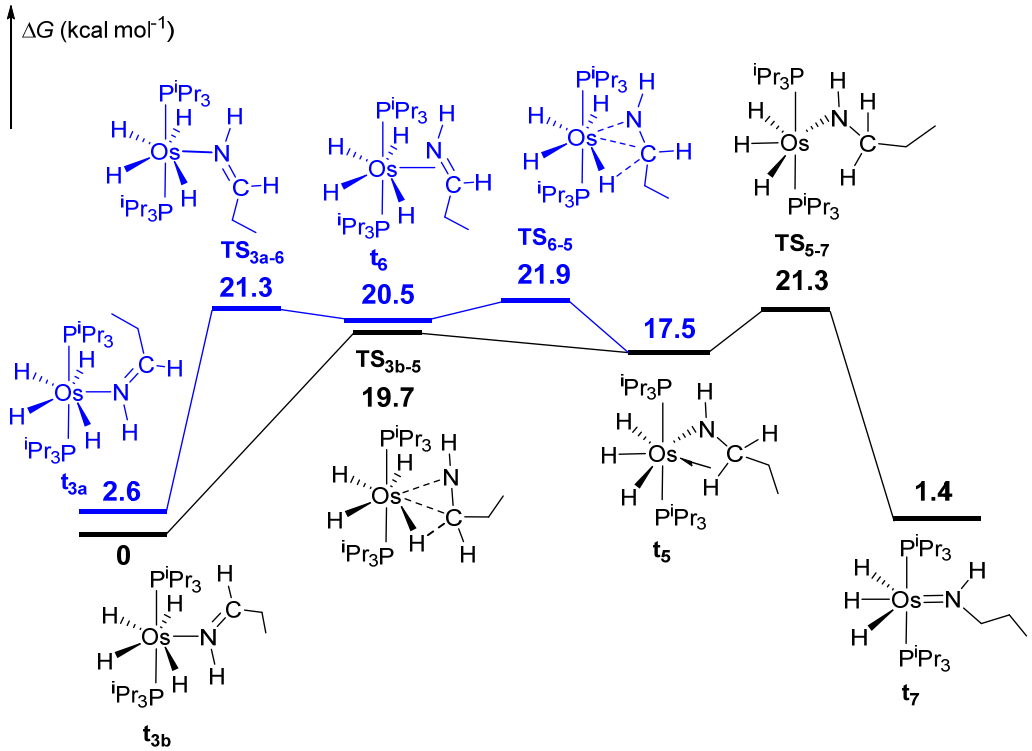

Figure S91. Computed energy profile for the insertion of the imine ligand into one of the Os-H bonds of **t_{3a}** (*cis*-imine) and **t_{3b}** (*trans*-imine).

TS_{3a-6}

Zero-point correction= 0.707374 (Hartree/Particle)
Thermal correction to Energy= 0.745391
Thermal correction to Enthalpy= 0.746335
Thermal correction to Gibbs Free Energy= 0.640132
Sum of electronic and zero-point Energies= -1659.874068
Sum of electronic and thermal Energies= -1659.836051
Sum of electronic and thermal Enthalpies= -1659.835106
Sum of electronic and thermal Free Energies= -1659.941309

t_6

Zero-point correction= 0.707548 (Hartree/Particle)
Thermal correction to Energy= 0.746177
Thermal correction to Enthalpy= 0.747121
Thermal correction to Gibbs Free Energy= 0.639498
Sum of electronic and zero-point Energies= -1659.874565
Sum of electronic and thermal Energies= -1659.835936
Sum of electronic and thermal Enthalpies= -1659.834992
Sum of electronic and thermal Free Energies= -1659.942615

$TS_{6\text{-}5}$

Zero-point correction= 0.706489 (Hartree/Particle)
Thermal correction to Energy= 0.744341
Thermal correction to Enthalpy= 0.745285
Thermal correction to Gibbs Free Energy= 0.640308
Sum of electronic and zero-point Energies= -1659.874118
Sum of electronic and thermal Energies= -1659.836265
Sum of electronic and thermal Enthalpies= -1659.835321
Sum of electronic and thermal Free Energies= -1659.940299

t_5

Zero-point correction= 0.710977 (Hartree/Particle)
Thermal correction to Energy= 0.748767
Thermal correction to Enthalpy= 0.749711
Thermal correction to Gibbs Free Energy= 0.644186
Sum of electronic and zero-point Energies= -1659.880549
Sum of electronic and thermal Energies= -1659.842759
Sum of electronic and thermal Enthalpies= -1659.841815
Sum of electronic and thermal Free Energies= -1659.947340

$TS_{3b\text{-}5}$

Zero-point correction= 0.707381 (Hartree/Particle)
Thermal correction to Energy= 0.745024
Thermal correction to Enthalpy= 0.745968
Thermal correction to Gibbs Free Energy= 0.641250
Sum of electronic and zero-point Energies= -1659.877732
Sum of electronic and thermal Energies= -1659.840089
Sum of electronic and thermal Enthalpies= -1659.839145
Sum of electronic and thermal Free Energies= -1659.943863

$TS_{5\text{-}7}$

Zero-point correction= 0.710336 (Hartree/Particle)
Thermal correction to Energy= 0.747978
Thermal correction to Enthalpy= 0.748922
Thermal correction to Gibbs Free Energy= 0.643450
Sum of electronic and zero-point Energies= -1659.874508

Sum of electronic and thermal Energies= -1659.836866
Sum of electronic and thermal Enthalpies= -1659.835922
Sum of electronic and thermal Free Energies= -1659.941394

t_7

Zero-point correction= 0.711905 (Hartree/Particle)
Thermal correction to Energy= 0.750233
Thermal correction to Enthalpy= 0.751177
Thermal correction to Gibbs Free Energy= 0.643941
Sum of electronic and zero-point Energies= -1659.905145
Sum of electronic and thermal Energies= -1659.866817
Sum of electronic and thermal Enthalpies= -1659.865873
Sum of electronic and thermal Free Energies= -1659.973108

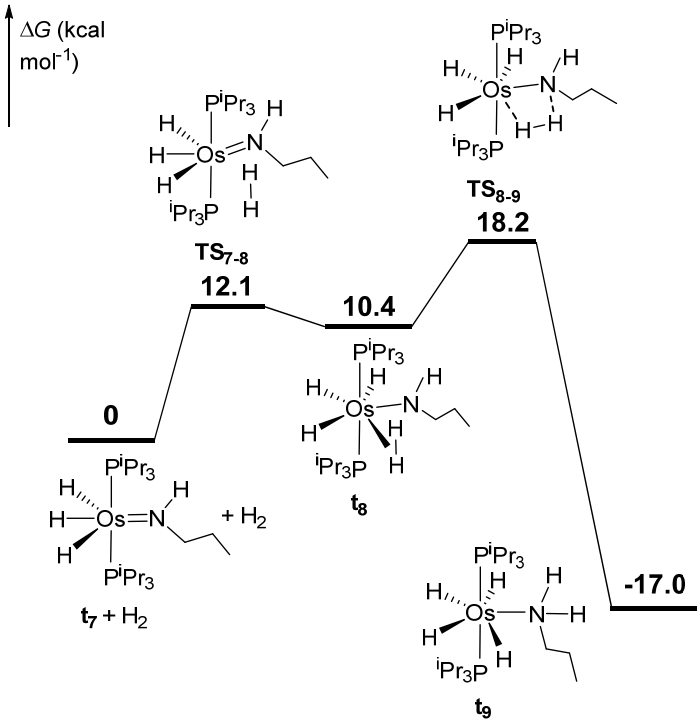

Figure S92. Computed energy profile for the reaction of the *n*-propylidene intermediate **t_7** with H_2: formation of amine intermediate **t_9** via dihydrogen intermediate **t_8**.

t_7+H_2

Zero-point correction= 0.724002 (Hartree/Particle)
Thermal correction to Energy= 0.765311
Thermal correction to Enthalpy= 0.766255
Thermal correction to Gibbs Free Energy= 0.653379
Sum of electronic and zero-point Energies= -1661.073066
Sum of electronic and thermal Energies= -1661.031757
Sum of electronic and thermal Enthalpies= -1661.030813

Sum of electronic and thermal Free Energies= -1661.143689

$TS_{7\text{-}8}$

Zero-point correction= 0.725905 (Hartree/Particle)
Thermal correction to Energy= 0.765277
Thermal correction to Enthalpy= 0.766222
Thermal correction to Gibbs Free Energy= 0.657757
Sum of electronic and zero-point Energies= -1661.056197
Sum of electronic and thermal Energies= -1661.016824
Sum of electronic and thermal Enthalpies= -1661.015880
Sum of electronic and thermal Free Energies= -1661.124344

t_8

Zero-point correction= 0.727753 (Hartree/Particle)
Thermal correction to Energy= 0.766900
Thermal correction to Enthalpy= 0.767844
Thermal correction to Gibbs Free Energy= 0.659215
Sum of electronic and zero-point Energies= -1661.058503
Sum of electronic and thermal Energies= -1661.019355
Sum of electronic and thermal Enthalpies= -1661.018411
Sum of electronic and thermal Free Energies= -1661.127040

$TS_{8\text{-}9}$

Zero-point correction= 0.727219 (Hartree/Particle)
Thermal correction to Energy= 0.765712
Thermal correction to Enthalpy= 0.766656
Thermal correction to Gibbs Free Energy= 0.659816
Sum of electronic and zero-point Energies= -1661.047310
Sum of electronic and thermal Energies= -1661.008816
Sum of electronic and thermal Enthalpies= -1661.007872
Sum of electronic and thermal Free Energies= -1661.114713

t_9

Zero-point correction= 0.732727 (Hartree/Particle)
Thermal correction to Energy= 0.771612
Thermal correction to Enthalpy= 0.772557
Thermal correction to Gibbs Free Energy= 0.663649
Sum of electronic and zero-point Energies= -1661.101643
Sum of electronic and thermal Energies= -1661.062758
Sum of electronic and thermal Enthalpies= -1661.061814
Sum of electronic and thermal Free Energies= -1661.170721

References

(1) Aracama, M.; Esteruelas, M. A.; Lahoz, F. J.; López, J. A.; Meyer, U.; Oro, L. A.; Werner, H. Synthesis, Reactivity, Molecular Structure, and Catalytic Activity of the Novel Dichlorodihydridoosmium(IV) Complexes $OsH_2Cl_2(PR_3)_2$ (PR_3 = P-*i*-Pr_3, PMe-*t*-Bu_2). *Inorg. Chem.* **1991**, *30*, 288–293.

(2) Blessing, R. H. An Empirical Correction for Absorption Anisotropy. *Acta Crystallogr.* **1995**, *A51*, 33. SADABS: Area-detector absorption correction; Bruker-AXS, Madison, WI, 1996.

(3) SHELXL-2016/6. Sheldrick, G. M. A short history of SHELX. *Acta Cryst.* **2008**, *A64*, 112-122.

(4) (a) Lee, C.; Yang, W.; Parr, R. G. Development of the Colle-Salvetti correlation-energy formula into a functional of the electron density. *Phys. Rev. B* **1988**, *37*, 785–789. (b) Becke, A. D. Density-functional exchange-energy approximation with correct asymptotic behavior. *J. Chem. Phys.* **1993**, *98*, 5648–5652. (c) Stephens, P. J.; Devlin, F. J.; Chabalowski, C. F.; Frisch, M. J. *Ab Initio* Calculation of Vibrational Absorption and Circular Dichroism Spectra Using Density Functional Force Fields. *J. Phys. Chem.* **1994**, *98*, 11623–11627.

(5) Grimme, S.; Antony, J.; Ehrlich, S.; Krieg, H. A consistent and accurate *ab initio* parametrization of density functional dispersion correction (DFT-D) for the 94 elements H-Pu. *J. Chem. Phys.* **2010**, *132*, 154104.

(6) Gaussian 09, Revision D.01, Frisch, M. J.; Trucks, G. W.; Schlegel H. B.; Scuseria, G. E.; Robb, M. A.; Cheeseman, J. R.; Scalmani, G.; Barone, V.; Mennucci, B.; Petersson, G. A.; Nakatsuji, H.; Caricato, M.; Li, X.; Hratchian, H. P.; Izmaylov, A. F.; Bloino, J.; Zheng, G.; Sonnenberg, J. L.; Hada, M.; Ehara, M.; Toyota, K.; Fukuda, R.; Hasegawa, J.; Ishida, M.; Nakajima, T.; Honda, Y.; Kitao, O.; Nakai, H.; Vreven, T.; Montgomery, J. A.; Peralta, Jr., J. E.; Ogliaro, F.; Bearpark, M.; Heyd, J. J.; Brothers, E.; Kudin, K. N.; Staroverov, V. N.; Keith, T.; Kobayashi, R.; Normand, J.; Raghavachari, K.; Rendell, A.; Burant, J. C.; Iyengar, S. S.; Tomasi, J.; Cossi, M.; Rega, N.; Millam, J. M.; Klene, M.; Knox, J. E.; Cross, J. B.; Bakken, V.; Adamo, C.; Jaramillo, J.; Gomperts, R.; Stratmann, R. E.; Yazyev, O.; Austin, A. J.; Cammi, R.; Pomelli, C.; Ochterski, J. W.; Martin, R. L.; Morokuma, K.; Zakrzewski, V. G.; Voth, G. A.; Salvador, P.; Dannenberg, J. J.; Dapprich, S.; Daniels, A. D.; Farkas, O.;

Foresman, J. B.; Ortiz, J. V.; Cioslowski, J.; Fox, D. J. Gaussian, Inc., Wallingford CT, 2013.

(7) Andrea, D.; Haeussermann, U. M.; Dolg, M.; Stoll, H.; Preuss, H. *Theor. Chim. Acta* **1990**, *77*, 123–141.

(8) Ehlers, A. W.; Bohme, M.; Dapprich, S.; Gobbi, A.; Hollwarth, A.; Jonas, V.; Kohler, K. F.; Stegmann, R.; Veldkamp, A.; Frenking, G. A set of f-polarization functions for pseudo-potential basis sets of the transition metals SC-Cu, Y-Ag and La-Au. *Chem. Phys. Lett.* **1993**, *208*, 111–114.

(9) (a) Hehre, W. J.; Ditchfield, R.; Pople, J. A. Self-Consistent Molecular Orbital Methods. XII. Further Extensions of Gaussian-Type Basis Sets for Use in Molecular Orbital Studies of Organic Molecules. *J. Chem. Phys.* **1972**, *56*, 2257–2261. (b) Francl, M. M.; Pietro, W. J.; Hehre, W. J.; Binkley, J. S.; Gordon, M. S.; DeFrees, D. J.; Pople, J. A. Self□consistent molecular orbital methods. XXIII. A polarization□type basis set for second□row elements. *J. Chem. Phys.* **1982**, *77*, 3654–3665.

(10) Marenich, A. V.; Cramer, C. J.; Truhlar, D. G. *J. Phys. Chem. B* **2009**, *113*, 6378–6396.

(11) AIST: Integrated Spectral Database System of Organic Compounds. (Data were obtained from the National Institute of Advanced Industrial Science and Technology (Japan)). (a) **a·HCl**: https://sdbs.db.aist.go.jp/sdbs/cgi-bin/landingpage?sdbsno=10120. (b) **i·HCl**: https://sdbs.db.aist.go.jp/sdbs/cgi-bin/landingpage?sdbsno=4739.

(12) Ghosh, C.; Konai, M. M.; Sarkar, P.; Samaddar, S.; Haldar, J. Designing Simple Lipidated Lysines: Bifurcation Imparts Selective Antibacterial Activity. *ChemMedChem* **2016**, *11*, 2367-2371.

(13) Montgomery, S. L.; Mangas-Sanchez, J.; Thompson, M. P.; Aleku, G. A.; Dominguez, B.; Turner, N. J. Direct Alkylation of Amines with Primary and Secondary Alcohols through Biocatalytic Hydrogen Borrowing. *Angew. Chem., Int. Ed.* **2017**, *56*, 10491-10494.

(14) Wiese, S.; Badiei, Y. M.; Gephart, R. T.; Mossin, S.; Varonka, M. S.; Melzer, M. M.; Meyer, K.; Cundari, T. R.; Warren, T. H. Catalytic C-H Amination with Unactivated Amines through Copper(II) Amides. *Angew. Chem., Int. Ed.* **2010**, *49*, 8850-8855.

(15) Miriyala, B.; Bhattacharyya, S.; Williamson, J. S. Chemoselective reductive alkylation of ammonia with carbonyl compounds: synthesis of primary and symmetrical secondary amines. *Tetrahedron*, **2004**, *60*, 1463-1471.

(16) Brinkmann, C.; Barrett, A. G. M.; Hill, M. S.; Procopiou, P. A. Heavier Alkaline Earth Catalysts for the Intermolecular Hydroamination of Vinylarenes, Dienes, and Alkynes. *J. Am. Chem. Soc*. **2012**, *134*, 2193–2207.

(17) Squiller, E. P.; Pajerski, A. D.; Whittle, R. R.; Richey, H. G. Jr. Preparation and Properties of RMgN< Compounds Having Coordinating Oxygen Atoms in the Amino Component. *Organometallics* **2006**, *25*, 2465-2469.

(18) Orito, K; Horibata, A.; Nakamura, T.; Ushito, H.; Nagasaki, H.; Yuguchi, M.; Yamashita, S.; Tokuda, M. Preparation of Benzolactams by $Pd(OAc)_2$-Catalyzed Direct Aromatic Carbonylation. *J. Am. Chem. Soc* **2004**, *126*, 14342-14343.

(19) Nacario, R.; Kotakonda, S.; Fouchard, D. M. D.; Tillekeratne, L. M. V.; Hudson, R. A. Reductive Monoalkylation of Aromatic and Aliphatic Nitro Compounds and the Corresponding Amines with Nitriles. *Org. Lett.* **2005**, *7*, 471-474.

(20) Largeron, M.; Fleury, M.-B. A Biomimetic Electrocatalytic System for the Atom-Economical Chemoselective Synthesis of Secondary Amines. *Org. Lett.* **2009**, *11*, 883-886.

(21) Candeias, N. R.; Gois, P. M. P.; Afonso, C. A. M. Rh(II)-Catalyzed Intramolecular C-H Insertion of Diazo Substrates in Water: Scope and Limitations. J. *Org. Chem.* **2006**, *71*, 5489-5497.